

**ESSENTIAL ROLES OF Pdia3/PLAA RECEPTOR COMPLEX AND
CAMKII IN $1\alpha,25(\text{OH})_2\text{D}_3$ AND Wnt5a CALCIUM-DEPENDENT
SIGNALING PATHWAYS IN OSTEOBLASTS AND CHONDROCYTES**

A Dissertation
Presented to
The Academic Faculty

by

Maryam Doroudi

In Partial Fulfillment
of the Requirements for the Degree
Doctor of Philosophy in the
School of Biology

Georgia Institute of Technology
May 2014

Copyright 2014 by Maryam Doroudi

**ESSENTIAL ROLES OF Pdia3/PLAA RECEPTOR COMPLEX AND
CAMKII IN $1\alpha,25(\text{OH})_2\text{D}_3$ AND Wnt5a CALCIUM-DEPENDENT
SIGNALING PATHWAYS IN OSTEOBLASTS AND CHONDROCYTES**

Approved by:

Dr. Barbara D. Boyan, Advisor
School of Biomedical Engineering
Georgia Institute of Technology

Dr. Al Merrill
School of Biology
Georgia Institute of Technology

Dr. Chong Shin
School of Biology
Georgia Institute of Technology

Dr. Zvi Schwartz
School of Engineering
Virginia Commonwealth University

Dr. Hanjoong Jo
School of Biomedical Engineering
Georgia Institute of Technology

Dr. Thomas Ziegler
School of Medicine
Emory University

Date Approved: March 19, 2014

ACKNOWLEDGEMENTS

First and foremost I would like to express my deepest appreciation and thanks to my advisors, Dr. Barbara Boyan and Dr. Zvi Schwartz, for their guidance and support in all stages of this thesis. Their enthusiasm for the vitamin D project was contagious and motivational for me, even during challenging times. Their mentorship played a significant role in shaping my vision for research and education. I am also thankful for the excellent example Dr. Boyan has provided as a successful woman scientist and leader. I must thank Dr. Don Ranly for sparking my interest in orthopedic research as an undergraduate student, which led me to join the Boyan-Schwartz lab. I would also like to extend my sincerest thanks to the other members of my committee, Dr. Chong Shin, Dr. Hanjoong Jo, Dr. Al Merrill and Dr. Thomas Ziegler, for their consistent encouragements and valuable comments during the completion of this thesis. I especially want to thank Dr. Thomas Ziegler, Dr. Vin Tangpricha, Dr. Henry Blumberg and Ms. Cheryl Sroka in Atlanta Clinical and Translational Science Institute for their mentorship and support during my certificate training.

In particular, I would like to thank Dr. Rene Olivares-Navarrete for his scientific advice and insightful suggestions. He was my primary resource for discussing my “quick” science questions and was instrumental in helping me power through the thesis project. I would also like to thank Ms. Sharon Hyzy for her excellent management of our lab and its army of students, and her outstanding support to conduct my Ph.D. research. I especially want to thank my collaborators, Dr. Jiaxuan Chen and Dr. Yun Wang, as we persevered through the vitamin D project.

The members of Boyan-Schwartz lab have contributed immensely to my personal and professional life at Georgia Institute of Technology. I would like to thank many of the past and current members of our lab: Dr. Jiaxuan Chen, Dr. Reyhaan Chaudhri, Dr. Jung Hwa Park, Dr. Chris Hermann, Dr. Christopher Lee, Dr. Rolando Gittens, Dr. Khairat Elbaradei, Dr. David Cohen, Alice Cheng, Qingfen Pan and Shirae Leslie for their guidance, support and friendship. I would also like to thank Crystal Branan, Leang Chun, Sri Vermula, Lauren Cason and Melissa Maczis for their assistance with cell culture; Jamie Lazin, Christopher Erdman and Megan Merritt for their technical support; Jenilee Shanks, Maribel Baker and Brentis Henderson for their administrative assistance.

I must thank the undergraduate students who assisted me over the course of my Ph.D. project: Chas Plaisance, Firaz Jamal and Subhendu De. I appreciate their hard work and enthusiasm for science.

I would also like to acknowledge the funding sources for my research which included the Price Gilbert, Jr. Foundation and Children's Healthcare of Atlanta and the National Center for Advancing Translational Sciences of the National Institutes of Health under award numbers UL1TR000454 and TL1TR000456.

Most of all, I would like to thank my family for their love and encouragement. Especially for my parents who raised me with a strong belief in education and supported me in all my pursuits. For my brother and sister who supported me. Finally for my loving, encouraging and supportive husband Wojciech whose endless support during all the stages of my Ph.D. training is so appreciated. Thank you.

Maryam Doroudi
Georgia Institute of Technology
March 2014

TABLE OF CONTENTS

	Page
ACKNOWLEDGMENTS	iii
LIST OF FIGURES	xi
LIST OF SYMBOLS AND ABBREVIATIONS	xiii
SUMMARY	xvi
<u>CHAPTER</u>	
1 SPECIFIC AIMS	1
2 BACKGROUND AND LITERATURE REVIEW	5
VITAMIN D METABOLISM	5
THE ROLE OF VITAMIN D IN PHYSIOLOGY AND DISEASE	6
BONE	6
CARTILAGE	9
MOLECULAR MECHANISM OF ACTIONS	11
DVR-MEDIATED GENE EXPRESSION	11
RAPID ACTIONS OF $1\alpha,25(\text{OH})_2\text{D}_3$	12
MODELS FOR STUDYING RAPID ACTIONS	12
MEMBRANE-MEDIATED SIGNALING BY $1\alpha,25(\text{OH})_2\text{D}_3$	12
PHOSPHOLIPASE A ₂	14
PHOSPHOLIPASE A ₂ ACTIVATING PROTEIN	15
CAVEOLAE	16
CALCIUM/CALMODULIN-DEPENDENT PROTEIN KINASE II	17
WNT SIGNALING AND FUNCTION	18

3	PHOSPHOLIPASE A ₂ ACTIVATING PROTEIN IS REQUIRED FOR 1 α ,25-DIHYDROXYVITAMIN D ₃ DEPENDENT RAPID ACTIVATION OF PROTEIN KINASE C VIA PDIA3	21
	INTRODUCTION	21
	MATERIALS AND METHODS	23
	Establishment of silenced and overexpressing MC3T3-E1 cell lines	24
	PLAA	24
	Cav1	26
	Pdia3	26
	Plasma membranes and caveolae isolation	27
	Western blots	28
	Regulation of PKC activity	28
	Regulation of PGE ₂ release	29
	Regulation of PLA ₂ activity	29
	Immunofluorescence Microscopy	30
	Immunoprecipitation	30
	Chemical crosslinking of PLAA to plasma membrane surface proteins	31
	Statistical analysis	32
	RESULTS	32
	Subcellular Localization of PLAA	32
	Effects of 1 α ,25(OH) ₂ D ₃ and BS ³ on Plasma Membrane Localization of PLAA	34
	Effect of PLAA Blocking on 1 α ,25(OH) ₂ D ₃ Membrane-mediated PKC Activation	36
	Effect of <i>Plaa</i> Silencing on 1 α ,25(OH) ₂ D ₃ Membrane-mediated Signaling	37

Effects of $1\alpha,25(\text{OH})_2\text{D}_3$ on Interactions between PLAA and Pdia3	38
DISCUSSION	41
CONCLUSION	45
4 MEMBRANE ACTIONS OF $1\alpha,25(\text{OH})_2\text{D}_3$ ARE MEDIATED BY CALCIUM/CALMODULIN-DEPENDENT PROTEIN KINASE II IN BONE AND CARTILAGE CELLS	47
INTRODUCTION	47
MATERIALS AND METHODS	49
Regulation of CaMKII Activity	51
Regulation of PLA ₂ Activity	53
Regulation of PGE ₂ Release	54
Regulation of PKC Activity	54
Regulation of Alkaline Phosphatase Activity	55
Regulation of Osteopontin Production	56
Plasma Membranes and Caveolae Isolation	56
Western Blots	57
Immunoprecipitation	57
Statistical Analysis	58
RESULTS	59
Effect of $1\alpha,25(\text{OH})_2\text{D}_3$ on CaMKII Activation in Growth Zone Chondrocytes and MC3T3-E1 Osteoblasts	59
Effect of CaMKII Inhibition On Rapid $1\alpha,25(\text{OH})_2\text{D}_3$ Membrane-Mediated Signaling and the Downstream Physiological Responses	59
Effects of <i>Camk2a</i> and <i>Camk2b</i> silencing on Rapid Actions of $1\alpha,25(\text{OH})_2\text{D}_3$ and the Downstream Physiological Responses	62
Roles of Pdia3, Cav-1 and Caveolae in $1\alpha,25(\text{OH})_2\text{D}_3$ Membrane-mediated Activation of CaMKII in MC3T3-E1 Osteoblasts	63

Role of PLAA in $1\alpha,25(\text{OH})_2\text{D}_3$ Membrane-mediated Activation of CaMKII in MC3T3-E1 Osteoblasts	66
Roles of Pdia3, Cav-1, Caveolae and PLAA in $1\alpha,25(\text{OH})_2\text{D}_3$ Membrane-mediated Activation of CaMKII in GC Chondrocytes	68
Role of CaM in $1\alpha,25(\text{OH})_2\text{D}_3$ Membrane-mediated Rapid Activation of CaMKII	69
DISCUSSION	72
CONCLUSION	76
5 SIGNALING COMPONENTS OF THE $1\alpha,25(\text{OH})_2\text{D}_3$ -DEPENDENT Pdia3 RECEPTOR COMPLEX ARE REQUIRED FOR Wnt5a CALCIUM-DEPENDENT SIGNALING	78
INTRODUCTION	78
MATERIALS AND METHODS	81
Time Course and Dose Response of PKC Activity to Wnt5a	82
Time Course of Wnt5a Effect on CaMKII Activity	83
Time Course of Wnt5a Effect on PLA ₂ Activity	83
Time Course of Wnt5a Effect on PGE ₂ Release	83
Role of Vitamin D Signaling Components on Wnt5a-induced PKC Activity	83
Role of Calmodulin on Wnt5a-induced PKC Activity	84
Role of PLAA on Wnt5a-induced PKC Activity	84
Effects of Wnt5a and $1\alpha,25(\text{OH})_2\text{D}_3$ Co-treatment on Regulation of PKC Activity	85
Roles of ROR2, FZD2 and FZD5 on $1\alpha,25(\text{OH})_2\text{D}_3$ -induced PKC Activity	85
Role of ROR2 on $1\alpha,25(\text{OH})_2\text{D}_3$ -induced CaMKII Activity	85
Role of ROR2 on PLAA-induced CaMKII Activity	85
Caveolae Isolation	86
Western Blots	86

Effects of $1\alpha,25(\text{OH})_2\text{D}_3$ and Wnt5a on Receptor Complex Interactions	87
Statistical Analysis	87
RESULTS	88
Rapid Effects of Wnt5a on PKC, CaMKII, PLA ₂ Activations and PGE ₂ Release	88
Roles of Pdia3, VDR, Cav-1 and Lipid Rafts in Wnt5a-mediated Rapid Activation of PKC	90
Roles of CaM, CaMKII- α , CaMKII- β , PLAA and PLA ₂ in Wnt5a-mediated rapid activation of PKC	91
Wnt5a and $1\alpha,25(\text{OH})_2\text{D}_3$ Co-treatment Studies	93
Roles of ROR2, FZD2 and FZD5 in $1\alpha,25(\text{OH})_2\text{D}_3$ -mediated PKC Activation and Their Subcellular Localization	94
Effects of $1\alpha,25(\text{OH})_2\text{D}_3$ Treatment on Interactions between $1\alpha,25(\text{OH})_2\text{D}_3$ Receptor Complex and Wnt5a Receptors Interactions	96
Effects of Wnt5a Treatment on Interactions between $1\alpha,25(\text{OH})_2\text{D}_3$ Receptor Complex and Wnt5a Receptors Interactions	98
DISCUSSION	100
CONCLUSION	106
6 CONCLUSIONS AND FUTURE DIRECTIONS	108
REFERENCES	114

LIST OF FIGURES

	Page
Figure 1.1: $1\alpha,25(\text{OH})_2\text{D}_3$ Biosynthesis	6
Figure 1.2: The Growth Plate	10
Figure 1.3: Proposed mechanism of $1\alpha,25(\text{OH})_2\text{D}_3$ stimulated rapid response in osteoblasts and chondrocytes	14
Figure 1.4: Mechanism of Wnt5a calcium-dependent pathway	20
Figure 3.1: Silencing Plaa in MC3T3-E1 cells	25
Figure 3.2: Subcellular localization of PLAA in growth zone chondrocytes and MC3T3-E1 osteoblasts	33
Figure 3.3: Effect of $1\alpha,25(\text{OH})_2\text{D}_3$ on plasma membrane localization of PLAA and Pdia3	35
Figure 3.4: Figure 3.4: Effect of PLAA blocking on $1\alpha,25(\text{OH})_2\text{D}_3$ membrane-mediated PKC activation in osteoblasts and chondrocytes	36
Figure 3.5: Effect of $1\alpha,25(\text{OH})_2\text{D}_3$ on PKC and PLA_2 activities and PGE_2 release in wild type and shPlaa MC3T3-E1 cells	38
Figure 3.6: Effect of $1\alpha,25(\text{OH})_2\text{D}_3$ on PLA_2 activity and PKC activity in wild type and silenced Pdia3 (shPdia3) and over-expressed Pdia3 (ovxPdia3) MC3T3-E1 cells	39
Figure 3.7: Western blot and confocal images of PLAA interaction studies	40
Figure 3.8: Western blot and confocal images of Pdia3 interaction studies	41
Figure 3.9: Proposed mechanism of $1\alpha,25(\text{OH})_2\text{D}_3$ stimulated rapid response in osteoblasts and chondrocytes	45
Figure 4.1: Effect of $1\alpha,25(\text{OH})_2\text{D}_3$ on CaMKII activation in growth zone chondrocytes and MC3T3-E1 osteoblasts	60
Figure 4.2: Effect of CaMKII inhibition on rapid $1\alpha,25(\text{OH})_2\text{D}_3$ membrane-mediated activation of CaMKII, PLA_2 , PKC and PGE_2 release and downstream physiological effects	62

Figure 4.3: Effect of $1\alpha,25(\text{OH})_2\text{D}_3$ on PLA_2 , PKC, CaMKII and alkaline phosphatase activities and PGE_2 and osteopontin production in wild type, shCamk2a and shCamk2b MC3T3-E1 cells	63
Figure 4.4: Effects of Pdia3 blocking, Pdia3, Vdr and Cav1 silencing and β -CD on $1\alpha,25(\text{OH})_2\text{D}_3$ -mediated rapid activation of CaMKII in MC3T3-E1 cells	65
Figure 4.5: Role of PLAA on rapid activation of CaMKII in MC3T3-E1 osteoblasts	67
Figure 4.6: Effects of Pdia3 and PLAA blocking and β -CD on $1\alpha,25(\text{OH})_2\text{D}_3$ -mediated rapid activation of CaMKII	68
Figure 4.7: Role of CaM on the rapid $1\alpha,25(\text{OH})_2\text{D}_3$ -mediated pathway and the downstream physiological effects	71
Figure 4.8: Proposed mechanism of $1\alpha,25(\text{OH})_2\text{D}_3$ stimulated rapid response in osteoblasts and chondrocytes	76
Figure 5.1: Effects of Wnt5a treatment on PKC, CaMKII, PLA_2 activations and PGE_2 release	90
Figure 5.2: Effects of Pdia3, Vdr and Cav1 silencing or blocking and β -CD on Wnt5a-mediated activation of PKC in MC3T3-E1 cells	91
Figure 5.3: Effects of CaM, CaMKII, PLAA and PLA_2 inhibition and Plaa, Camk2a and Camk2b silencing on Wnt5a-mediated activation of PKC in MC3T3-E1 cells	92
Figure 5.4: Effect of $1\alpha,25(\text{OH})_2\text{D}_3$ in Wnt5a-dependent PKC activation and effect of Wnt5a in $1\alpha,25(\text{OH})_2\text{D}_3$ regulation of PKC activity	94
Figure 5.5: Role of FZD2, FZD5 and ROR2 in $1\alpha,25(\text{OH})_2\text{D}_3$ -dependent PKC activation and their subcellular localization	95
Figure 5.6: Effect of $1\alpha,25(\text{OH})_2\text{D}_3$ treatment on interactions between $1\alpha,25(\text{OH})_2\text{D}_3$ receptor complex and Wnt5a receptors	97
Figure 5.7: Effect of Wnt5a treatment on interactions between $1\alpha,25(\text{OH})_2\text{D}_3$ receptor complex and Wnt5a receptors	99

LIST OF SYMBOLS AND ABBREVIATIONS

$1\alpha,25(\text{OH})_2\text{D}_3$	$1\alpha,25$ -dihydroxy vitamin D_3
α -MEM	Minimum essential medium alpha
AA	Arachidonic acid
BS^3	bis(sulfosuccinimidyl) substrate
CaM	Calmodulin
CaMKII	Calcium/calmodulin dependent protein kinase II
CaMKII- α	Calcium/calmodulin dependent protein kinase II alpha
Camk2a	Gene encoding CaMKII- α protein in mouse and rat
CaMKII- β	Calcium/calmodulin dependent protein kinase II beta
Camk2b	Gene encoding CaMKII- β protein in mouse and rat
Cav-1	Caveolin-1
Cav1	Gene encoding Cav-1 protein in mouse and rat
Cox-1	Cyclooxygenase-1
CREB	cAMP response element-binding protein
DMEM	Dulbecco's modified Eagle's medium
DR-3	Direct repeat 3
ELISA	Enzyme-linked immunosorbent assay
GAPDH	Glyceraldehyde 3-phosphate dehydrogenase
GC	Growth zone chondrocyte
FZD	Frizzled
FZD2	Frizzled homolog 2
FZD5	Frizzled homolog 5

LPL	Lysophospholipid
MAPK	Mitogen-activated protein kinase
MMP	Matrix metalloproteinase
mRNA	Messenger ribonucleotide acid
PCR	Polymerase chain reaction
Pdia3	Protein disulfide isomerase associated 3
Pdia3	Gene encoding Pdia3 protein in mouse and rat
PGE ₂	Prostaglandin E ₂
PKC	Protein kinase C
PLA ₂	Phospholipase A ₂
PLAA	Phospholipase A ₂ activating protein
Plaa	Gene encoding PLAA protein in mouse and rat
PLC	Phospholipase C
PTH	Parathyroid hormone
shCav-1	Silenced Cav1 MC3T3-E1 osteoblast
shCamk2a	Silenced Camk2a MC3T3-E1 osteoblast
shCamk2b	Silenced Camk2b MC3T3-E1 osteoblast
shPdia3	Silenced Pdia3 MC3T3-E1 osteoblast
shPlaa	Silenced Plaa MC3T3-E1 osteoblast
ROR2	Receptor tyrosine kinase-like orphan receptor 2
RXR	Retinoid X receptor
VDR	Vitamin D receptor
Vdr	Gene encoding VDR protein in mouse and rat

VDRE

Vitamin D responsive element

Wnt5a

Wingless-related MMTV integration site 5A

WT

Wild type

SUMMARY

The vitamin D metabolite 1,25-dihydroxyvitamin D₃ [1 α ,25(OH)₂D₃] plays an important role in the regulation of musculoskeletal growth and differentiation. 1 α ,25(OH)₂D₃ mediates its effects on cells, including chondrocytes and osteoblasts, through the classical nuclear 1 α ,25(OH)₂D₃ receptor. Additionally, recent evidence indicates that several cellular responses to 1 α ,25(OH)₂D₃ are mediated via a rapid, calcium-dependent membrane-mediated pathway. These actions of 1 α ,25(OH)₂D₃ can be blocked by antibodies to protein-disulfide isomerase family A, member 3 (Pdia3), indicating that it is part of the receptor complex; however, the pathway which is activated by this receptor is not fully understood. The overall goal of this thesis was to examine the roles of phospholipase A₂ activating protein and calcium calmodulin-dependent kinase II in 1 α ,25(OH)₂D₃ rapid membrane-mediated signaling. We further investigated the interaction between two pathways regulating growth plate cartilage and endochondral bone formation, 1 α ,25(OH)₂D₃ and Wnt5a, at the receptor complex level.

In the first study, evidence is provided that phospholipase A₂ (PLA₂) activating protein (PLAA) is required for 1 α ,25(OH)₂D₃ rapid membrane-mediated signaling. PLAA, Pdia3, and caveolin-1 (Cav-1) were detected in plasma membranes and caveolae of growth zone chondrocytes (GC) and MC3T3-E1 cells. Pdia3-immunoprecipitated samples were positive for PLAA only after 1 α ,25(OH)₂D₃ treatment. Cav-1 was detected when immunoprecipitated with anti-Pdia3 and anti-PLAA in both vehicle and 1 α ,25(OH)₂D₃ treated cells. These observations were confirmed by immunohistochemistry. 1 α ,25(OH)₂D₃ failed to activate PLA₂ and protein kinase C (PKC) or cause prostaglandin E₂ (PGE₂) release in PLAA-silenced cells. PLAA-antibody successfully blocked the PLAA protein and consequently suppressed PKC activity in

GC and MC3T3-E1 cells. Crosslinking studies confirmed the localization of PLAA on the extracellular face of the plasma membrane in untreated MC3T3-E1 cells. Taken together, our results suggest that PLAA is an important mediator of $1\alpha,25(\text{OH})_2\text{D}_3$ rapid membrane mediated signaling. $1\alpha,25(\text{OH})_2\text{D}_3$ likely causes conformational changes that bring Pdia3 into proximity with PLAA, and aiding in transducing the signal from caveolae to the plasma membrane.

In the second study, the roles of CaM and CaMKII as mediators of $1\alpha,25(\text{OH})_2\text{D}_3$ -stimulated PLAA-dependent activation of cPLA₂ and PKC α , and downstream biological effects. The results indicated that $1\alpha,25(\text{OH})_2\text{D}_3$ and PLAA-peptide increased CaMKII activity within 9 minutes. Silencing Cav1, Pdia3 or Plaa in osteoblasts suppressed CaMKII this effect. Similarly, antibodies against PLAA or Pdia3 blocked $1\alpha,25(\text{OH})_2\text{D}_3$ -dependent CaMKII. Caveolae disruption abolished activation of CaMKII by $1\alpha,25(\text{OH})_2\text{D}_3$ or PLAA. CaMKII-specific and CaM-specific inhibitors reduced cPLA₂ and PKC activities, PGE₂ release and osteoblast maturation markers in response to $1\alpha,25(\text{OH})_2\text{D}_3$. Camk2a-silenced but not Camk2b-silenced osteoblasts showed comparable effects. Immunoprecipitation showed increased interaction of CaM and PLAA in response to $1\alpha,25(\text{OH})_2\text{D}_3$. The results indicate that membrane actions of $1\alpha,25(\text{OH})_2\text{D}_3$ via Pdia3 triggered the interaction between PLAA and CaM, leading to dissociation of CaM from caveolae, activation of CaMKII, and downstream PLA₂ activation, and suggest that CaMKII plays a major role in membrane-mediated actions of $1\alpha,25(\text{OH})_2\text{D}_3$.

Wnt5a and $1\alpha,25(\text{OH})_2\text{D}_3$ are important regulators of endochondral bone formation. In osteoblasts and growth plate chondrocytes, $1\alpha,25(\text{OH})_2\text{D}_3$ initiates rapid effects via its membrane-associated receptor protein disulfide isomerase A3 (Pdia3) in caveolae, activating phospholipase A₂ (PLA₂)-activating protein (PLAA), calcium/calmodulin-dependent protein kinase II (CaMKII), and PLA₂, resulting in protein kinase C (PKC) activation. Wnt5a initiates its

calcium-dependent effects via release of intracellular calcium, activating PKC and CaMKII. We investigated the requirement for components of the Pdia3 receptor complex in Wnt5a calcium-dependent signaling. We determined that Wnt5a signals through a CaMKII/PLA₂/PGE₂/PKC cascade. Silencing or blocking Pdia3, PLAA, or vitamin D receptor (VDR), and inhibition of calmodulin (CaM), CaMKII, or PLA₂ inhibited Wnt5a-induced PKC activity. Wnt5a activated PKC in Caveolin-1-silenced cells, but methyl-beta-cyclodextrin reduced its stimulatory effect. 1 α ,25(OH)₂D₃ reduced Wnt5a-stimulated PKC. In contrast, Wnt5a had a biphasic effect on 1 α ,25(OH)₂D₃-stimulated PKC activation; 50ng/ml Wnt5a caused a 2-fold increase in 1 α ,25(OH)₂D₃-stimulated PKC but higher Wnt5a concentrations reduced 1 α ,25(OH)₂D₃-stimulated PKC activation. Western blots showed that Wnt receptors receptor tyrosine kinase-like orphan receptor 2 (ROR2), Frizzled2 (FZD2), and Frizzled5 (FZD5) localized to caveolae. Blocking ROR2, but not FZD2 or FZD5, abolished the stimulatory effects of 1 α ,25(OH)₂D₃ on PKC and CaMKII. 1 α ,25(OH)₂D₃ membrane receptor complex components (Pdia3, PLAA, Caveolin-1, CaM) interacted with Wnt5a receptors/co-receptors (ROR2, FZD2, FZD5) in immunoprecipitation studies, interactions that changed with either 1 α ,25(OH)₂D₃ or Wnt5a treatment. This study demonstrates that 1 α ,25(OH)₂D₃ and Wnt5a mediate their effects via similar receptor components and suggests that these pathways may interact.

CHAPTER 1

SPECIFIC AIMS

The vitamin D metabolite 1,25-dihydroxyvitamin D₃ [1 α ,25(OH)₂D₃] plays an important role in controlling calcium homeostasis, regulating normal development of the cartilaginous growth plate and modulating bone formation (1-5). 1 α ,25(OH)₂D₃ regulates chondrocytes and osteoblasts via two different mechanisms: the classical pathway that is vitamin D receptor (VDR) mediated, and rapid membrane-initiated signaling (6-8). Growth zone chondrocytes isolated from the rat costochondral growth plate and MC3T3-E1 osteoblasts respond to 1 α ,25(OH)₂D₃ with a rapid increase in protein kinase C alpha (PKC α) activity (9,10). Although various signaling proteins have been implicated in 1 α ,25(OH)₂D₃-mediated membrane signaling, some pivotal signaling molecules involved in this pathway have yet to be determined. We have previously shown that direct activation of phospholipase A₂ mimics the effects of 1 α ,25(OH)₂D₃ treatment on growth zone chondrocytes and MC3T3-E1 osteoblasts (10,11). Recent studies have also demonstrated that activation of calcium calmodulin-dependent kinase II is required for the actions of phospholipase A₂. Based on these data, we hypothesize that phospholipase A₂ activating protein (PLAA) and calcium calmodulin-dependent kinase II (CaMKII) are required for 1 α ,25(OH)₂D₃ rapid membrane-mediated signaling. Previous works from our lab have shown that 1 α ,25(OH)₂D₃ and Wnt5a are important regulators of osteoblast maturation. They are also known to mediate their actions via calcium-dependent pathways. In this study, we will examine the requirement for protein disulfide isomerase 3 (Pdia3) receptor complex in Wnt5a pathway. We hypothesize that signaling components of 1 α ,25(OH)₂D₃ receptor complex are required for calcium-dependent actions of Wnt5a.

The overall objective of this project was to determine the roles of Pdia3/PLAA receptor complex and CaMKII in $1\alpha,25(\text{OH})_2\text{D}_3$ and Wnt5a membrane-mediated signaling pathways in chondrocytes and osteoblasts. The overall objective was addressed through the following specific aims.

Specific Aim 1: Determine the role of phospholipase A₂ activating protein in $1\alpha,25(\text{OH})_2\text{D}_3$ rapid membrane-mediated pathway.

Caveolae and Cav-1 are required for rapid $1\alpha,25(\text{OH})_2\text{D}_3$ -dependent PKC signaling, and Pdia3 is co-localized with Cav-1 in plasma membranes and lipid rafts (12-14). However, it is not clear whether PLAA is present in caveolae and if it interacts with Cav-1 and Pdia3 receptor complex in the presence of $1\alpha,25(\text{OH})_2\text{D}_3$. Previous studies demonstrated that $1\alpha,25(\text{OH})_2\text{D}_3$ treatment for 9 minutes increases PLA₂ and PKC activities and PGE₂ release in GC chondrocytes and MC3T3-E1 osteoblasts (9,15,16). Also, past studies using a 21 amino acid PLAA peptide as the activator of PLA₂ have shown that this peptide mimics the effects of $1\alpha,25(\text{OH})_2\text{D}_3$ on growth zone chondrocytes and MC3T3-E1 osteoblasts (10,11). Based on these data, if PLAA plays a critical role in $1\alpha,25(\text{OH})_2\text{D}_3$ membrane-mediated signaling, then silencing PLAA should decrease the levels of activities of PLA₂, PKC and release of PGE₂ in response to $1\alpha,25(\text{OH})_2\text{D}_3$. The *hypothesis* was that phospholipase A₂ activating protein is required to mediate $1\alpha,25(\text{OH})_2\text{D}_3$ rapid membrane-mediated signaling. Subcellular localization of PLAA under different treatments was determined, the influence of $1\alpha,25(\text{OH})_2\text{D}_3$ on interactions between PLAA, Pdia3, and Cav-1 was tested using immunoprecipitation and immunostaining, and the effect of PLAA knockdown on rapid actions of $1\alpha,25(\text{OH})_2\text{D}_3$ was studied in MC3T3-E1 osteoblasts.

Specific Aim 2: Determine the role of calcium calmodulin-dependent kinase II in $1\alpha,25(\text{OH})_2\text{D}_3$ rapid membrane-mediated pathway.

Treatment of MC3T3-E1 cells with $1\alpha,25(\text{OH})_2\text{D}_3$ activates CaMK, which subsequently results in phosphorylation of CREB (17). Recently, it has been reported that MC3T3-E1 osteoblasts possess all CaMK isoforms. Specifically, it has been reported in vascular smooth muscle cells that transient silencing of CaMKII- α abolishes norepinephrine-induced increases in arachidonic acid (18). However, the role of CaMKII in $1\alpha,25(\text{OH})_2\text{D}_3$ -dependent membrane-mediated signaling is unclear. It is important to elucidate the role of CaM KII in osteoblasts in response to $1\alpha,25(\text{OH})_2\text{D}_3$. The *hypothesis* was that calcium calmodulin-dependent kinase II is required for $1\alpha,25(\text{OH})_2\text{D}_3$ -stimulated rapid activation of phospholipase A₂. The activation of CaMKII under different treatments was quantified, the effect of $1\alpha,25(\text{OH})_2\text{D}_3$ receptor complex knockdown was investigated, and the specific roles of two CaMKII isoforms were evaluated in $1\alpha,25(\text{OH})_2\text{D}_3$ membrane-mediated signaling.

Specific Aim 3: Determine the requirement for $1\alpha,25(\text{OH})_2\text{D}_3$ receptor signaling components in Wnt5a calcium-dependent signaling.

Wnt5a and $1\alpha,25(\text{OH})_2\text{D}_3$ are important regulators of growth plate cartilage and endochondral bone formation. *In vitro* studies have demonstrated that Wnt5a promotes osteoblast maturation (19,20) and osteoblasts isolated from Wnt5a^{-/-} mice exhibit down-regulation of osteoblastic differentiation markers compared to the wild type (21). Wnt5a calcium-dependent signaling involves activation of heterotrimeric G proteins, PLC, PKC, CaMKII, and the phosphatase calcineurin, (22-26) which are also used by the $1\alpha,25(\text{OH})_2\text{D}_3$ rapid membrane-mediated pathway. However, the requirement for $1\alpha,25(\text{OH})_2\text{D}_3$ membrane-associated receptor

complex have not been elucidated in Wnt5a pathway. The *hypothesis* was that signaling components of $1\alpha,25(\text{OH})_2\text{D}_3$ receptor complex are required for calcium-dependent actions of Wnt5a. The activation of PKC, CaMKII, PLA₂ and PGE₂ release with Wnt5a treatment was quantified in chondrocytes and osteoblasts, the effects of knockdown or inhibition of $1\alpha,25(\text{OH})_2\text{D}_3$ receptor signaling components on Wnt5a pathway was investigated, and the impacts of $1\alpha,25(\text{OH})_2\text{D}_3$ and Wnt5a on interactions between receptor components was tested using immunoprecipitation.

The outcomes of this study were expected to show that Pdia3/PLAA receptor complex and CaMKII are necessary for Wnt5a and $1\alpha,25(\text{OH})_2\text{D}_3$ membrane-mediated pathways. The research was significant because it provided greater insight into mechanisms underlying $1\alpha,25(\text{OH})_2\text{D}_3$ and Wnt5a calcium-dependent signaling which holds great promise to identify mechanisms of diseases associated with aberrations in these signaling pathways and will promote the development of novel therapeutic targets.

CHAPTER 2

BACKGROUND AND LITERATURE REVIEW

VITAMIN D METABOLISM

Photochemical synthesis of vitamin D₃ (cholecalciferol) occurs in the epidermis and dermis of humans when ultraviolet B radiation (UVB) of sunlight is absorbed by a precursor molecule, 7-dehydrocholesterol (27). Vitamin D₃ acquired from isomerization of 7-dehydrocholesterol or intestinal absorption of dietary sources such as egg yolk, fish liver oil, sun-dried mushrooms or fortified food (28), binds to vitamin D binding protein (DBP) in the blood. Decreased sun exposure reduces vitamin D₃ synthesis. In the liver, vitamin D₃ is hydroxylated by 25-hydroxylase (25-OHase; encoded by *CYP27A1*) to 25-hydroxyvitamin D₃ [25(OH)D₃] (29), which is then converted to 1 α ,25-dihydroxyvitamin D₃ [1 α ,25(OH)₂D₃] by 1 α -hydroxylase (1 α -OHase; encoded by *CYP27B1*) in the kidney or other tissues expressing 1 α -hydroxylase (15,28,30-33). Moreover, 24-hydroxylase (encoded by *CYP24A1*) activity in kidneys converts 25(OH)D₃ to 24R,25(OH)₂D₃ (34). The active secosteroid 1 α ,25(OH)₂D₃ (calcitriol) has different effects on diverse target tissues, and regulates cell proliferation, differentiation and apoptosis (35,36). The 1 α ,25(OH)₂D₃ biosynthesis process is highly regulated via mechanisms involving feedback regulation of its synthesis and catabolism by 24-hydroxylase. Furthermore, this process is one of the key endocrine systems controlling plasma concentration of calcium and phosphorus (37). The major role of 1 α ,25(OH)₂D₃ is to preserve calcium and phosphorus homeostasis in vertebrates (38). In bone, 1 α ,25(OH)₂D₃ regulates the formation of osteoid matrix and mineralization (39). Additionally, 1 α ,25(OH)₂D₃ has been reported to regulate immune system (40-43) and cardiovascular functions (44,45). Low levels of vitamin D₃ cause rickets in children

and exacerbate osteoporosis and fractures in adults. In addition, Vitamin D₃ plays an important role in reducing risk of heart disease, multiple sclerosis, and cancer (46-49).

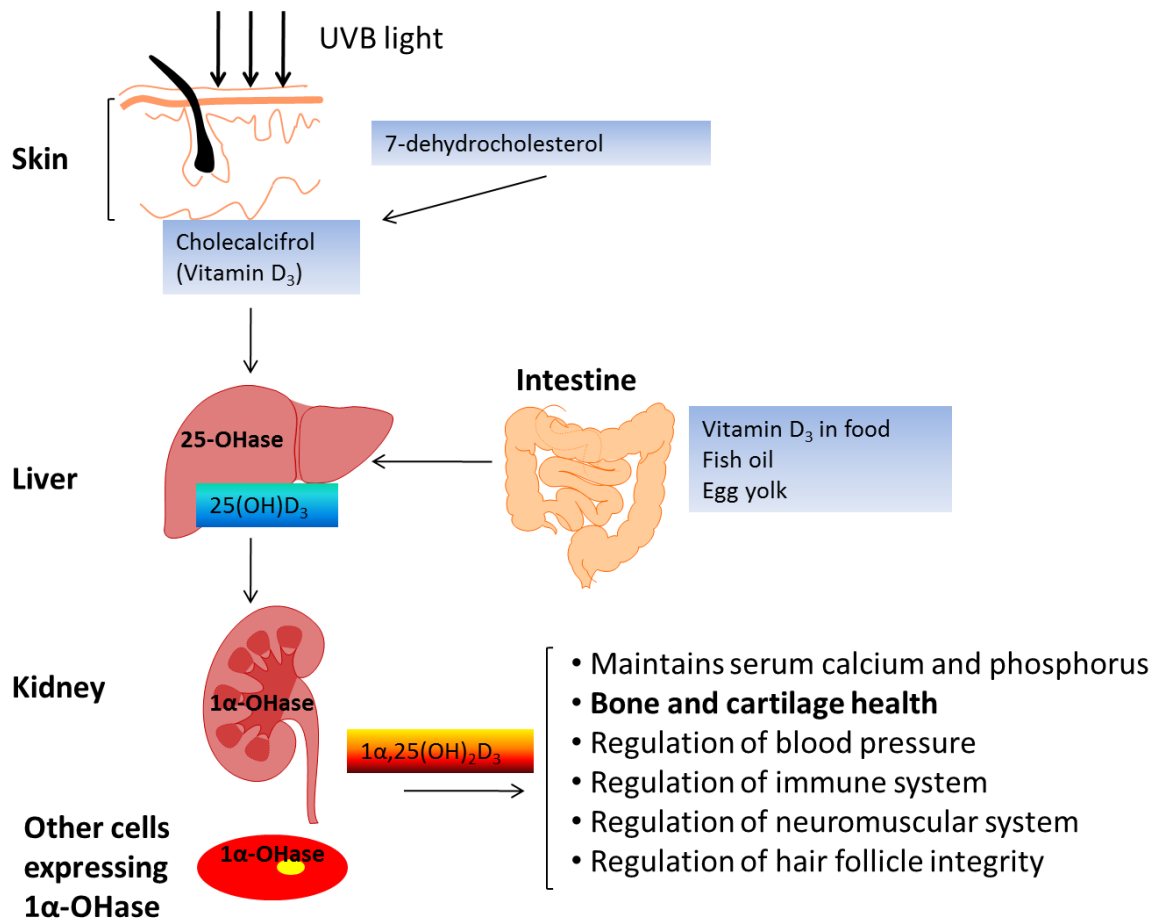


Figure 1.1: 1α,25(OH)₂D₃ Biosynthesis. The process of biosynthesis of 1α,25(OH)₂D₃ from its precursor, 7-dehydrocholesterol, is a multistep procedure involving the actions of ultraviolet irradiation, 25-hydroxylase and 1α-hydroxylase.

THE ROLE OF VITAMIN D IN PHYSIOLOGY AND DISEASE

Bone

Vitamin D is an important regulator of intestinal absorption of calcium (50). When the body needs calcium, intestinal calcium absorption increases, which activates parathyroid hormone (PTH) secretion, which in turn stimulates 1α,25(OH)₂D₃ biosynthesis (51). The increase

in $1\alpha,25(\text{OH})_2\text{D}_3$ levels triggers intestinal calcium absorption. However, if the body has been deprived of calcium, despite the activation of intestinal absorption of calcium, the described mechanism is unable to bring calcium in. In this scenario, highly elevated levels of PTH and $1\alpha,25(\text{OH})_2\text{D}_3$ mobilize calcium from bones, that, together with an increased renal reabsorption of calcium, raise plasma levels of calcium (37). Therefore, calcium homeostasis is maintained in the body at the expense of skeleton. If the latter mechanism persists due to insufficient calcium intake or aberrations in intestinal calcium absorption pathways, calcium homeostasis becomes dependent on skeletal calcium until its reduced mass alarms a serious structural problem. Such conditions result in fractures and osteoporosis.

Furthermore, case studies of postmenopausal women have indicated that the absence of estrogen causes development of structural disorders similar to that of blood calcium absorption from the skeleton. This condition suppresses PTH release and subsequently reduces synthesis of vitamin D (37). Moreover, the reduction in $1\alpha,25(\text{OH})_2\text{D}_3$ and PTH levels suppresses bone remodeling, a highly important process responsible for bone resorption and formation and is necessary to maintain healthy bone structures. Therefore, suppression of $1\alpha,25(\text{OH})_2\text{D}_3$ biosynthesis plays an important role in initiating onset of skeletal disorders in women following menopause. Daily supplementation of vitamin D to these patients have proven to increase calcium absorption, increase trabecular bone volume and reduce fracture rate (52). These findings indicate the role of $1\alpha,25(\text{OH})_2\text{D}_3$ as a potential therapeutic candidate for postmenopausal osteoporosis. It is also important to note that vitamin D supplements co-administered without calcium have not proven to prevent fractures (53).

Vitamin D-mediated signaling regulates mechanisms involved in osteoblast biology, function and differentiation. Osteoblasts are known to respond to a selection of resorptive

signals, including $1\alpha,25(\text{OH})_2\text{D}_3$ and parathyroid hormone (PTH), by secreting receptor activator of NF- κ B ligand (RANKL) (54). RANKL is a member of tumor necrosis family (TNF) superfamily, and is an essential regulator of osteoclastogenesis (55,56). It mediates its effects via binding its receptor, RANK, stimulating a range of signaling pathways such as mitogen activated protein kinase (MAP), Src, phosphatidylinositol 3-kinase (PI3K)/AK and IKK/I κ B/ NF- κ B. Downstream from activation of these pathways, important transcription factors including c-fos and NF- κ B are activated, which in turn induce osteoclastic differentiation of hematopoietic progenitor cells (54). The promoter region of the *RANKL* gene contains a functional vitamin D responsive element (VDRE) through which its transcription is regulated by $1\alpha,25(\text{OH})_2\text{D}_3$ (57-59). Osteoprotegerin (OPG) is a member of tumor necrosis family (TNF) superfamily, and it serves as an inhibitor of osteoclastogenesis (60). This protein acts as a soluble decoy receptor for RANKL, which inhibits the interaction of RANKL with its RANK receptor. Osteoblasts secrete OPG and $1\alpha,25(\text{OH})_2\text{D}_3$ has been reported to regulate osteoprotegerin gene expression (60-62).

Roles of $1\alpha,25(\text{OH})_2\text{D}_3$ in differentiation and maturation of osteoblasts in tissue culture has been extensively studied over the past two decades. $1\alpha,25(\text{OH})_2\text{D}_3$ regulates the expression of osteoblast phenotypic markers. $1\alpha,25(\text{OH})_2\text{D}_3$ stimulates osteocalcin and osteopontin production and increases mineralized nodule formation in osteoblasts (63,64). Genetic approaches, in which the *CYP27B1* gene was knocked out to investigate bone formation in mice lacking the ability to synthesize $1\alpha,25(\text{OH})_2\text{D}_3$, have shown that knockout animals develop osteopenia, reduced bone size, hyperparathyroidism and hypocalcemia. Similar to results obtained from *CYP27B1*^{-/-} animals, VDR-deficient (VDR^{-/-}) and double knockout mice (VDR^{-/-} x *CYP27B1*^{-/-}) develop comparable phenotypes.

Cartilage

Cartilage is a dense non-vascular tissue produced by chondrocytes. Cartilaginous tissue is composed of a specialized extracellular matrix, which is primarily type II collagen and proteoglycans. Proteoglycans of a mature tissue consist of a core protein and highly sulfated glycosaminoglycan side chains, which result in a hydration state that can resist compressive loads. Cartilaginous tissue is found in the ear, nose, trachea, xyphoid, fracture callus growth plate of long bones, mandibular condyle and costochondral joints.

Growth of endochondral bone encompasses a series of events including proliferation, changes in cell morphology and expression of markers specific for chondrocytes and osteoblasts. In the growth plate, resting zone chondrocytes form clusters of rounded and randomly arranged chondrocytes residing at the ends of long bones. Resting zone chondrocytes mature into rapidly dividing chondrocytes in the proliferative zone, organizing themselves in columns parallel to the long axis of bone (65). Failure of these cells to thrive results in termination of growth at the end of long bones. As chondrocytes mature, proliferative cells undergo cell cycle arrest and increase in size, forming the prehypertrophic and hypertrophic zones of the growth plate which referred to as growth zone chondrocytes (GC) (65). Subsequently, the cartilage matrix calcifies and gives rise to the zone of ossification (65). Regulation and maintenance of these events are important for proper formation and function of the growth plate.

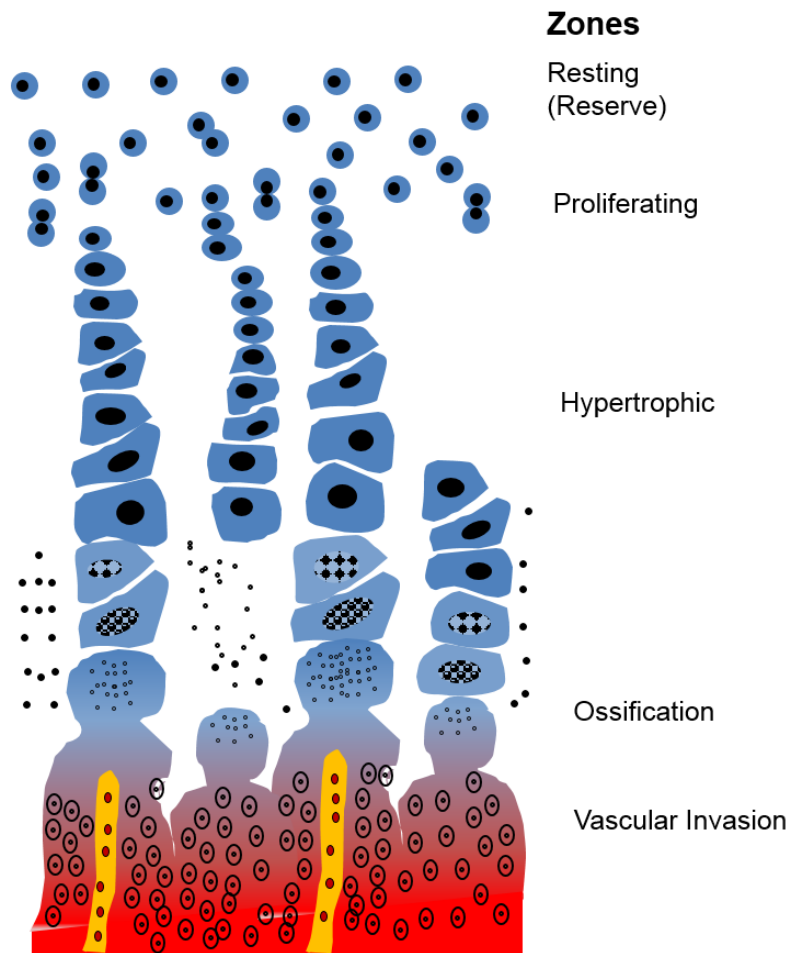


Figure 1.2: The Growth Plate. The growth plate is divided into four zones: the resting (reserve) zone, the proliferating zone, the hypertrophic zone and the zone of provisional calcification. The resting zone is the germinal layer of the growth plate. In the proliferative zone, chondrocytes assume a flattened morphology and begin to divide and organize themselves into columns. The hypertrophic zone is the layer in which chondrocytes begin to terminally differentiate and become enlarged, leading to cell death. Zone of provisional calcification is the area where with the death of chondrocytes and increase in alkaline phosphatase activity, chondrocyte columns become calcified. Matrix calcification is required for subsequent invasion by blood vessels.

Previous reports by our lab and other groups have found that a complex network of interacting signaling pathways induced by hormones and growth factors appear to regulate the behavior of growth plate chondrocytes and endochondral bone ossification (19,66-68). Among these factors, vitamin D metabolites have been shown to play an important role in the regulation

of growth plate chondrocytes. In the absence of $1\alpha,25(\text{OH})_2\text{D}_3$ or in mammals that lack the ability to respond to this metabolite, the hypertrophic zone is enlarged and extracellular matrix of cartilage fails to calcify, which in turn results in a condition called rickets (69,70). The symptoms of this disorder include bone pain or tenderness, dental deformities, impaired growth, increased bone fractures and skeletal deformities (bowlegs and asymmetrical skull) (71). Crystallographic studies of rachitic bones indicate that their mineral crystals are less mature than those of non-rachitic control bones (72). This condition can be treated by restoring systemic levels of $1\alpha,25(\text{OH})_2\text{D}_3$ by supplementing patients with vitamin D_3 in co-administration with calcium. Mouse models that lack functional vitamin D receptor also exhibit rachitic growth plates (73,74). This condition can be treated by restoring serum calcium concentration.

Several studies have found that $1\alpha,25(\text{OH})_2\text{D}_3$ is an important regulator of chondrocyte hypertrophy (75-78). In the growth plate, $1\alpha,25(\text{OH})_2\text{D}_3$ inhibits proliferation and induces terminal differentiation and apoptosis. It also activates matrix metalloproteinases (MMPs), such as stromelysin-1 (MMP-3) and 72-kD gelatinase (MMP-2) (79,80). Additionally, recent studies have found that the primary role of $24\text{R},25(\text{OH})_2\text{D}_3$ is to maintain the pool of chondrocytes in the resting zone region of the growth plate by promoting cell survival (80-82). $24\text{R},25(\text{OH})_2\text{D}_3$ stimulates production of sulfated glycosaminoglycans and reduces MMP activities (80).

MOLECULAR MECHANISM OF ACTIONS

A. VDR-MEDIATED GENE EXPRESSION

Once $1\alpha,25(\text{OH})_2\text{D}_3$ is inside the target cell, it binds to vitamin D receptor (VDR). The association of $1\alpha,25(\text{OH})_2\text{D}_3$ with VDR promotes its heterodimerization with retinoid X receptor (RXR). $1\alpha,25(\text{OH})_2\text{D}_3$ binding enhances the association of VDR to vitamin D response elements

(VDRE) in the promoter region of target genes. VDREs consist of two direct hexameric repeats with a three-nucleotide spacer; referred to as direct repeat 3 (DR-3) elements. The binding affinity of VDR-DR-3 is weaker than that of VDR/RXR-DR-3. $1\alpha,25(\text{OH})_2\text{D}_3$ binding with VDR promotes the high affinity binding of VDR/RXR to the DR-3 region of VDRE. VDR occupies the proximal (3' half-site) and RXR occupies the distal (5' half site) sites of DR-3 (83). Ultimately, this interaction assures target gene selectivity of the $1\alpha,25(\text{OH})_2\text{D}_3$ /VDR/RXR complex, and consequently influences the rate of RNA polymerase II-mediated transcription.

B. RAPID ACTIONS OF $1\alpha,25(\text{OH})_2\text{D}_3$

Models for Studying Rapid Actions

Over the past two decades, the rat costochondral chondrocyte culture system has been used in our lab to study the membrane-mediated actions of $1\alpha,25(\text{OH})_2\text{D}_3$ and $24\text{R},25(\text{OH})_2\text{D}_3$. This powerful model encompasses both resting zone chondrocytes and growth zone chondrocytes (upper hypertrophic and hypertrophic). Previously, our lab demonstrated that growth zone chondrocytes express both the classical vitamin D receptor (VDR) and the plasma membrane associated receptor, protein disulfide isomerase family A (Pdia3; aka 1,25-MARS, ERp60, ERp57 and Grp58) (15,84,85). The mouse MC3T3-E1 subclone 4 line, originally isolated from the fetal mouse calvaria, exhibits high levels of osteoblast differentiation after growth in media supplemented with ascorbic acid. This subclone expresses osteoblast markers such as osteocalcin and bone sialoprotein (86), as well as VDR and Pdia3 (10,87). This cell line is a powerful model for studying the effects of $1\alpha,25(\text{OH})_2\text{D}_3$ membrane-mediated response on *in vitro* osteoblast differentiation.

Membrane-mediated Signaling by $1\alpha,25(\text{OH})_2\text{D}_3$

Rat costochondral cartilage growth plate chondrocytes and MC3T3-E1 osteoblasts respond to $1\alpha,25(\text{OH})_2\text{D}_3$ with a rapid increase in protein kinase C alpha (PKC α) activity (9,10). This rapid response is specific to the $1\alpha,25(\text{OH})_2\text{D}_3$ stereoisomer; $1\beta,25(\text{OH})_2\text{D}_3$ fails to stimulate PKC-dependent signaling, indicating a receptor-mediated mechanism (88). In growth zone chondrocytes, $1\alpha,25(\text{OH})_2\text{D}_3$ causes a rapid increase in phospholipase A₂ (PLA₂) and phosphatidylinositol-specific phospholipase C beta (PLC β) (11,89). PLA₂ action generates arachidonic acid (AA) and lysophospholipid (LPL) (89). AA can increase PKC α activity directly (90). Alternatively, AA may be metabolized further into PGE₂ via constitutive cyclooxygenase-1 (Cox-1), which acts via its EP1 receptor to increase cyclic AMP (91). Phosphatidylinositol-specific PLC β is activated via G α_q and lysophospholipid, generating diacylglycerol (DAG) and inositol 1,4,5-trisphosphate (IP3) (89,92). DAG binds PKC α and triggers its recruitment to the plasma membrane (93). IP3 activates the release of Calcium ions from the endoplasmic reticulum, required for PKC α activation. These actions of $1\alpha,25(\text{OH})_2\text{D}_3$ can be blocked by antibodies to protein-disulfide isomerase family A, member 3 (Pdia3, also known as ERp60, ERp57, Grp58, and 1,25-MARRS), indicating that it is part of the receptor complex.

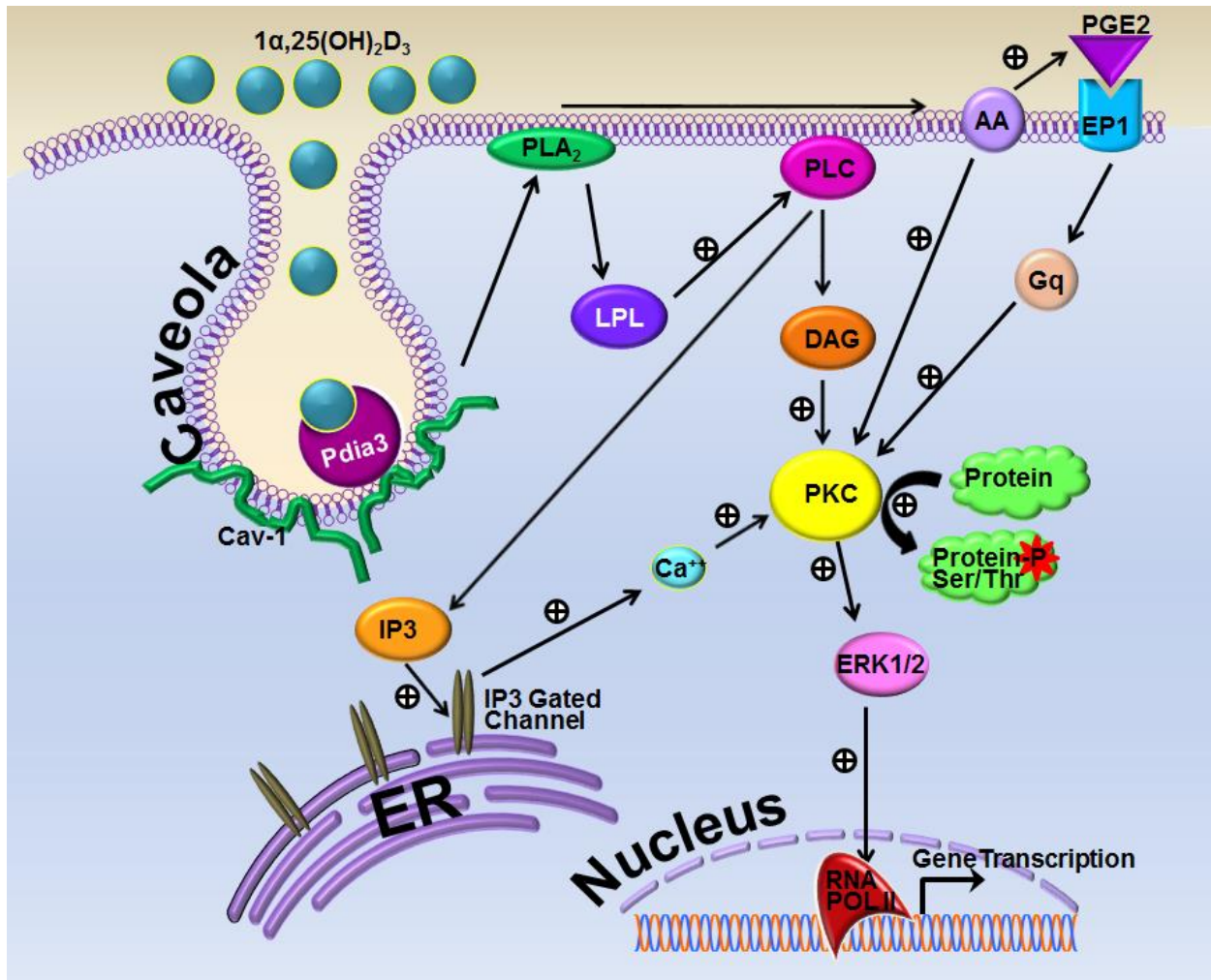


Figure 1.3: Proposed mechanism of $1\alpha,25(\text{OH})_2\text{D}_3$ stimulated rapid response in osteoblasts and chondrocytes. $1\alpha,25(\text{OH})_2\text{D}_3$ binds its membrane associated receptor, Pdia3, in caveolae. This binding stimulates phospholipase C (PLC), resulting in diacylglycerol (DAG)-mediated activation of protein kinase C (PKC). Additionally, $1\alpha,25(\text{OH})_2\text{D}_3$ activates phospholipase A₂ (PLA₂), leading to release of arachidonic acid (AA) and prostaglandin E₂ (PGE₂) production. PGE₂ binds its membrane-associated receptor, EP1, and positively regulates PKC activation. Together, these actions result in activation of mitogen activated protein kinase (MAPK) to induce differentiation and maturation of osteoblasts and chondrocytes.

Phospholipase A₂

PLA₂ designates a superfamily of diverse intracellular and secreted enzymes that catalyze the hydrolysis of sn-2 ester of glycerophospholipid, resulting in production of a free fatty acid and lysophospholipid. The products of their enzymatic activity have been implicated in a number

of physiological responses, including signal transduction processes, lipid metabolism, and host defense (94-96). PLA₂ isoforms are divided into three classes based on their structure, subcellular localization, or function: 1- large, cytosolic PLA₂ (cPLA₂) 2- calcium-independent PLA₂ (iPLA₂) and 3- small, secreted PLA₂ (sPLA₂) (96). Proper regulation of PLA₂ is crucial to control the levels of lipid metabolism. Multiple studies have demonstrated the pivotal role PLA₂ plays in calcium-dependent signaling pathways, including 1 α ,25(OH)₂D₃-dependent membrane-mediated signaling (11,97-100) and estrogen-dependent rapid signaling (101). Stimulation of PLA₂ activity using agents such as bee venom melittin and snake venom mastoparan mimics the effects of 1 α ,25(OH)₂D₃ on PKC in growth zone chondrocytes. Conversely, inhibition of PLA₂ activity using agents such as AACOCF₃, OEPC, and quinacrine abolishes the stimulatory effect of 1 α ,25(OH)₂D₃ (10,89). Importantly, in growth plate chondrocytes, PLA₂ activation is upstream of PLC β , and AA is released within 15 seconds following treatment, suggesting that PLA₂ is coupled to Pdia3.

Phospholipase A₂ Activating Protein

Human phospholipase A₂ activating protein (PLAA) has a region of 38% homology with melittin (102), and it also exhibits homology with the G-protein beta subunit, suggesting that it is membrane-associated (103). PLAA mRNA is expressed in growth plate chondrocytes *in vivo* and in chondrocytes isolated from the growth zone of rat costochondral growth plates *in vitro* (11). Previous studies using a 21 amino acid PLAA peptide as the activator of PLA₂ have demonstrated that this peptide mimics the effects of 1 α ,25(OH)₂D₃ on growth zone chondrocytes and MC3T3-E1 osteoblasts (10,11). PLA₂ inhibitors such as quinacrine and AACOCF₃ blocked the effect of PLAA peptide on PLA₂ and PKC, suggesting that the full-length protein acts

upstream of PLA₂ (11). This supports the hypothesis that PLAA links the Pdia3 receptor complex with PLA₂.

Caveolae

Caveolae (Latin for little caves; singular: caveola), a subset of lipid rafts, are 50-100 nm plasma membrane invaginations that are highly enriched with cholesterol and glycosphingolipids (104-106). Sphingolipids interact with each other through their polar head groups and cholesterol molecules are inserted between the associated sphingolipids (105,106). These regions of the plasma membrane are characterized by the presence of coat proteins called caveolins (Cav-1, Cav-2, and Cav-3; with molecular masses between 18-22 kD) and serve as signaling platforms (107-113). The lipid composition of caveolae provides a relative insolubility in cold non-ionic detergents, a biophysical property used to isolate these plasma membrane domains (114-117). However, detergent-based methods have been shown to alter the molecular composition of caveolae, thus a detergent-free method is used to isolate caveolae (118-120). Several steroid hormone receptors, including estrogen receptors α and β , androgen receptors, and vitamin D receptor (VDR) have been identified in caveolae (121-124). Cav-1 is expressed in most cell types, including growth zone chondrocytes, MC3T3-E1 osteoblasts, adipocytes, endothelial cells, fibroblasts, smooth muscle cells and epithelial cells (12,108,125-130). Cav-2 and Cav-3 have been reported to form caveolae invaginations; however, Cav-2 does not play an essential role in this process (131,132). We previously showed that intact caveolae and Cav-1 are required for rapid $1\alpha,25(\text{OH})_2\text{D}_3$ -dependent PKC signaling, and Pdia3 is co-localized with Cav-1 in plasma membranes and in lipid rafts (12-14). Mice lacking functional Cav-1 exhibit a longer costochondral growth plate, and the number of columns of chondrocytes in the hypertrophic zone is greater than that of wild type (12). Caveolae domains of the plasma membrane play an

important role in regulation of signaling pathways. Changes in caveolae function lead to severe conditions, including prion disease and cancer (133-135).

Calcium/calmodulin-dependent Protein Kinase II

Calmodulin (CaM) is a calcium binding protein that mediates many of the cellular effects of calcium. (136). CaM is expressed in all eukaryotes and it is found in various subcellular locations such as cytoplasm, plasma membrane and organelle membranes (136). Many of the downstream targets of CaM, such as calcium calmodulin kinase II (CaMKII), protein phosphatases, nitric oxide synthase and calcium pumps, are unable to bind to calcium themselves; therefore, CaM serves as a calcium sensor and signal transducer for these proteins. CaM activates CaMKII by displacement of its auto-inhibitory domains (136). CaMKII belongs to the family of serine/threonine kinases. It is activated in response to calcium signals, phosphorylating several downstream proteins (137). To date, over 30 isoforms of CaMKII have been identified. The molecular mass of these isoforms ranges from 52 to 83 KDa. These isoforms are the results of alternative messenger RNA splicing of four *Camk2* genes, known as *Camk2a*, *Camk2b*, *Camk2d*, and *Camk2g* (138,139). It has also been reported that MC3T3-E1 osteoblasts possess all CaMK types (CaMKI, CaMKII, and CaMKIV), and treating these cells with $1\alpha,25(\text{OH})_2\text{D}_3$ activates CaMK. which subsequently results in phosphorylation of cAMP response element-binding protein (CREB) and eventually regulation of osteoprotegerin (*OPG*) expression (17). Parallel to these studies, another group has reported that CaMKII- α regulates the CREB/activating transcription factors (ATF) and ERK signaling pathways in osteoblasts (140). However, the role of CaMKII in $1\alpha,25(\text{OH})_2\text{D}_3$ -dependent membrane-mediated signaling in osteoblasts and chondrocytes is unclear.

WNT SIGNALING AND FUNCTION

Wnts constitute a large family of cysteine-rich secreted glycoproteins that regulate a wide range of developmental and physiological processes (141). Currently, at least 19 members of the Wnt superfamily have been identified in humans and mice, with each member exhibiting a unique expression pattern and distinct function during development. Wnts regulate cellular functions, including proliferation, differentiation, survival, migration and polarity, by stimulating a group of signal transduction pathways (142-144). These signaling proteins act through three different pathways: the canonical Wnt/ β -catenin pathway (145); the Wnt calcium-dependent pathway (26); and the planar cell polarity pathway involving jun N-terminal kinase (JNK) (146-148). Several members of Wnt superfamily, Wnt5a, Wnt5b and Wnt-11, which activate the non-canonical calcium-dependent pathway, are expressed by growth plate chondrocytes (149).

Wnt5a is one of the most extensively studied members of the Wnt superfamily. Genome sequence analysis has identified Wnt5a as an evolutionary conserved protein (150,151). Wnt5a palmitoylation is necessary for its binding to frizzled 5 (FZD5) receptor, while its glycosylation has been shown to be essential for its secretion (152). Wnt5a is expressed in growth zone chondrocytes (149) and plays an important role in chondrocyte transition between different zones of the growth plate. Animals lacking functional Wnt5a exhibit a significant delay in chondrocyte hypertrophy and skeletal ossification compared to the wild type (153), suggesting that Wnt5a plays a critical role in skeletal growth and development.

Wnts mediate their effects via a wide range of receptors. Thus far, 10 frizzled receptors have been identified for Wnts. Frizzled proteins belong to the seven-pass transmembrane class of receptors carrying a cysteine-rich domain (CRD) in their extracellular region, which serves as their Wnt binding domain (154). In mammalian models, Wnt5a mediates its calcium-dependent

signaling via frizzled-2 (FZD2) and frizzled-5 (FZD5) (155,156). In addition to frizzled proteins, receptor tyrosine kinase-like orphan receptor 2 (ROR2) serves as a co-receptor to mediate the actions of Wnt5a. ROR2 is a single-pass transmembrane protein with a cysteine-rich domain in its extracellular region, which has been implicated in Wnt binding (157,158). ROR2 is expressed by chondrocytes of the growth plate, and ROR2^{-/-} mice display a delayed hypertrophic region in their growth plate (159). Animals lacking functional ROR2 display skeletal abnormalities including shortened limbs and tails, facial deformities and dwarfism, suggesting that ROR2 plays a critical role in skeletal growth and development (159,160).

Wnt5a has been shown to regulate the calcium signaling pathway (161-163). Wnt5a mutant zebrafish exhibit a reduction in frequencies of calcium fluxes, whereas overexpression of Wnt5a or FZD2 increases frequencies of calcium transients in the enveloping layers (164). Wnt5a induces a rapid activation of phospholipase C (PLC) and release of intracellular calcium. This increase in intracellular calcium concentration activates calcium sensitive enzymes such as PKC, CaMKII, and calcineurin, and subsequently leads to activation of NFAT transcription factor (22-26).

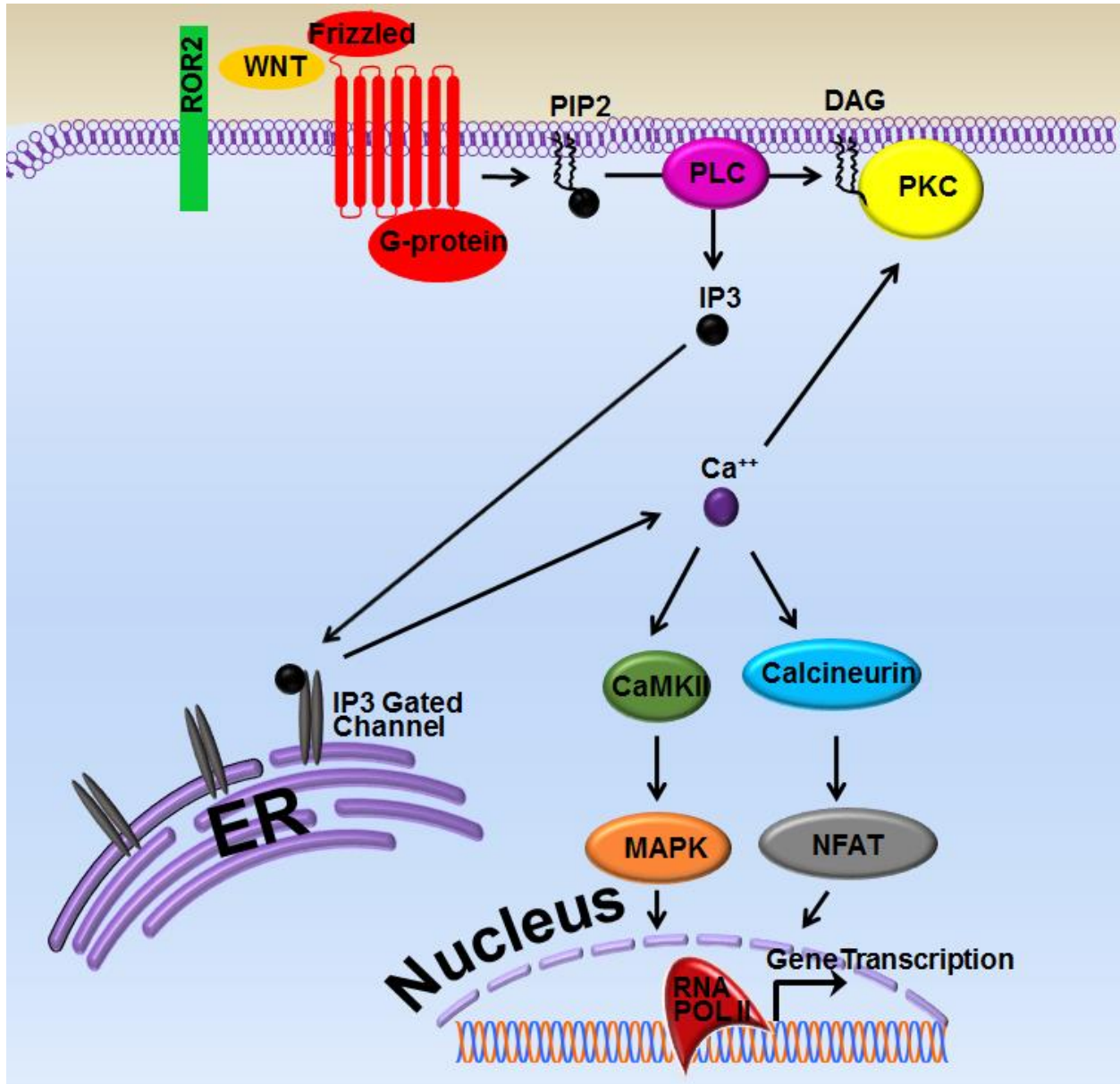


Figure1.4: Mechanism of Wnt5a calcium-dependent pathway. Wnt5a binds its membrane associated receptor, frizzled-2 (FZD2) or frizzled-5 (FZD5), and its co-receptor, receptor tyrosine kinase-like orphan receptor 2 (ROR2). This binding stimulates phospholipase C (PLC), resulting in diacylglycerol (DAG)-mediated activation of protein kinase C (PKC). Additionally, Wnt5a activates calcium/calmodulin-dependent protein kinase II (CaMKII) leading to activation of mitogen activated protein kinase (MAPK). Wnt5a also induces an increase in calcineurin activity, which in turn activates transcription factors from the NFAT family. Together, these actions result in alterations of cellular functions.

CHAPTER 3

PHOSPHOLIPASE A₂ ACTIVATING PROTEIN IS REQUIRED FOR 1 α ,25-DIHYDROXYVITAMIN D₃ DEPENDENT RAPID ACTIVATION OF PROTEIN KINASE C VIA PDIA3

INTRODUCTION

1 α ,25-dihydroxyvitamin D₃ [1 α ,25(OH)₂D₃] regulates chondrocytes and osteoblasts via two different mechanisms: the classical pathway that is vitamin D receptor (VDR) mediated, and rapid membrane initiated signaling (6-8). Growth zone chondrocytes isolated from the rat costochondral cartilage growth plate and MC3T3-E1 osteoblasts respond to 1 α ,25(OH)₂D₃ with a rapid increase in protein kinase C alpha (PKC α) activity (9,10). This rapid response is specific to the 1 α ,25(OH)₂D₃ stereoisomer; 1 β ,25(OH)₂D₃ fails to stimulate PKC-dependent signaling, indicating a receptor-mediated mechanism (88). In GC cells, 1 α ,25(OH)₂D₃ causes a rapid increase in phospholipase A₂ (PLA₂) and phosphatidylinositol-specific phospholipase C beta (PLC β) (11,89). PLA₂ action generates arachidonic acid (AA) and lysophospholipid (LPL) (89). AA can either increase PKC α activity directly (90), or it is processed further to PGE₂, which acts via its EP1 receptor to increase cyclic AMP (91). Phosphatidylinositol-specific PLC β is activated via G α_q and lysophospholipid, generating diacylglycerol (DAG) and inositol 1,4,5-trisphosphate (IP3) (89,92). DAG binds PKC α and triggers its recruitment to the plasma membrane (93). IP3 activates the release of calcium ions from the endoplasmic reticulum, required for PKC α activation. These actions of 1 α ,25(OH)₂D₃ can be blocked by antibodies to protein-disulfide isomerase family A, member 3 (Pdia3, also known as ERp60, ERp57, Grp58, and 1,25-MARRS), indicating that it is part of the receptor complex.

Multiple studies have demonstrated the pivotal role PLA₂ plays in 1 α ,25(OH)₂D₃-dependent membrane-mediated signaling (11,97-100). Stimulation of PLA₂ activity using agents such as bee venom melittin and snake venom mastoparan, mimics the effects of 1 α ,25(OH)₂D₃ on PKC in growth zone chondrocytes. Conversely, inhibition of PLA₂ activity using agents such as AACOCF₃, OEPC and quinacrine, abolishes the stimulatory effect of 1 α ,25(OH)₂D₃ (10,89). Importantly, in growth plate chondrocytes, 1 α ,25(OH)₂D₃ treatment results in release of arachidonic acid within 15 seconds and PLA₂ activation is upstream of PLC β , that PLA₂ is coupled to Pdia3.

Human phospholipase A₂ activating protein (PLAA) is a likely candidate for mediating the signal from Pdia3 to PLA₂. PLAA has three conserved domains including an N-terminal β -propeller WD40 domain, a central PLAA family ubiquitin binding domain (PFU), and a C-terminal PLAP, Ufd3p, and Lub1p domain (PUL). It has a region of 38% homology with melittin (102), and it also exhibits homology with the G-protein beta subunit WD40 domain, suggesting that it is membrane-associated (103). PLAA mRNA is expressed in growth plate chondrocytes *in vivo* and in chondrocytes isolated from the growth zone of rat costochondral growth plates *in vitro* (11). Previous studies using a 21 amino acid PLAA peptide as the activator of PLA₂ have demonstrated that this peptide mimics the effects of 1 α ,25(OH)₂D₃ on growth zone chondrocytes and MC3T3-E1 osteoblasts (10,11). PLA₂ inhibitors such as quinacrine and AACOCF₃ blocked the effect of PLAA peptide on PLA₂ and PKC, suggesting that the full-length protein acts upstream of PLA₂ (11), supporting the hypothesis that PLAA links the Pdia3 receptor complex with PLA₂.

We previously showed that disruption of caveolae structures using cholesterol chelating agents such as methyl-beta-cyclodextrin or whole-animal knockout of caveolin-1 (Cav-1)

abolished the rapid $1\alpha,25(\text{OH})_2\text{D}_3$ -dependent PKC signaling in chondrocytes, and that Pdia3 is co-localized with Cav-1 in plasma membranes and in lipid rafts (12-14). It has also been reported that Pdia3-silenced MC3T3-E1 osteoblasts rapidly activate PKC in response to PLAA peptide treatment suggesting that PLAA is downstream of Pdia3 (10). However, it is not clear whether PLAA is present in caveolae and if it interacts with Cav-1 and Pdia3. In this study, we first examined if PLAA is required to mediate $1\alpha,25(\text{OH})_2\text{D}_3$ stimulated rapid membrane signaling in chondrocytes and osteoblasts. Second, we determined the subcellular localization of this protein. Third, we evaluated how PLAA interacts with the Pdia3 receptor complex in the presence of $1\alpha,25(\text{OH})_2\text{D}_3$.

MATERIALS AND METHODS

Reagents

PLA₂ activating peptide (PLAA) was purchased from Enzo Life Sciences International, Inc. (Plymouth Meeting, PA). $1\alpha,25(\text{OH})_2\text{D}_3$ was purchased from Biomol (Plymouth Meeting, PA). The anti-PLAA polyclonal antibody was designed and developed by Strategic Diagnostics Inc. (Newark, DE), using Genomic Antibody Technology™. The selected 100 amino acid long region was 100% identical among three rat PLAA isoforms and 97% identical to mouse PLAA. Rabbit antiserum against the N-terminal peptide of Pdia3 was purchased from Alpha Diagnostic International (San Antonio, TX) (165). A polyclonal antibody to Cav-1 was purchased from Santa Cruz Biotechnology (sc-894, Santa Cruz, CA); pan cadherin polyclonal antibody was from Abcam (ab6529, San Francisco, CA); and a monoclonal antibody to glyceraldehyde-3-phosphate dehydrogenase (GAPDH) was from Millipore (MAB374, Billerica, MA, USA).

Establishment of silenced and overexpressing MC3T3-E1 cell lines

1. PLAA

Wild type mouse MC3T3-E1 osteoblast-like cells (CRL-2593) were purchased from ATCC (Manassas, VA, USA). Stable knock down of *Plaa* was achieved using MISSION™ shRNA lentiviral transduction particles (SHVRS-NM_172695, Sigma Aldrich, St. Louis, MO). Five different sequences were generated against the *Plaa* mRNA and were incorporated into the lentivirus particles. MC3T3-E1 cells were plated at a density of 20,000 cells/cm² in 24-well plates, and cultured in minimum essential medium alpha (α -MEM) supplemented with 10% fetal bovine serum (FBS), 1% penicillin/streptomycin (P/S) and 8 μ g/ml hexadimethrine bromide (500 μ l/well). In our system, lentiviral particles transfected MC3T3-E1 cells at a multiplicity of infection (MOI) of 7.5. The selection of successfully transfected cells was achieved by culturing cells containing the *Plaa* shRNA or empty vectors for 2 weeks in medium containing 2.0 μ g/ml of puromycin. The success of silencing *Plaa* was evaluated by measuring the expression of *Plaa* mRNA in comparison to wild type cells using real-time PCR and by Western blots using anti-PLAA antibody.

To determine *Plaa* expression, confluent cultures of wild type and *Plaa* silenced MC3T3-E1 cells were incubated with fresh media for 12 hours and RNA was harvested using the TRIzol® (Invitrogen, Carlsbad, CA) extraction method. RNA was quantified using a Nanodrop spectrophotometer (Thermo Fisher Scientific, Waltham, MA). 1 μ g of RNA was reverse transcribed to create the cDNA template using a High Capacity Reverse Transcription cDNA kit (Applied Biosystems, Carlsbad, CA). To quantify the expression of *Plaa*, real-time PCR was performed with *Plaa*-specific primers (F: 5'-AGA GAT GGT GAA GAA GCG-3'; R: 5'-ACCTGGCTCATTGAGATGTTCC-3') using the Step One Plus Real-time PCR System and

Power SYBR[®] Green PCR Master Mix (Applied Biosystems). Primers were designed using the beacon designer software and synthesized by Eurofins MWG Operon (Huntsville, AL). The stably transduced cell line with the highest silencing of *Plaa* (87% reduction) was chosen.

A stably silenced MC3T3-E1 cell line was established for *Plaa* (shPlaa), confirmed by Western blots of whole cell lysates (Fig. 3.1A). Of the five clones examined, RT-PCR indicated that mRNA for *Plaa* was significantly reduced in clone 906 compared with wild type cells (Fig. 3.1B). Western blots of plasma membranes from wild type MC3T3-E1 cells showed strong bands for PLAA, but the intensity of these bands was largely decreased in clone 906 cells (Fig. 3.1C). Similarly, wild type MC3T3-E1 cells exhibited intense immunofluorescence signal for PLAA, but this signal was reduced significantly in clone 906 cells (Fig. 3.1D).

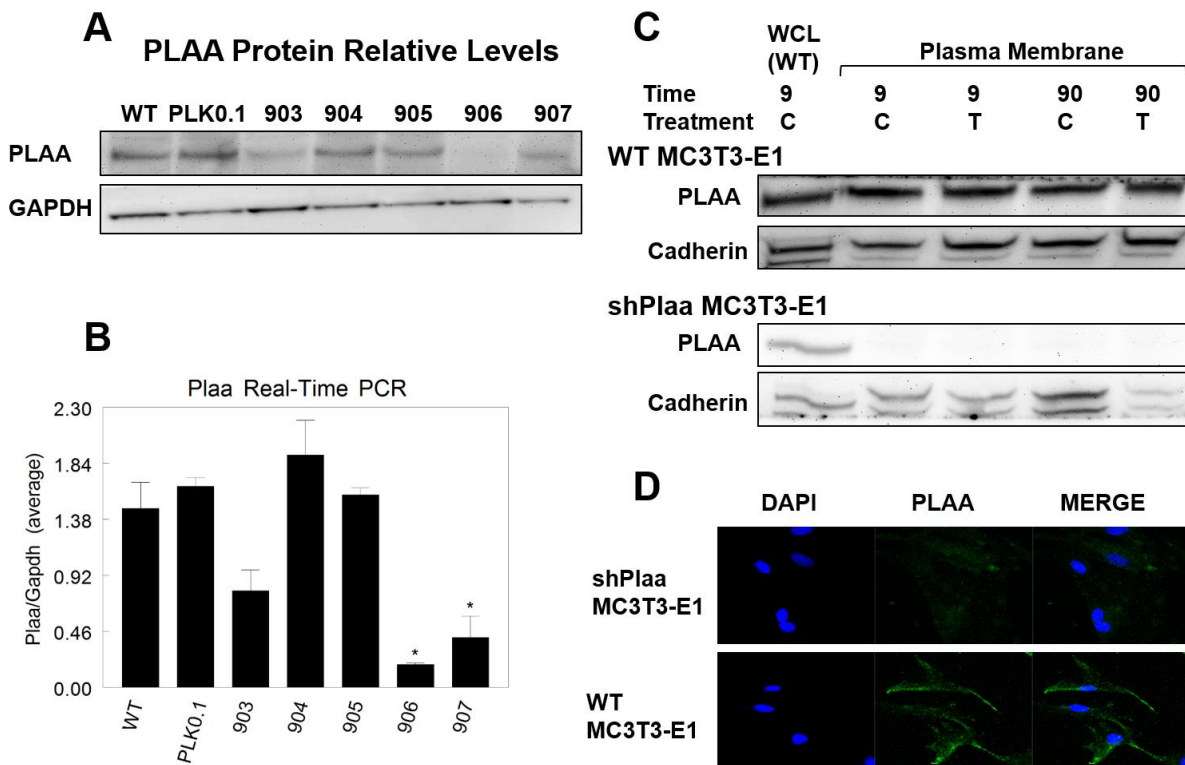


Figure 3.1: Silencing Plaa in MC3T3-E1 cells. (A) Western blot of whole cell lysates. *Top*: Blotting image for PLAA. *Bottom*: Blotting image for GAPDH (loading control). (B) Real-time

PCR. Plaa levels relative to Gapdh control. * $p < 0.05$, versus WT. (C) Western blot of whole cell lysates of wild type MC3T3-E1 and plasma membranes of wild type and shPlaa MC3T3-E1 cells. *Top*: Blotting image for PLAA in the plasma membrane of wild type MC3T3-E1 cells. Cadherin serves as a loading control. *Bottom*: Blotting image for PLAA in the plasma membrane of shPlaa MC3T3-E1 cells. Whole cell lysates of wild type MC3T3-E1 cells were loaded as a positive control for PLAA. Cadherin serves as the plasma membrane loading control. (D) Confocal microscopy of wild type and shPlaa MC3T3-E1 cells. *blue*: nucleus, *green*: PLAA. Cells were permeabilized before staining.

2. Cav1

Stable knockdown of Cav1 (shCav-1) was achieved by transducing wild type MC3T3-E1 cells with Cav1 shRNA lentiviral transduction particles (data not shown) (87). Greater than 90% silencing of Cav1 in clone 662 was confirmed using real-time PCR and by Western blots using anti-Cav-1 antibody. The method used to quantify Cav1 gene expression is as described for PLAA. Cav1-specific primers used in this part of the study (F: 5'- GAT TGA CTT TGA AGA TGT GAT TGC -3'; R: 5'- ACA GTG AAG GTG GTG AAG C -3') were designed using the beacon designer software and synthesized by Eurofins MWG Operon.

3. Pdia3

Pdia3 silenced (shPdia3) and over-expressing (ovxPdia3) MC3T3-E1 cell lines were generated previously (10). For these studies, we used the cell line with the highest silencing of Pdia3 (80% reduction). ovxPdia3 cells showed 100% over-expression of Pdia3 compared to the wild type.

Cell culture

Wild type MC3T3-E1, shPlaa, and shCav-1 cells, as well as shPdia3 and ovxPdia3 cells were plated at 10,000 cells/cm³, and cultured in puromycin-free α -MEM containing 10% FBS and 1% P/S. To induce osteoblastic differentiation of MC3T3-E1 cells, the media were replaced with α -MEM supplemented with 10% FBS, 1% P/S and 1% ascorbic acid, 24 hours after plating

and then every 48 hours. After 10 days in culture, the cells were used for experiments described below.

Costochondral cartilage growth zone chondrocytes used in these experiments were isolated from 100-125-g male Sprague-Dawley rats (Harlan, Indianapolis, IN). The rats were at the end of their adolescent growth spurt; therefore, their long bones were growing at a reduced rate. The culture system used in this study was described previously in detail (11,166). Confluent cultures (approximately day 7) were used for the experiments described below.

Plasma membranes and caveolae isolation

Plasma membranes and caveolae were isolated using a detergent-free method as described previously (121). Confluent, fourth passage growth zone chondrocytes and MC3T3-E1 cells (cultured for 10 days post-plating) were treated with either 10^{-8} M $1\alpha,25(\text{OH})_2\text{D}_3$ or vehicle (ethanol) for 9 minutes. The cells were harvested by scraping while in isolation buffer (0.25 M sucrose, 1 mM EDTA, 20 mM Tricine, pH 7.8) and were homogenized using a tissue grinder (20 strokes; 10 strokes clockwise and 10 strokes counter-clockwise). Homogenates were centrifuged at 20,000 X *g* for 10 minutes. The pellet, including nucleus, mitochondria, and endoplasmic reticulum was discarded, and the supernatant was collected, and placed on top of isolation buffer containing 30% Percoll (GE Healthcare, Piscataway, NJ). The samples were centrifuged at 84,000 X *g* for 30 minutes. Syringe needles (18G) were used to collect the plasma membrane fraction from the gradient column. The isolated fraction was layered over a 10-20% OptiPrep gradient (Sigma Aldrich), and the gradient was centrifuged at 52,000 X *g* for another 4 hours. Plasma membrane sub-fractions were collected from the top to the bottom of the tube, which resulted in isolation of thirteen fractions. Caveolae were observed as an opaque band, which was collected in fraction 3.

To verify that PLAA and Pdia3 were in caveolae, MC3T3-E1 osteoblasts were treated with 10mM methyl-beta-cyclodextrin (β -CD) for 1 hour in a serum-free medium to disrupt the caveolar structure, as described previously (12). Plasma membranes were isolated as above. 2.5.

Western blots

Proteins were separated using polyacrylamide gel electrophoresis. Whole cell lysates, plasma membranes, and plasma membrane fractions (50 μ g protein) were loaded onto NuSep 4-20% LongLife Gels (NuSep, Lawrenceville, GA), and at the end of the run, the proteins were transferred from gels to nitrocellulose membranes using an iBlot Dry Blotting System (Invitrogen). Next, the membrane was incubated with 1% bovine serum albumin (BSA) in phosphate buffered saline (PBS). Subsequently, the membranes were incubated with antibodies against PLAA, Pdia3, Cav-1, pan cadherin or GAPDH overnight. The membranes were incubated with goat anti-rabbit or goat anti-mouse horseradish peroxidase-conjugated secondary antibodies (Bio-Rad, Hercules, CA) in PBS containing 1% BSA after washing three times with PBS containing 0.05% Tween-20. The membranes were incubated with the secondary antibody only for one hour. Following three washes with PBS containing 0.05% Tween-20 (three times, ten minutes each), membranes were developed using either the SuperSignal West Pico Chemiluminescent System (Thermo Fisher Scientific) or the LumiSensorTM Plus Chemiluminescent HRP Substrate kit (GenScript, Piscataway, NJ, USA) and imaged with the VersaDoc imaging system (Bio-Rad).

Regulation of PKC activity

To study the effect of *Plaa* silencing on $1\alpha,25(\text{OH})_2\text{D}_3$ -dependent PKC activation, wild type and shPlaa MC3T3-E1 cells were treated for 15 minutes with 10^{-10} to 10^{-8} M $1\alpha,25(\text{OH})_2\text{D}_3$. After washing the cell layers with PBS, the cells were lysed in RIPA buffer (20 mM Tris-HCl,

150 mM NaCl, 5mM disodium EDTA, 1% Nonidet P-40). PKC activity was measured using a commercially available kit (Protein Kinase C Biotrak Enzyme Assay, RPN77, GE Healthcare). PKC data were normalized to total protein (Pierce BCA Protein Assay, Thermo Fisher Scientific).

To determine if PLAA is required for PKC activation, MC3T3-E1 cells were pretreated with the anti-PLAA antibody for 30 minutes, and next treated with 10^{-8} M $1\alpha,25(\text{OH})_2\text{D}_3$ for 15 minutes. The cell layers were collected for subsequent PKC assay. To investigate the effects of PLAA blocking on PKC activity in growth zone cartilage cells, the chondrocytes were pretreated with the anti-PLAA antibody for 30 minutes, and next treated with 10^{-8} M $1\alpha,25(\text{OH})_2\text{D}_3$ for 9 minutes. The cell layers were collected for subsequent PKC assay.

Regulation of PGE₂ release

To study the effect of *Plaa* silencing on $1\alpha,25(\text{OH})_2\text{D}_3$ mediated PGE₂ release, wild type and shPlaa MC3T3-E1 cells were treated for 15 minutes with 10^{-10} to 10^{-8} M $1\alpha,25(\text{OH})_2\text{D}_3$. At the end of the incubation, the media were acidified and PGE₂ was measured using a commercially available kit (Prostaglandin E₂ [¹²⁵I]-RIA kit, NEK020001K, Perkin Elmer, Waltham, MA). PGE₂ data were normalized to total DNA (Quant-iT™ PicoGreen® dsDNA Assay kit, P11496, Invitrogen).

Regulation of PLA₂ activity

To determine if PLAA is required for $1\alpha,25(\text{OH})_2\text{D}_3$ mediated PLA₂ activation, wild type and shPlaa MC3T3-E1 cells were treated for 15 minutes with 10^{-10} to 10^{-8} M $1\alpha,25(\text{OH})_2\text{D}_3$. After washing the cell layers with PBS, the cells were lysed and the lysates assayed for PLA₂ activity using a commercially available kit (cPLA₂ Assay kit, 765021, Cayman Chemical, Ann Arbor, MI).

Immunofluorescence Microscopy

Growth zone chondrocytes and wild type MC3T3-E1 cells were plated at 10,000 cells/cm² on glass chamber slides and cultured for 24 hours in their appropriate medium. The next day, the cells were treated with either 10⁻⁸ M 1 α ,25(OH)₂D₃ or vehicle for 9 minutes and 90 minutes. After washing the cell layers with PBS, they were fixed in 4% paraformaldehyde for 20 minutes. The fixed cell layers were incubated with antibodies to PLAA, Pdia3 and caveolin-1 in 1% BSA overnight. At the end of the incubation time, the cell layers were washed with PBS and incubated with goat anti-rabbit Alexa Fluor 594 or goat anti-mouse Alexa Fluor 488 (Invitrogen) in 1% BSA for one hour. At the end of the incubation period, cells were washed with PBS and then were incubated with Hoechst 33342 (Invitrogen) for 10 minutes. After washing cells with PBS, they were imaged using a Zeiss LSM 510 NLO with META MPE confocal microscope.

Immunoprecipitation

MC3T3-E1 cells and GC chondrocytes were treated with either 10⁻⁸ M 1 α ,25(OH)₂D₃ or vehicle (ethanol) for 9 minutes and 90 minutes. The cell layers were washed with PBS and the cells were lysed and sonicated in RIPA buffer (20 mM Tris-HCl, 150 mM NaCl, 5mM disodium EDTA, 1% Nonidet P-40) containing 100mM NaF, protease inhibitor cocktail (Sigma Aldrich) and 1 mM phenylmethylsulfonyl fluoride (PMSF). In order to preclear the cell extracts, protein samples (1mg) were incubated with 5 μ g of rabbit IgG (1 hour, 4°C) and next incubated with protein A-agarose beads (EMD Chemicals, Gibbstown, NJ, USA) for 2 hours at 4°C. The beads were pelleted by centrifugation at 1,000 X g (1 minute, 4°C). Pre-cleared protein samples were mixed with either anti-PLAA or anti-Pdia3 antibodies and incubated at 4°C overnight with continuous agitation. Protein A-agarose beads were added to the mixture and the mixture was incubated at 4°C for two additional hours. The beads were pelleted and the pellets washed three

times with PBS. Precipitated proteins were eluted by boiling beads in Tris-glycine SDS sample loading buffer (Bio-Rad) containing 5.0% beta-mercaptoethanol for 5 minutes. The immunoprecipitated samples were subjected to Western blot (refer to section 2.5). In order to lower the background in the images, a ONE-HOUR IP-Western Kit (Genscript) was used.

Chemical crosslinking of PLAA to plasma membrane surface proteins

MC3T3-E1 osteoblasts were treated with either 10^{-8} M $1\alpha,25(\text{OH})_2\text{D}_3$ or vehicle (ethanol) for 9 minutes. The cell layers were washed with PBS, and the 11.4-A° non-cleavable, membrane-impermeable crosslinker bis(sulfosuccinimidyl) substrate (BS^3) (Thermo Fisher Scientific) (167) was added to chemically crosslink exposed membrane proteins (10 mM BS^3 in PBS, 20ml per T175 flask, 1 hour, 4°C). BS^3 induces amine-to-amine covalent bonds between the neighboring proteins, and these bonds are not sensitive to chemical reduction; therefore, gel electrophoretic separation of proteins can be performed under reducing conditions, which was beneficial for the subsequent immunoblotting step. After 1 hour, the reaction was terminated by quenching the reaction with 100 mM glycine in PBS (10 minutes, 4°C). The cell layer was washed with PBS and the cells were lysed and sonicated in RIPA buffer containing 100mM NaF, protease inhibitor cocktail, and 1 mM PMSF.

To determine if the ability of $1\alpha,25(\text{OH})_2\text{D}_3$ to stimulate PKC activity requires PLAA mobility, we cross-linked PLAA to its neighboring membrane surface proteins, and assessed $1\alpha,25(\text{OH})_2\text{D}_3$ membrane-mediated PKC activation. Wild type MC3T3-E1 cells were treated with 10mM BS^3 for 30 minutes in serum-free medium, and next treated with 10^{-8} M $1\alpha,25(\text{OH})_2\text{D}_3$ for 15 minutes. The cell layers were collected for subsequent PKC assay.

Statistical analysis

For each experiment, each data point represents the means \pm SEM for six individual cultures. Each experiment was repeated at least three times to ensure the validity of the data. The data presented are from a single representative experiment. Significance was determined by analysis of variance and post hoc testing performed using Bonferroni's modification of Student's *t* test for multiple comparisons. $P \leq 0.05$ were considered significant.

RESULTS

Subcellular Localization of PLAA

Western blots of whole cell lysates demonstrated that MC3T3-E1 osteoblasts possess Pdia3, PLAA and Cav-1 (Fig. 3.2A,B,C). Western blots of the plasma membrane fractions of these cells indicated that Pdia3, PLAA, and Cav-1 were present in the plasma membranes with their greatest concentration in fraction 3, which represents caveolae microdomains (Fig. 3.2A, B, C). Based on the intensity of PLAA bands in Western blots of caveolae fractions isolated from MC3T3-E1 osteoblasts, $1\alpha,25(\text{OH})_2\text{D}_3$ did not change the levels of PLAA protein in these plasma membrane microdomains (Fig. 3.2C). Pdia3 and Cav-1 were also present in whole cell lysates of GC chondrocytes (Fig. 3.2D, E ,F) and in plasma membranes with their highest abundance in caveolae (Fig. 3.2D). Similar to MC3T3-E1 cells, PLAA was present in other fraction 3 as well (Fig. 3.2E). Intensity analysis of PLAA bands indicated that $1\alpha,25(\text{OH})_2\text{D}_3$ treatment did not alter the levels of PLAA in caveolae of GC chondrocytes (Fig. 3.2F).

Treatment of MC3T3-E1 osteoblasts with β -CD altered the abundance of PLAA and Pdia3 in the plasma membrane. Comparison of the intensity of PLAA bands on the Western blot relative to cadherin bands as a loading control, showed that β -CD reduced the intensity of PLAA

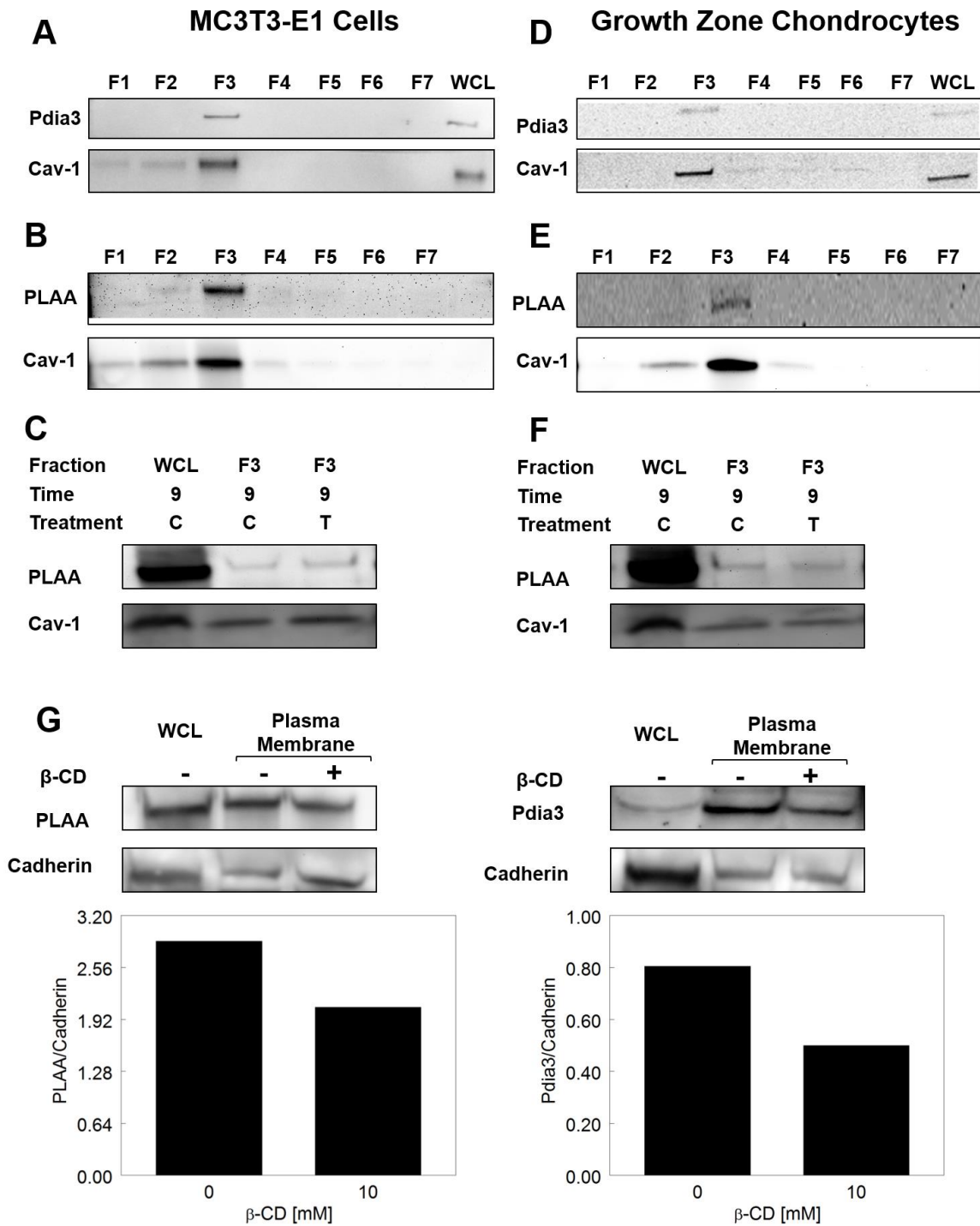


Figure 3.2: Subcellular localization of PLAA in growth zone chondrocytes and MC3T3-E1 osteoblasts. (A) Caveolae localization of Pdia3 in MC3T3-E1 osteoblasts (B) Caveolae localization of PLAA in MC3T3-E1 osteoblasts. (C) The effect of $1\alpha,25(\text{OH})_2\text{D}_3$ on caveolae localization of PLAA in MC3T3-E1 cells. (D) Caveolae localization of Pdia3 in GC cells. (E) Caveolae localization of PLAA in GC chondrocytes. (F) The effect of $1\alpha,25(\text{OH})_2\text{D}_3$ on caveolae

localization of PLAA in GC cells. (G) Effect of β -CD on plasma membrane localization of PLAA and Pdia3 in MC3T3-E1 osteoblasts. MC3T3-E1 osteoblasts were treated with 10mM β -CD for 1 hour in a serum-free medium. Plasma membranes were isolated and subjected to Western blot. (C: control group, T: $1\alpha,25(\text{OH})_2\text{D}_3$ treated group)

bands by 30% compared to cells with no β -CD treatment (Fig. 3.2G). Comparison of the intensity of Pdia3 bands on the Western blot relative to cadherin bands, showed nearly a 40% reduction in the intensity of Pdia3 bands compared to cells with no β -CD treatment (Fig. 3.2G).

Effects of $1\alpha,25(\text{OH})_2\text{D}_3$ and BS^3 on Plasma Membrane Localization of PLAA

PLAA was exposed on the membrane surface. Western blots of whole cell lysates of MC3T3-E1 cells showed the presence of PLAA (Fig. 3.3A). However, when MC3T3-E1 cells were treated with BS^3 to crosslink plasma membrane surface proteins, there was a decrease in the apparent 73 kDa PLAA band (Fig. 3.3B). Concomitant appearance of a higher molecular weight band was observed only in whole cell lysates of cells exposed to BS^3 . The higher molecular weight indicates that the PLAA protein formed complexes with other plasma membrane proteins facing the extracellular matrix. The positive control protein, cadherin, also exhibited a shift to a higher molecular weight region (Fig. 3.3B). Comparison of the intensity of PLAA bands on the Western blot relative to GAPDH bands, as a loading control, showed that BS^3 reduced the intensity of PLAA bands by 50% compared to cells with no BS^3 treatment and with cells treated for 9 minutes with $1\alpha,25(\text{OH})_2\text{D}_3$ and BS^3 , respectively (Fig. 3.3C). Comparison of the intensity of cadherin bands on the Western blot relative to GAPDH bands, showed nearly a 50% reduction in the intensity of cadherin bands compared to cells with no BS^3 treatment (Fig. 3.3D).

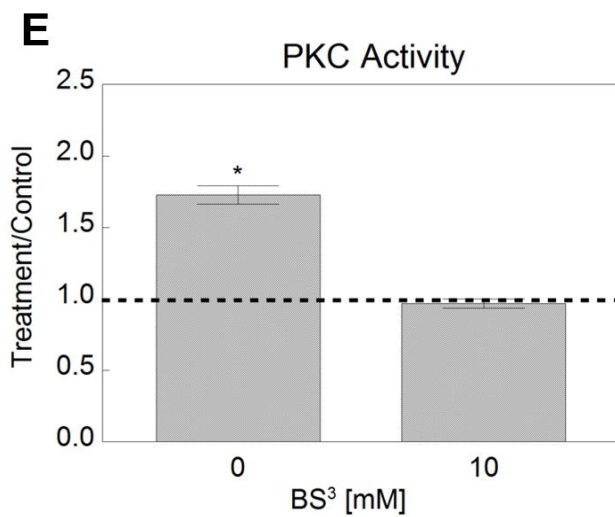
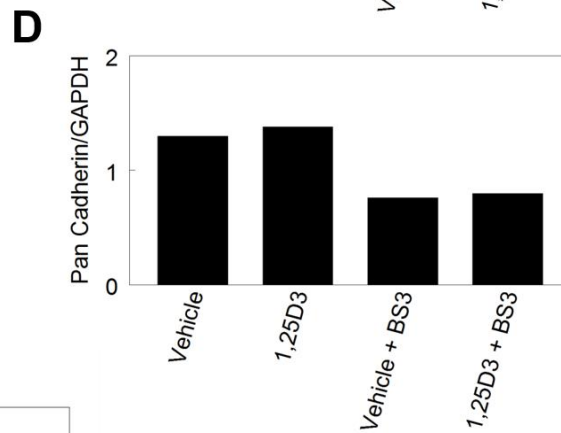
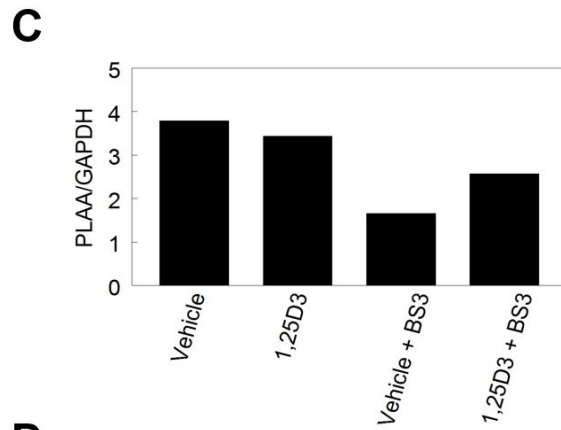
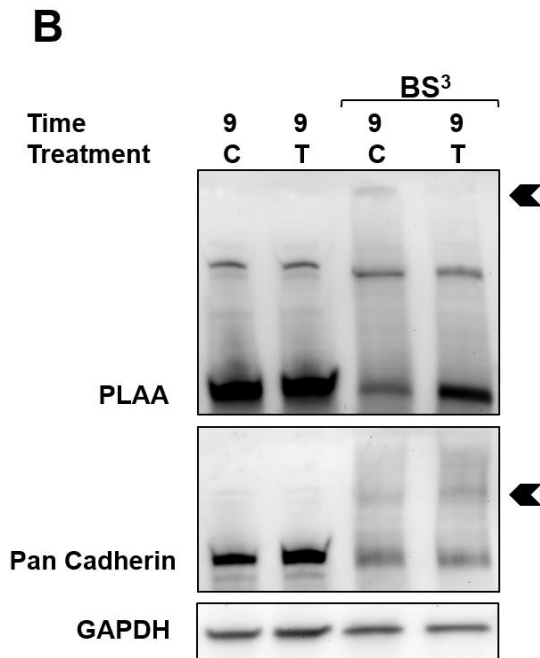
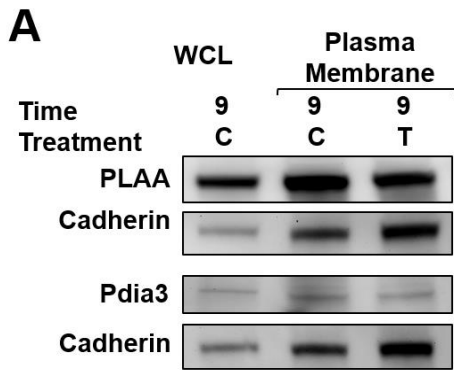


Figure 3.3: Effect of $1\alpha,25(\text{OH})_2\text{D}_3$ on plasma membrane localization of PLAA and Pdia3. (A) MC3T3-E1 cells were treated with $1\alpha,25(\text{OH})_2\text{D}_3$ for 9 minutes. Presence of PLAA, Pdia3 and cadherin in the plasma membrane were examined by Western blot. (B) The effect of BS^3 pretreatment on PLAA crosslinking with plasma membrane surface proteins. MC3T3-E1 cells were treated with $1\alpha,25(\text{OH})_2\text{D}_3$ for 9 minutes, and subsequently incubated with BS^3 for 1 hour. The whole cell lysates were subjected to Western blot: PLAA (top), Cadherin (middle), or GAPDH (bottom). (C) Relative intensity analysis of PLAA bands relative to GAPDH. (D) Relative intensity analysis of cadherin bands relative to GAPDH. (E) Effect of BS^3 on $1\alpha,25(\text{OH})_2\text{D}_3$ membrane-mediated PKC activation in MC3T3-E1 osteoblasts. MC3T3-E1 cells were pretreated with treated with BS^3 for 1 hour, and next treated with $1\alpha,25(\text{OH})_2\text{D}_3$ for 9 minutes. The cell layers were collected for PKC activity assay. * $p < 0.05$, treatment *versus* control. (C: control group, T: $1\alpha,25(\text{OH})_2\text{D}_3$ treated group)

Treatment of MC3T3-E1 cells with BS^3 altered the response of cells to $1\alpha,25(\text{OH})_2\text{D}_3$. The rapid stimulatory effect of $1\alpha,25(\text{OH})_2\text{D}_3$ on PKC was completely abrogated with BS^3 treatment (Fig. 3.3E).

Effect of PLAA Blocking on $1\alpha,25(\text{OH})_2\text{D}_3$ Membrane-mediated PKC Activation

Anti-PLAA antibody significantly reduced the $1\alpha,25(\text{OH})_2\text{D}_3$ -dependent increase in PKC activity in MC3T3-E1 osteoblasts (Fig. 3.4A), whereas, IgG had no effect. Similarly, a significant reduction was observed in PKC activity in response to $1\alpha,25(\text{OH})_2\text{D}_3$ when GC chondrocytes were pretreated with anti-PLAA antibody (Fig. 3.4B). Conversely, IgG had no effect on stimulation of PKC activity by $1\alpha,25(\text{OH})_2\text{D}_3$.

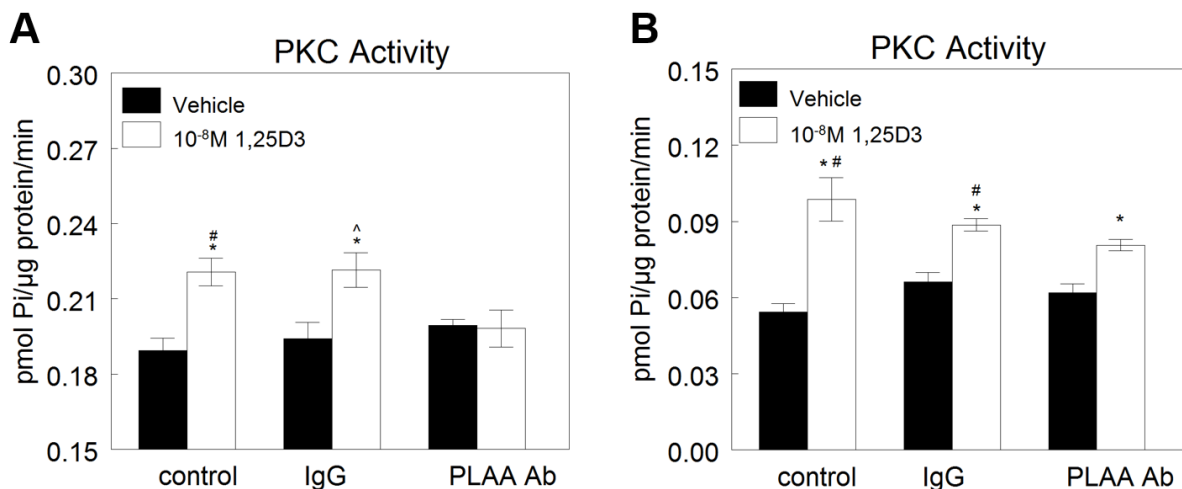


Figure 3.4: Effect of PLAA blocking on $1\alpha,25(\text{OH})_2\text{D}_3$ membrane-mediated PKC activation in osteoblasts and chondrocytes. MC3T3-E1 osteoblasts (A) and growth zone chondrocytes (B) were pretreated with PLAA-antibody for 30 minutes, and next they were treated with $1\alpha,25(\text{OH})_2\text{D}_3$ for 15 minutes and 9 minutes, respectively. PKC activity was measured as described and normalized to total protein level. * $p < 0.05$, treatment *versus* control; # $p < 0.05$, PLAA Ab *versus* control; ^ $p < 0.05$, PLAA Ab *versus* IgG. Each figure is a representative experiment, repeated three times with similar results.

Effect of *Plaa* Silencing on $1\alpha,25(\text{OH})_2\text{D}_3$ Membrane-mediated Signaling

Unlike wild type MC3T3-E1 cells, shPlaa cells did not respond to $1\alpha,25(\text{OH})_2\text{D}_3$ with an increase in PLA₂ activity (Fig. 3.5A). Similarly, $1\alpha,25(\text{OH})_2\text{D}_3$ had no effect on PGE₂ release (Fig. 3.5B) and PKC activity (Fig. 3.5C) in shPlaa MC3T3-E1 cells. These effects were specific to PLAA since the MC3T3-E1 cells transfected with empty vectors responded to $1\alpha,25(\text{OH})_2\text{D}_3$ like the wild type cells (Fig. 3.5D).

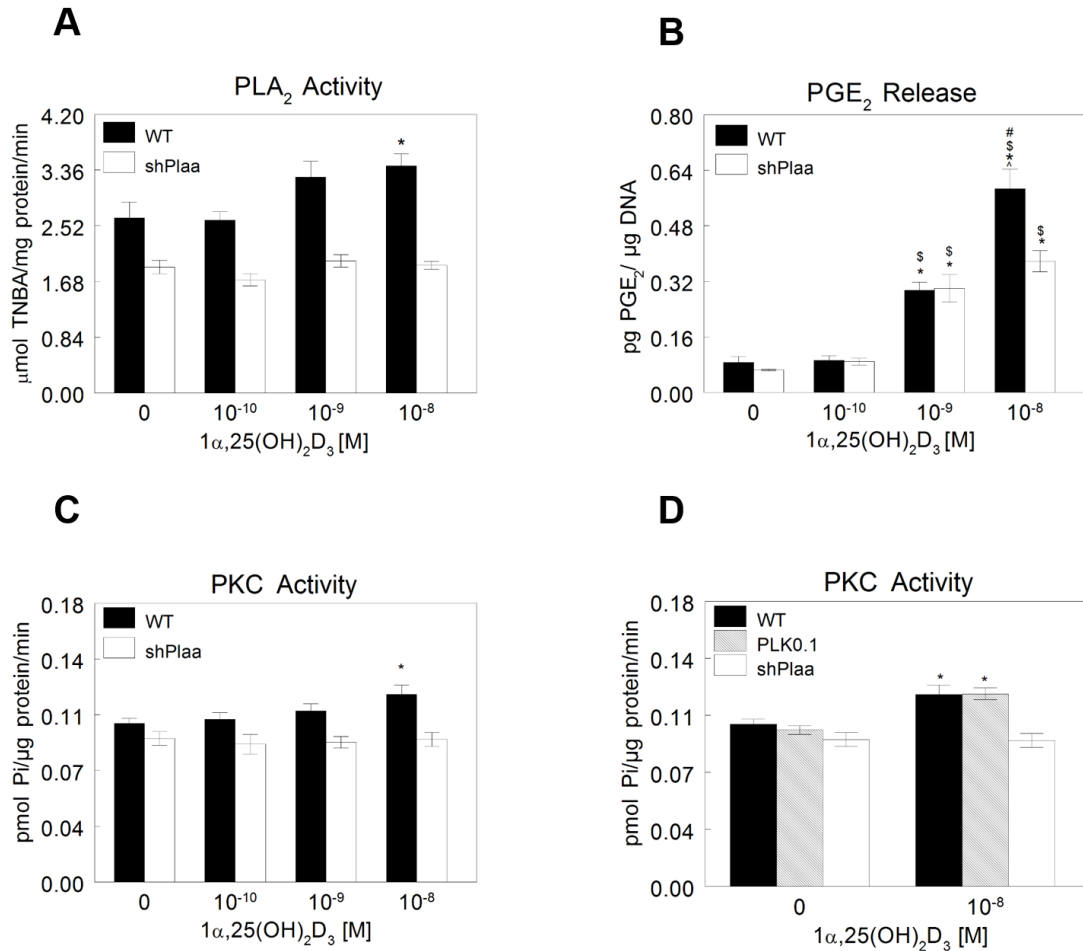


Figure 3.5: Effect of 1α,25(OH)₂D₃ on PLA₂ and PKC activities and PGE₂ release in wild type and shPlaa MC3T3-E1 cells. (A) 1α,25(OH)₂D₃ effect on PLA₂ activity of WT and shPlaa MC3T3-E1 cells. (B) The effect of 1α,25(OH)₂D₃ on PGE₂ release of WT and shPlaa MC3T3-E1 cells. (C) 1α,25(OH)₂D₃ effect on PKC of WT and shPlaa MC3T3-E1 cells. (D) 1α,25(OH)₂D₃ effect on PKC of WT, empty vector and shPlaa MC3T3-E1 cells. **p*<0.05, treatment versus control; §*p*<0.05, versus 10⁻¹⁰M 1α,25(OH)₂D₃; #*p*<0.05, versus 10⁻⁹M 1α,25(OH)₂D₃; ^*p*<0.05, versus 10⁻⁸M shPlaa 1α,25(OH)₂D₃ treated group. Each figure is a representative experiment repeated three times with similar results.

Effects of 1α,25(OH)₂D₃ on Interactions between PLAA and Pdia3

The stimulatory effect of PLAA on PLA₂ in response to 1α,25(OH)₂D₃ is downstream of Pdia3. 1α,25(OH)₂D₃ did not stimulate PLA₂ activity in MC3T3-E1 cells silenced for Pdia3 (Fig.3.6A). In contrast, cells overexpressing Pdia3 showed increased PLA₂ activity compared to

wild type MC3T3-E1 cells (Fig. 1.6A). As shown previously, $1\alpha,25(\text{OH})_2\text{D}_3$ had no effect on PKC in shPdia3 cells, and enhanced PKC activity in ovxPdia3 cells (Fig. 3.6B).

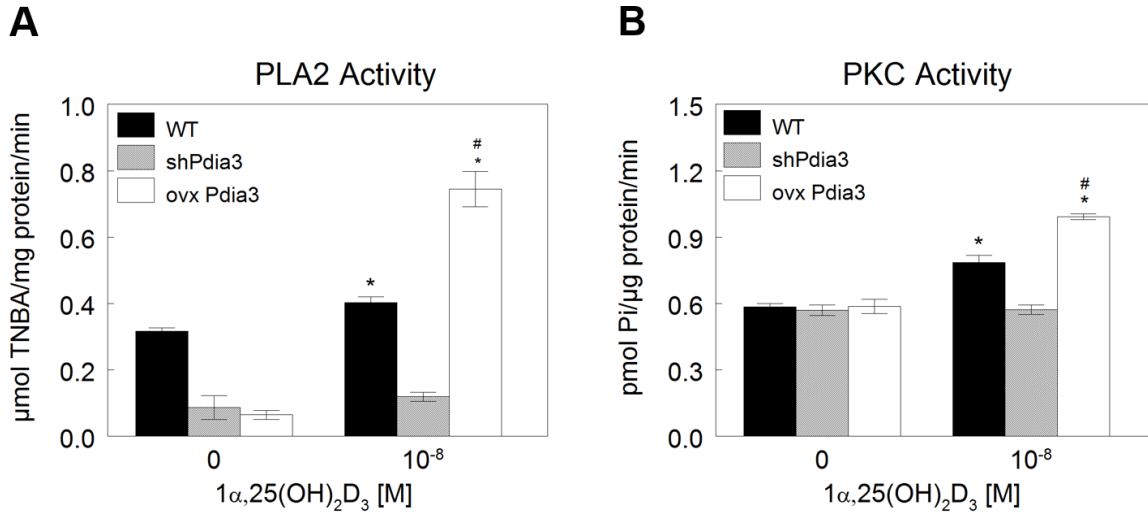


Figure 3.6: Effect of $1\alpha,25(\text{OH})_2\text{D}_3$ on PLA₂ activity and PKC activity in wild type and silenced *Pdia3* (shPdia3) and over-expressed *Pdia3* (ovxPdia3) MC3T3-E1 cells. (A) The effect of $1\alpha,25(\text{OH})_2\text{D}_3$ on PLA₂ activity of WT, shPdia3 and ovxPdia3 MC3T3-E1 cells. (B) $1\alpha,25(\text{OH})_2\text{D}_3$ effect on PKC activity of WT and shPdia3 and ovxPdia3 MC3T3-E1 cells. * $p < 0.05$, treatment versus control; # $p < 0.05$, versus 10^{-8} M $1\alpha,25(\text{OH})_2\text{D}_3$ WT; % $p < 0.05$, versus 10^{-8} M $1\alpha,25(\text{OH})_2\text{D}_3$ ovxPdia3. Each figure is a representative experiment, repeated two times with similar results.

Confocal microscopy of MC3T3-E1 cells stained with antibodies against PLAA and Cav-1 indicated that the two proteins were co-localized (Fig. 3.7A). When cells were treated with $1\alpha,25(\text{OH})_2\text{D}_3$, PLAA and Cav-1 appeared to increase their interaction and immunoprecipitates of MC3T3-E1 cell lysates using anti-PLAA antibodies confirmed this (Fig. 3.7B). Pdia3 was not present in anti-PLAA antibody immunoprecipitates of cells treated with vehicle, but it was present when the cells were treated with $1\alpha,25(\text{OH})_2\text{D}_3$ for 9 minutes (Fig. 3.7B).

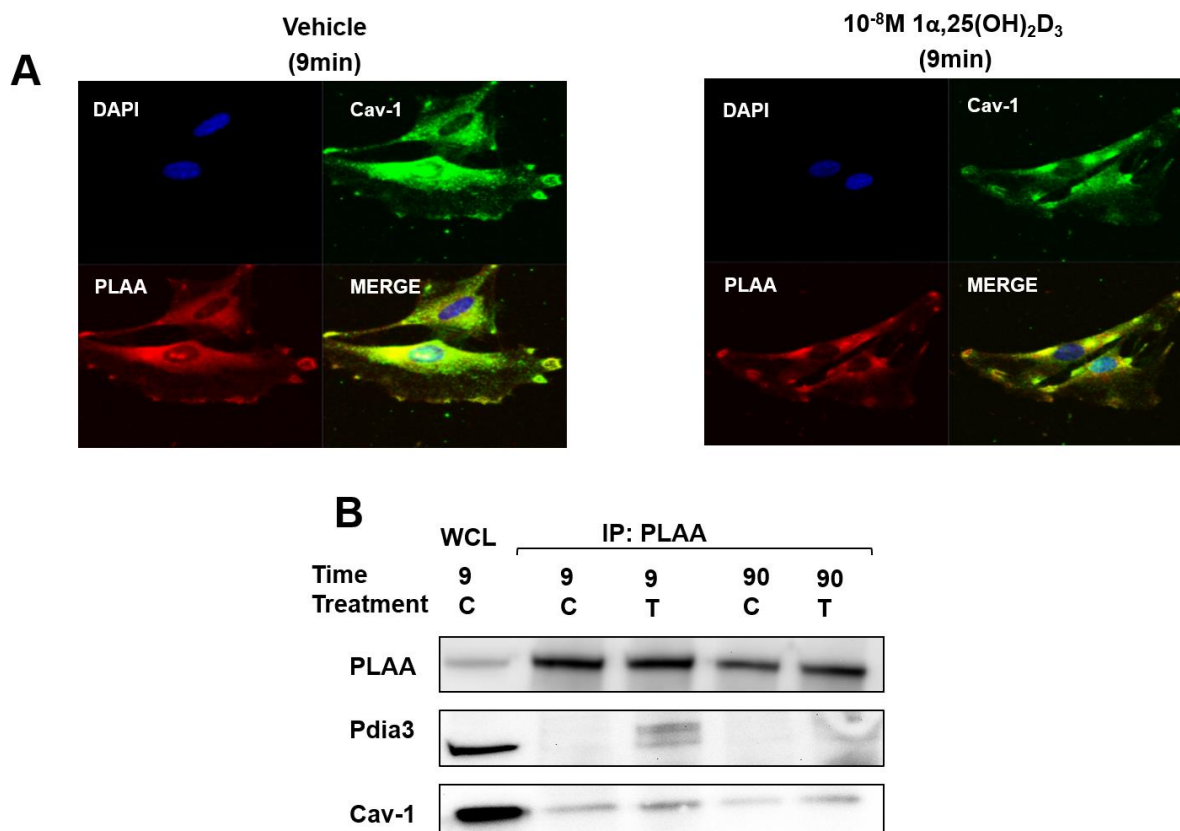


Figure 3.7: Western blot and confocal images of PLAA interaction studies. (A) Confocal image of the effect of $1\alpha,25(\text{OH})_2\text{D}_3$ on PLAA-Cav-1 colocalization in MC3T3-E1. Green: Cav-1; red: PLAA; yellow: merge. (B) The effect of $1\alpha,25(\text{OH})_2\text{D}_3$ on PLAA's interaction with Pdia3 and Cav-1. PLAA was immunoprecipitated and subjected to Western blot. The membranes were incubated with the anti-Pdia3 and anti-Cav-1 antibodies. (C: control group, T: $1\alpha,25(\text{OH})_2\text{D}_3$ treated group)

Confocal microscopy indicated that Pdia3 and Cav-1 were present in the cells and were co-localized (Fig. 3.8A), but when antibodies to Pdia3 were used to precipitate whole cell lysates; Western blots showed that only Cav-1 and Pdia3 were present in the immunoprecipitates (Fig. 3.8B). However, PLAA was present in the immunoprecipitates of cells treated with $1\alpha,25(\text{OH})_2\text{D}_3$. In contrast, anti-Pdia3 immunoprecipitates of Cav-1 silenced MC3T3-E1 cells treated with $1\alpha,25(\text{OH})_2\text{D}_3$ lacked PLAA (Fig. 3.8C).

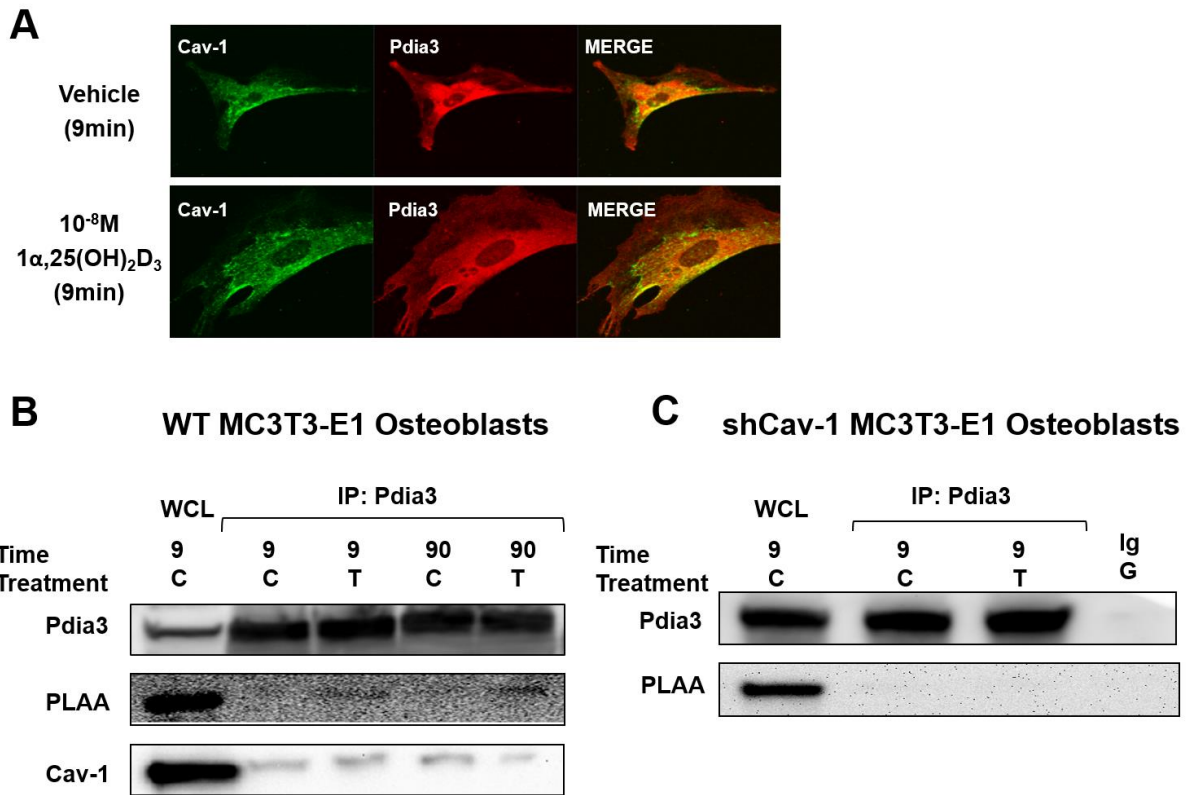


Figure 3.8: Western blot and confocal images of Pdia3 interaction studies. (A) Confocal image of the effect of $1\alpha,25(\text{OH})_2\text{D}_3$ on Pdia3-Cav-1 colocalization in MC3T3-E1 osteoblasts. Green: Cav-1; red: Pdia3; yellow: merge. (B) The effect of $1\alpha,25(\text{OH})_2\text{D}_3$ on Pdia3's interaction with PLAA and Cav-1. Pdia3 was immunoprecipitated and subjected to Western blot. The membranes were incubated with anti-PLAA and anti-Cav-1 antibodies. (C) The effect of $1\alpha,25(\text{OH})_2\text{D}_3$ on Pdia3's interaction with PLAA in shCav-1 MC3T3-E1 cells. Pdia3 was immunoprecipitated and subjected to Western blot. The membranes were incubated with anti-PLAA antibody. (C: control group, T: 1,25D3 treated group)

DISCUSSION

Previous studies have shown that a 21 amino acid PLAA peptide activates PLA_2 in cells sensitive to $1\alpha,25(\text{OH})_2\text{D}_3$ (11) as well as in other cells types (168), however little is known about the function of the full length protein in rapid signaling by steroid hormones, or its subcellular localization in osteoblasts and chondrocytes. This study demonstrated that PLAA is

required to mediate the rapid effects of $1\alpha,25(\text{OH})_2\text{D}_3$ on osteoblasts and chondrocytes, including PLA_2 activation, PGE_2 release, and PKC activation.

The failure of $1\alpha,25(\text{OH})_2\text{D}_3$ to stimulate rapid responses in shPlaa MC3T3-E1 cells supports the hypothesis that PLAA is a pivotal member of the $1\alpha,25(\text{OH})_2\text{D}_3$ rapid signaling pathway. Immunoprecipitation studies demonstrated that PLAA only interacts with the $1\alpha,25(\text{OH})_2\text{D}_3$ membrane associated receptor, Pdia3, in the presence of the hormone. This suggests that PLAA serves as a mediator to transfer the signal from the ligand-receptor complex to PLA_2 . Whether PLAA directly binds to PLA_2 and triggers its activation, or if it stimulates PLA_2 activation through activation of other protein kinases is still not known and requires further investigation.

We previously demonstrated that disruption of caveolae structures using cholesterol chelating agents such as β -CD or whole-animal knockout of caveolin-1 (Cav-1) abolished the rapid $1\alpha,25(\text{OH})_2\text{D}_3$ -dependent PKC signaling in chondrocytes (12). In this study we found caveolae must be functionally intact for the localization of Pdia3 and PLAA in the plasma membrane to occur. β -CD, which alters the chemical structure of lipid rafts and caveolae by depleting cholesterol, reduces the abundance of Pdia3 and PLAA in plasma membranes. Moreover, anti-PLAA antibody blocking studies and BS^3 crosslinking experiments confirmed the localization of PLAA on the extracellular face of the plasma membrane. These results are in agreement with studies looking at the localization of melittin in host cells (169). It is unclear why the BS^3 crosslinker failed to crosslink PLAA with plasma membrane surface proteins in $1\alpha,25(\text{OH})_2\text{D}_3$ treated cells. One possibility is that $1\alpha,25(\text{OH})_2\text{D}_3$ induced a caveolae-mediated endocytosis mechanism causing internalization of PLAA and its loss from the plasma membrane.

We previously demonstrated that anti-Pdia3 antibody blocking caused a significant reduction in $1\alpha,25(\text{OH})_2\text{D}_3$ -stimulated PKC activation (84). We proposed two explanations for such an effect. First, anti-Pdia3 antibody may block $1\alpha,25(\text{OH})_2\text{D}_3$ docking to its receptor protein. Second, anti-Pdia3 antibody may prevent the interaction between Pdia3 and other signaling proteins. In this study, we propose that anti-PLAA antibody may also work by either blocking $1\alpha,25(\text{OH})_2\text{D}_3$ docking to its receptor Pdia3 or by preventing the interaction between PLAA and Pdia3.

PLAA has homology with melittin (102), which is known to selectively interact with negatively charged lipids (170-172). Cholesterol is a major component of eukaryotic plasma membrane that is rich in lipid rafts and caveolae microdomains (173). Several studies in recent years have proposed that the rigid ring system in the structure of the cholesterol molecule could potentially form a stable complex with tryptophan in melittin, and consequently inhibit the lytic activity of this molecule (169,174). PLAA protein has multiple tryptophan residues in its structure suggesting that it may have the same mode of interaction as melittin with the plasma membrane. In agreement with studies done on melittin-cholesterol interactions, our results from plasma membrane fractionation studies showed that PLAA is localized in caveolae structures that are rich in cholesterol. PLAA peptide acts like melittin with respect to PKC activation, and the effects of both of these agents are additive with $1\alpha,25(\text{OH})_2\text{D}_3$, suggesting that they mediate their effects via similar mechanisms (11). However, different mechanisms may also be involved. While melittin mediates its effects via enhancing the interaction between the enzyme and its substrate, PLAA mediates its effects via enhancing the interaction between two proteins (175).

The present study supports the hypothesis that Pdia3 and Cav-1 play pivotal roles in mediating rapid membrane associated $1\alpha,25(\text{OH})_2\text{D}_3$ -dependent signaling via PLA_2 and PKC

(10,12). $1\alpha,25(\text{OH})_2\text{D}_3$ failed to stimulate rapid responses in shPdia3 MC3T3-E1 cells; there were significantly higher levels of PLA₂ and PKC activities in response to $1\alpha,25(\text{OH})_2\text{D}_3$ in ovxPdia3 MC3T3-E1 cells compared to wild type cells; and Pdia3 associated with PLAA in the presence of $1\alpha,25(\text{OH})_2\text{D}_3$. Moreover, in shCav-1 osteoblasts, Pdia3 failed to interact with PLAA in the presence of $1\alpha,25(\text{OH})_2\text{D}_3$ supporting the hypothesis that Cav-1 serves as a scaffolding protein creating the environment required for the interaction between Pdia3 and PLAA to occur.

Taken together with previously published studies (91), the results suggest the following pathway (Fig. 3.9): $1\alpha,25(\text{OH})_2\text{D}_3$ binds the Pdia3-Cav-1 membrane receptor complex in caveolae, triggering binding of PLAA to Pdia3. Next, PLA₂ is activated resulting in production of arachidonic acid, which is further metabolized via Cox-1 to release PGE₂. In GC cells, PGE₂ binds its EP1 receptor, a G-protein coupled receptor, activating PLC. Activated PLC hydrolyzes phosphatidylinositol 4,5-bisphosphate (PIP₂) releasing inositol 1,4,5-triphosphate (IP₃) and diacylglycerol (DAG), both of which function as second messengers. In this cascade, IP₃ activates IP₃ receptors on the smooth endoplasmic reticulum, opening the calcium channels, and increasing the intracellular calcium. Increased intracellular calcium and DAG work together to activate protein kinase C, and subsequently lead to the activation of ERK1/2. Eventually, $1\alpha,25(\text{OH})_2\text{D}_3$ induces caveolae-mediated endocytosis of $1\alpha,25(\text{OH})_2\text{D}_3$ -receptor complex, causing internalization of PLAA and Pdia3 and their loss from the plasma membrane.

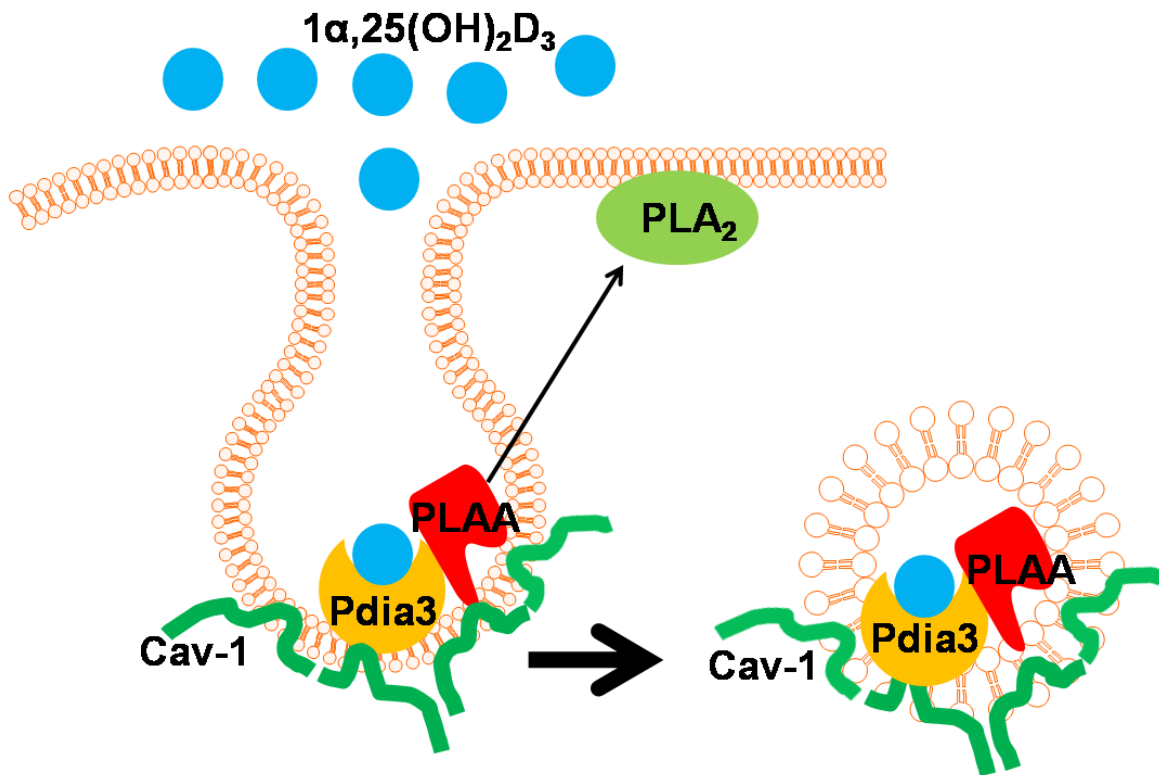


Figure 3.9: Proposed mechanism of $1\alpha,25(\text{OH})_2\text{D}_3$ stimulated rapid response in osteoblasts and chondrocytes.

CONCLUSION

In conclusion, we found a detailed mechanism of $1\alpha,25(\text{OH})_2\text{D}_3$ dependent rapid activation of protein kinase C via PLAA in chondrocytes and osteoblasts. PLAA is required for mediating the Pdia3-mediated actions of $1\alpha,25(\text{OH})_2\text{D}_3$ on growth zone chondrocytes and MC3T3-E1 osteoblasts. PLAA is localized with Pdia3 in caveolae domains of the plasma membrane, and they form protein complexes with Cav-1. PLAA interacts with Pdia3 only in the presence of $1\alpha,25(\text{OH})_2\text{D}_3$, suggesting it serves as one of the mediators of membrane-mediated actions of $1\alpha,25(\text{OH})_2\text{D}_3$. When MC3T3-E1 osteoblasts were treated with the BS³ crosslinker, appearance of a higher molecular band suggested that PLAA is a plasma membrane surface

protein. In agreement with crosslinking studies, anti-PLAA antibodies were able to block the effect of $1\alpha,25(\text{OH})_2\text{D}_3$ on rapid activation of PKC. When PLAA was stably knocked down in MC3T3-E1 osteoblasts, $1\alpha,25(\text{OH})_2\text{D}_3$ failed to rapidly activate PLA_2 and PKC or cause PGE_2 release. Recently, it has been reported that $1\alpha,25(\text{OH})_2\text{D}_3$ also mediates its effect through the activation of Src pathway in C2C12 skeletal muscle cells (176,177). Whether $1\alpha,25(\text{OH})_2\text{D}_3$ mediates its effects through activation of Src pathway in osteoblasts is still unknown and requires further investigation.

CHAPTER 4

MEMBRANE ACTIONS OF $1\alpha,25(\text{OH})_2\text{D}_3$ ARE MEDIATED BY CALCIUM/CALMODULIN-DEPENDENT PROTEIN KINASE II IN BONE AND CARTILAGE CELLS

INTRODUCTION

$1\alpha,25$ -dihydroxyvitamin D₃ [$1\alpha,25(\text{OH})_2\text{D}_3$], one of the bioactive metabolites of vitamin D₃, elicits its effects via two different mechanisms: the classical pathway that is vitamin D receptor (VDR) mediated, and rapid membrane signaling pathways (1-3). In growth zone chondrocytes (GC) from the costochondral cartilage and MC3T3-E1 osteoblasts, $1\alpha,25(\text{OH})_2\text{D}_3$ triggers a rapid increase in phospholipase A₂ (PLA₂) activity, releasing arachidonic acid (AA) within 15 seconds (4,5) and causing increased protein kinase C alpha (PKC α) activity within 3 minutes (6). AA can either increase PKC α activity directly (7), or it is processed further to prostaglandin E₂ (PGE₂), which acts via its EP1 receptor to increase cyclic AMP and ultimately PKC (4). PLA₂ generates lysophospholipid (LPL) in addition to AA (8). We have shown that LPL produced in response to $1\alpha,25(\text{OH})_2\text{D}_3$ -dependent activation of PLA₂ together with G α_q activates phosphatidylinositol-specific phospholipase C beta (PLC β), generating diacylglycerol (DAG) and inositol 1,4,5-trisphosphate (IP₃) (8,9). DAG binds PKC α and triggers its recruitment to the plasma membrane (10). IP₃ activates the release of Ca²⁺ ions from the endoplasmic reticulum, required for PKC α activation.

This implicates PLA₂ activation as a key component of the Pdia3-dependent signaling pathway. We previously reported that PLA₂ activating protein (PLAA) is required to process the signal from the Pdia3 receptor complex to cytosolic PLA₂ (cPLA₂) (11). Anti-PLAA antibodies

as well as *Plaa* knockdown both block $1\alpha,25(\text{OH})_2\text{D}_3$ -dependent stimulation of PLA_2 (11). PLAA exists in plasma membrane caveolae of osteoblasts and chondrocytes where it interacts directly with *Pdia3* and caveolin-1 (*Cav-1*) to initiate the rapid signaling via PLA_2 . $1\alpha,25(\text{OH})_2\text{D}_3$ treatment does not change the abundance of PLAA in caveolae (11), indicating that other mechanisms are involved in mediating the signal from caveolae to cPLA_2 in the plasma membrane. However, the signaling molecules linking PLAA to cPLA_2 remain to be identified.

Previous studies have demonstrated that melittin, a bee venom PLA_2 activator homologous to PLAA, binds to calmodulin (CaM) in the presence of Ca^{2+} (12), suggesting that CaM is a likely candidate for mediating the $1\alpha,25(\text{OH})_2\text{D}_3$ signal from PLAA. The calmodulin inhibitor, W-7 blocks norepinephrine-induced prostacyclin synthesis in vascular smooth muscle cells, which is suggestive of CaM's action upstream of cPLA_2 (13). CaM is a highly conserved 17 kDa soluble protein, which serves as a major Ca^{2+} sensor in eukaryotic cells (14). Upon Ca^{2+} binding, CaM binds its target proteins, including Ca^{2+} /calmodulin-dependent protein kinase II (CaMKII; encoded by the *Camk2* gene). Such protein interaction alters the function of target proteins, thereby transducing the Ca^{2+} signals. CaM has a diverse subcellular distribution profile including the cytoplasm (15), within organelles (16) and associated with the plasma membrane (17) or organelle membranes (18), indicative of differing functions.

cPLA_2 activity has also been reported to be regulated by CaMKII (19). As noted above for CaM, norepinephrine-induced cPLA_2 activation and AA release are inhibited in vascular smooth muscle cells treated with the CaMKII inhibitor, KN-93 or with the *Camk2* antisense oligonucleotide (19). This suggests that CaMKII may play a role in transducing the $1\alpha,25(\text{OH})_2\text{D}_3$ signal to cPLA_2 as well. To date, over 30 various splice-variants of four *Camk2* isoforms, *Camk2a*, *Camk2b*, *Camk2d* and *Camk2g* have been identified. Activated CaMKII

modulates the activity of several transcription factors, including cAMP-responsive element-binding protein (CREB) (20), which has been shown to be phosphorylated via a $1\alpha,25(\text{OH})_2\text{D}_3$ -dependent mechanism (21). CREB is known to bind to two AP-1 sites and a cAMP responsive element-like site on the osteopontin promoter, participating in the induction of osteopontin gene expression (22). $1\alpha,25(\text{OH})_2\text{D}_3$ stimulates alkaline phosphatase activity (4) and osteopontin production (23), markers of osteoblast maturation, via its membrane-mediated events. Whether CaMKII mediates the biological consequences of rapid responses to $1\alpha,25(\text{OH})_2\text{D}_3$ is not known.

In this study, we first examined $1\alpha,25(\text{OH})_2\text{D}_3$ stimulated rapid activation of CaMKII in MC3T3-E1 osteoblasts and GC chondrocytes. Second, we investigated the roles of CaM and CaMKII in $1\alpha,25(\text{OH})_2\text{D}_3$ rapid signaling and its consequent biological effects using MC3T3-E1 cell model. Third, we evaluated the effects of $1\alpha,25(\text{OH})_2\text{D}_3$ treatment on interactions between CaM and the Pdia3 receptor complex.

MATERIALS AND METHODS

Reagents

PLAA was purchased from Enzo Life Sciences International, Inc. (Plymouth Meeting, PA). $1\alpha,25(\text{OH})_2\text{D}_3$ was purchased from Biomol (Plymouth Meeting, PA). The anti-PLAA polyclonal antibody was designed and developed by Strategic Diagnostics Inc. (Newark, DE), using Genomic Antibody Technology™. The selected 100 amino acid long region was 100% identical among three rat PLAA isoforms and 97% identical to mouse PLAA. Rabbit antiserum against the N-terminal peptide of Pdia3 was purchased from Alpha Diagnostic International (San Antonio, TX) (165). A polyclonal antibody to Cav-1 was purchased from Santa Cruz Biotechnology (sc-894, Santa Cruz, CA); cPLA₂ polyclonal antibody was from Cell Signaling

Technology (2832, Danvers, MA); pan CaMKII monoclonal antibody (4436) and CaMKII- α polyclonal antibody (3357) were from Cell Signaling Technology (Danvers, MA); pan cadherin polyclonal antibody was from Abcam (ab6529, San Francisco, CA); and a monoclonal antibody to CaM was from Millipore (05-173, Billerica, MA); KN-93 and myristoylated calmodulin kinase IINtide were from EMD Biosciences (Billerica, MA).

Cell Culture

Wild-type mouse MC3T3-E1 osteoblast-like cells (CRL-2593) were purchased from ATCC (Manassas, VA, USA). Silenced *Pdia3* (shPdia3), silenced *Plaa* (shPlaa), silenced *Cav1* (shCav-1) and silenced *Vdr* (shVdr) MC3T3-E1 cells were generated and characterized in our lab previously (10,125,178). Stable knockdown of *Camk2a* was achieved using MISSION™ shRNA lentiviral transduction particles (SHVRS-NM_009792, Sigma Aldrich, St. Louis, MO). Five different sequences were generated against the *Camk2a* mRNA and were incorporated into the lentiviral particles. MC3T3-E1 cells were plated at a density of 20,000 cells/cm² in 24-well plates, and cultured in minimum essential medium alpha (α -MEM) supplemented with 10% fetal bovine serum (FBS), 1% penicillin/streptomycin (P/S) and 8 μ g/ml hexadimethrine bromide (500 μ l/well). In our system, lentiviral particles transfected MC3T3-E1 cells at a multiplicity of infection (MOI) of 7.5. The selection of successfully transfected cells was achieved by culturing cells containing the *Camk2a* shRNA or empty vectors for 2 weeks in medium containing 2.0 μ g/ml of puromycin. The success of silencing *Camk2a* was evaluated by measuring the expression of CaMKII- α protein in comparison to wild-type cells using Western blots and anti-CaMKII- α antibody. A stably silenced MC3T3-E1 cell line was established for *Camk2a* (shCamk2a), confirmed by Western blots of whole cell lysates. Of the five clones examined, Western blots of whole cell lysates from wild-type MC3T3-E1 cells showed strong bands for

CaMKII- α , but the intensity of these bands was decreased by 84% compared to the wild-type in clone 71 cells (data not shown). Stable knockdown of *Camk2b* was achieved by transducing wild-type MC3T3-E1 cells with *Camk2b* shRNA lentiviral transduction particles (SHVRS-NM_007595, Sigma Aldrich) as described above. Western blots of whole cell lysates of the five examined clones showed 89% reduction in intensity of CaMKII- β band in clone 475 using anti-pan CaMKII antibody (data not shown).

Wild-type MC3T3-E1, shPlaa, shCav-1, shPdia3, shVdr, shCamk2a and shCamk2b MC3T3-E1 cells were plated at 10,000 cells/cm², and cultured in puromycin-free α -MEM containing 10% fetal bovine serum (FBS) and 1% penicillin/streptomycin (P/S). To induce osteoblastic differentiation of MC3T3-E1 cells, the media were replaced with α -MEM supplemented with 10% FBS, 1% P/S and 1% ascorbic acid 24 hours after plating and then every 48 hours. After 10 days in culture, shPlaa, shCav-1, shPdia3 and shVdr cells were used for experiments. Cultures of shCamK2a and shCamK2b were used at approximately day 4 after plating.

Costochondral cartilage growth zone chondrocytes (GC) used in these experiments were isolated from 100 to 125 g male Sprague-Dawley rats (Harlan, Indianapolis, IN). The rats were at the end of their adolescent growth spurt; therefore, their long bones were growing at a reduced rate. The culture system used in this study was described previously in detail (11,166). Confluent cultures (approximately day 7) were used for the experiments described below.

Regulation of CaMKII Activity

To determine the time-point at which $1\alpha,25(\text{OH})_2\text{D}_3$ activates CaMKII, GC and MC3T3-E1 cells were treated for 3, 6, 9 and 15 minutes with 10^{-8} M $1\alpha,25(\text{OH})_2\text{D}_3$ and cell layer lysates were assayed for CaMKII activity using a commercial kit (SignaTECT® Ca²⁺/Calmodulin-

Dependent Protein Kinase Assay System, V8161, Promega). To determine if $1\alpha,25(\text{OH})_2\text{D}_3$ activates CaMKII in a dose-dependent manner, MC3T3-E1 cells were treated with 10^{-10} to 10^{-8} M $1\alpha,25(\text{OH})_2\text{D}_3$ for 15 minutes.

KN-93 is a cell-permeable inhibitor of CaMKII that binds to the CaM binding site of the enzyme and prevents the association of CaM with CaMKII (179). Myristoylated calmodulin kinase IINtide (mer-CaMKIINtide) is a 28-residue cell-permeable CaMKII inhibitor peptide derived from CaMKIIN, an endogenous inhibitory protein of CaMKII, with high selectivity for inhibition of CaMKII and little effect on CaMKI, CaMKIV, CaMKK or PKC (180). The peptide sequence corresponds to inhibitory domain of CaMKII- α and CaMKII- β (180). To determine the effects of KN-93 or mer-CaMKIINtide on $1\alpha,25(\text{OH})_2\text{D}_3$ dependent CaMKII activation in growth plate chondrocytes, confluent GC cells were pretreated with either KN-93 or mer-CaMKIINtide at 1.25, 2.5 and 5 μM concentrations for 30 minutes. Next, cells were treated with 10^{-8} M $1\alpha,25(\text{OH})_2\text{D}_3$ for 15 minutes. Cell layer lysates were assayed for CaMKII activity.

To determine whether $1\alpha,25(\text{OH})_2\text{D}_3$ activates CaMKII via a Pdia3-dependent mechanism, MC3T3-E1 osteoblasts were pretreated with anti-Pdia3 antibody for 30 minutes, and next treated with 10^{-8} M $1\alpha,25(\text{OH})_2\text{D}_3$ for 15 minutes. Cell layers were collected for subsequent CaMKII assay. To assess the roles of Pdia3 and VDR in activation of CaMKII by $1\alpha,25(\text{OH})_2\text{D}_3$, wild-type, silenced-Pdia3 and silenced-Vdr MC3T3-E1 cells were treated with 10^{-8} M $1\alpha,25(\text{OH})_2\text{D}_3$ for 15 minutes. Cell layer lysates were collected were assayed for CaMKII activity.

To determine the requirement for intact caveolae in the regulation of CaMKII by $1\alpha,25(\text{OH})_2\text{D}_3$ we used two approaches. Methyl-beta-cyclodextrin ($\beta\text{-CD}$) is a chemical that does not enter cells but can bind cholesterol and remove it from the plasma membranes leading to

disruption of lipid rafts and caveolae. To determine the effects of β -CD on CaMKII activation, MC3T3-E1 osteoblasts were treated with 10 mM β -CD for 30 minutes in serum-free medium, as described previously (12). At the end of the incubation, the cell layers were rinsed with serum free medium and then treated with 10^{-8} M $1\alpha,25(\text{OH})_2\text{D}_3$ for 15 minutes. The cell layer lysates were collected for CaMKII assay. To determine the effects of *Cav1* silencing on CaMKII activity, wild-type and silenced-Cav-1 MC3T3-E1 cells were treated with 10^{-8} M $1\alpha,25(\text{OH})_2\text{D}_3$ for 15 minutes prior to assay.

In order to examine the relationship between PLAA and CaMKII, MC3T3-E1 cells were pretreated with anti-PLAA antibody for 30 minutes, and next treated with 10^{-8} M $1\alpha,25(\text{OH})_2\text{D}_3$ for 15 minutes. In addition, wild-type and silenced-Plaa MC3T3-E1 cells were treated with 10^{-8} M $1\alpha,25(\text{OH})_2\text{D}_3$ for 15 minutes prior to assay of CaMKII activity. The direct effect of PLAA on CaMKII was determined by treating MC3T3-E1 cells with 10^{-8} to 10^{-6} M PLAA peptide for 15 minutes prior to assay of cell layer lysates. Whether caveolae are required for PLAA-mediated CaMKII activation, MC3T3-E1 osteoblasts were treated with 10 mM β -CD for 30 minutes in a serum-free medium as described above. After rinsing with serum free medium, cells were treated with 10^{-6} M PLAA peptide for 15 minutes, followed by CaMKII assay.

GC chondrocytes were used to investigate the role of CaM in $1\alpha,25(\text{OH})_2\text{D}_3$ -dependent CaMKII activation. Confluent cultures were pretreated with the CaM inhibitor W-7 at 0.1, 1 and 10 μM concentrations for 30 minutes. Next, cells were treated with 10^{-8} M $1\alpha,25(\text{OH})_2\text{D}_3$ for 15 minutes. Cell layer lysates were assayed for CaMKII activity.

Regulation of PLA_2 Activity

To determine if CaMKII is required for $1\alpha,25(\text{OH})_2\text{D}_3$ -dependent PLA_2 activation, confluent GC chondrocytes were treated for 30 minutes with 1.25, 2.5 and 5 μM of either KN-93

or mer-CaMKIINtide, followed by 10^{-8} M $1\alpha,25(\text{OH})_2\text{D}_3$ for 15 minutes. After washing the cell layers with PBS, the cell layers were lysed and assayed for PLA₂ activity using a commercially available kit (cPLA₂ Assay kit, 765021, Cayman Chemical, Ann Arbor, MI). PLA₂ data were normalized to total protein (Pierce BCA Protein Assay, Thermo Fisher Scientific).

Regulation of PGE₂ Release

To determine if CaMKII is involved in $1\alpha,25(\text{OH})_2\text{D}_3$ -activated PGE₂ release, confluent GC chondrocytes were treated for 30 minutes with 1.25, 2.5 and 5 μM of either KN-93 or mer-CaMKIINtide, followed by 10^{-8} M $1\alpha,25(\text{OH})_2\text{D}_3$ for 15 minutes. At the end of the incubation, the media were acidified and PGE₂ was measured using a commercially available kit (Prostaglandin E₂ [¹²⁵I]-RIA kit, NEK020001K, Perkin Elmer, Waltham, MA). PGE₂ data were normalized to total DNA (Quant-iT™ PicoGreen® dsDNA Assay kit, P11496, Invitrogen).

CaM was inhibited by treating GC chondrocytes with 0.6, 2.5 and 10 μM W-7 for 30 minutes. Next, cells were treated with 10^{-8} M $1\alpha,25(\text{OH})_2\text{D}_3$ for 15 minutes. At the end of the incubation, the media were acidified and PGE₂ was measured. PGE₂ data were normalized to total DNA.

Regulation of PKC Activity

To determine whether CaMKII mediates the stimulatory effects of $1\alpha,25(\text{OH})_2\text{D}_3$ on PKC, GC chondrocytes were treated for 30 minutes with 1.25, 2.5 and 5 μM of either KN-93 or mer-CaMKIINtide, followed by 10^{-8} M $1\alpha,25(\text{OH})_2\text{D}_3$ for 15 minutes. Cell layers were washed with PBS and lysed in RIPA buffer (20 mM Tris-HCl, 150 mM NaCl, 5mM disodium EDTA, 1% Nonidet P-40). PKC activity was measured using a commercially available kit (Protein Kinase C Biotrak Enzyme Assay, RPN77, GE Healthcare). PKC data were normalized to total protein (Pierce BCA Protein Assay, Thermo Fisher Scientific).

The special role of CaM was determined by treating the cells for 30 minutes with 0.6, 2.5 and 10 μM W-7, followed by 10^{-8} M $1\alpha,25(\text{OH})_2\text{D}_3$ for 15 minutes.

Camk2a and *Camk2b* silencing was used to determine which CaMKII isoform was responsible for the rapid response to $1\alpha,25(\text{OH})_2\text{D}_3$. Wild-type and *Camk2a* and *Camk2b* silenced MC3T3-E1 cells were treated for 15 minutes with 10^{-8} M $1\alpha,25(\text{OH})_2\text{D}_3$. Cell layer lysates were assayed for PLA₂, PKC and CaMKII activities as described above. PLA₂, PKC and CaMKII were normalized to total protein. PGE₂ data were normalized to total DNA.

Regulation of Alkaline Phosphatase Activity

Changes in alkaline phosphatase specific activity, an early marker of osteoblast maturation, were used as an outcome measure of the $1\alpha,25(\text{OH})_2\text{D}_3$ rapid membrane-mediated signaling. The requirement for CaMKII in $1\alpha,25(\text{OH})_2\text{D}_3$ rapid membrane-mediated alkaline phosphatase activation was assessed by pretreating wild-type MC3T3-E1 cells with 5 μM of mer-CaMKIINtide for 30 minutes, followed by 10^{-8} M $1\alpha,25(\text{OH})_2\text{D}_3$ for 15 minutes. At the end of the treatment, the media were replaced by fresh media. 24 hours later, the cell layers were lysed by sonication in 0.05% Triton X-100 (Sigma Aldrich). Alkaline phosphatase specific activity was measured by determining *p*-nitrophenol (pNP) release from *p*-nitrophenylphosphate (pNPP) at pH 10.2 in lysates. Enzyme activity data were normalized to total protein content.

The requirements for CaMKII- α and CaMKII- β were assessed by treating wild-type, sh*Camk2a* and sh*Camk2b* MC3T3-E1 cells with 10^{-8} M $1\alpha,25(\text{OH})_2\text{D}_3$ for 15 minutes. At the end of the incubation, the media were replaced by fresh media. 24 hours later, the cell layers were lysed and assayed for alkaline phosphatase activity. The requirement for CaM in $1\alpha,25(\text{OH})_2\text{D}_3$ rapid membrane-mediated alkaline phosphatase activation was assessed by pre-incubating wild-type MC3T3-E1 cells with 5 μM of W-7 as described above.

Regulation of Osteopontin Production

Alterations in osteopontin levels secreted into the media were used as an outcome measure of the $1\alpha,25(\text{OH})_2\text{D}_3$ rapid membrane-mediated signaling. This was assessed by pretreating wild-type MC3T3-E1 cells with 5 μM of mer-CaMKIINtide for 30 minutes followed by 10^{-8} M $1\alpha,25(\text{OH})_2\text{D}_3$ for 15 minutes. At the end of the treatment, the media were replaced by fresh media. 24 hours later osteopontin in the media was measured by ELISA using a commercial mouse osteopontin ELISA kit (R&D Systems, Minneapolis, MN). Osteopontin values were normalized to total DNA. The requirements for CaMKII- α and CaMKII- β and CaM was determined as above.

Plasma Membranes and Caveolae Isolation

Plasma membranes and caveolae were isolated using a detergent-free method as described previously (121). MC3T3-E1 cells (cultured for 10 days post-plating) were treated with either 10^{-8} M $1\alpha,25(\text{OH})_2\text{D}_3$ or vehicle (ethanol) for 15 minutes. The cells were harvested by scraping while in isolation buffer (0.25 M sucrose, 1 mM EDTA, 20 mM Tricine, pH 7.8) and were homogenized using a tissue grinder (20 strokes; 10 strokes clockwise and 10 strokes counter-clockwise). Homogenates were centrifuged at 20,000 X g for 10 minutes. The pellet, including nucleus, mitochondria, and endoplasmic reticulum was discarded and the supernatant was collected, and placed on top of isolation buffer containing 30% Percoll (GE Healthcare, Piscataway, NJ). The samples were centrifuged at 84,000 X g for 30 minutes. Syringe needles (5G) were used to collect the plasma membrane fraction from the gradient column. The isolated fraction was layered over a 10-20% OptiPrep gradient (Sigma Aldrich), and the gradient was centrifuged at 52,000 X g for another 4 hours. Plasma membrane sub-fractions were collected

from the top to the bottom of the tube, which resulted in isolation of thirteen fractions. Caveolae were observed as an opaque band, which was collected in fraction 3.

Western Blots

Proteins were separated using polyacrylamide gel electrophoresis. Whole cell lysates, plasma membranes, and plasma membrane fractions (50µg protein) were loaded onto 4–20% Mini-PROTEAN® TGX™ precast polyacrylamide gels (Bio-Rad, Hercules, CA), and at the end of the run, the proteins were transferred from gels to nitrocellulose membranes using an iBlot Dry Blotting System (Invitrogen). Next, the membrane was incubated with 1% bovine serum albumin (BSA) in PBS. Subsequently, the membranes were incubated with antibodies against CaMKII, CaM, cPLA₂, Cav-1, pan cadherin or GAPDH overnight. The membranes were incubated with goat anti-rabbit or goat anti-mouse horseradish peroxidase-conjugated secondary antibodies (Bio-Rad, Hercules, CA) in PBS containing 1% BSA after washing three times with PBS containing 0.05% Tween-20. The membranes were incubated with the secondary antibody only for one hour. Following three washes with PBS containing 0.05% Tween-20 (three times, ten minutes each), membranes were developed using the LumiSensor™ Plus Chemiluminescent HRP Substrate kit (GenScript, Piscataway, NJ) and imaged with the VersaDoc imaging system (Bio-Rad, Hercules, CA).

Immunoprecipitation

MC3T3-E1 osteoblasts were treated with either 10⁻⁸ M 1α,25(OH)₂D₃ or vehicle (ethanol) for 15 minutes. The cell layers were washed with PBS, lysed and sonicated in RIPA buffer containing 100mM NaF, protease inhibitor cocktail (Sigma Aldrich) and 1 mM phenylmethylsulfonyl fluoride (PMSF). In order to preclear the cell extracts, protein samples (1mg) were incubated with 5µg of rabbit IgG (1 hour, 4°C) and next incubated with protein A-

agarose beads (EMD Chemicals, Gibbstown, NJ, USA) for 2 hours at 4°C. The beads were pelleted by centrifugation at 1,000 *X g* (1 minute, 4°C). To immunoprecipitate the Pdia3 protein complex, pre-cleared protein samples were mixed with anti-Pdia3 antibodies and incubated at 4°C overnight with continuous agitation. Protein A-agarose beads were added to the mixture and the mixture was incubated at 4°C for two additional hours. The beads were pelleted and the pellets washed three times with PBS. Precipitated proteins were eluted by boiling beads in Tris-glycine SDS sample loading buffer (Bio-Rad) containing 5.0% beta-mercaptoethanol for 5 minutes. The immunoprecipitated samples were subjected to Western blot. In order to lower the background in the images, a ONE-HOUR IP-Western Kit (Genscript) was used.

To immunoprecipitate PLAA and CaM protein complexes, the Dynabeads® Protein A immunoprecipitation kit (Invitrogen) was used. Anti-CaM and anti-PLAA antibodies were covalently coupled to the Dynabeads Protein A according to the manufacturer's protocol. Pre-cleared protein samples were mixed with either anti-PLAA or anti-CaM antibodies coated Dynabeads and incubated at 4°C overnight with continuous agitation. Dynabeads were recovered using a magnet and were washed three times with PBS containing 0.05% Tween-20. Precipitated proteins were eluted by resuspending the beads in Elution Buffer and boiling beads in Tris-glycine SDS sample loading buffer (Bio-Rad) containing 5.0% (v/v) beta-mercaptoethanol for 5 minutes. The immunoprecipitated samples were subjected to Western blot. A ONE-HOUR IP-Western Kit (Genscript) was used to lower the background in the images.

Statistical Analysis

For each experiment, each data point represents the mean \pm standard error of the mean (SEM) for six individual cultures. Each experiment was repeated at least three times to ensure the validity of the data. Statistical analysis was performed using the GraphPad Prism software

(version 5, GraphPad Software, Inc., San Diego, CA). Statistical significance was assessed by analysis of variance and post hoc testing performed using Bonferroni's modification of Student's t-test for multiple comparisons. P-values <0.05 were considered significant.

RESULTS

Effect of $1\alpha,25(\text{OH})_2\text{D}_3$ on CaMKII Activation in Growth Zone Chondrocytes and MC3T3-E1 Osteoblasts

Following an initial decrease in CaMKII activity, $1\alpha,25(\text{OH})_2\text{D}_3$ caused a time and dose dependent increase in CaMKII activity in chondrocytes and osteoblasts. This effect was rapid, occurring by 6 minutes in GC cells (Fig. 4.1A) and within 9 minutes in MC3T3-E1 cells (Fig.4.1B). $1\alpha,25(\text{OH})_2\text{D}_3$ caused a significant increase in CaMKII activity only at its highest experimental dose, 10^{-8} M, in GC cells (Fig. 4.1C) and MC3T3-E1 osteoblasts (Fig. 4.1D).

Effect of CaMKII Inhibition On Rapid $1\alpha,25(\text{OH})_2\text{D}_3$ Membrane-Mediated Signaling and the Downstream Biological Responses

The $1\alpha,25(\text{OH})_2\text{D}_3$ -stimulated increase in CaMKII activity was blocked by the CaMKII inhibitor KN-93 in a dose dependent manner (Fig. 4.2A). The effect of KN-93 on $1\alpha,25(\text{OH})_2\text{D}_3$ -dependent cPLA₂ activity was also dose-dependent, at the highest concentration of inhibitor, activity was 50% that of the control cultures (Fig. 4.2B). Similarly, KN-93 blocked production of PGE₂ in response to $1\alpha,25(\text{OH})_2\text{D}_3$ (Fig. 4.2C) as well as the stimulatory effect of $1\alpha,25(\text{OH})_2\text{D}_3$ on PKC activity (Fig. 4.2D). Treatment of the cells with mer-CaMKIINtide had comparable effects to KN-93 on CaMKII (Fig. 4.2E), cPLA₂ (Fig. 4.2F), PGE₂ release (Fig. 4.2G) and PKC (Fig. 4.2H). Moreover, mer-CaMKIINtide significantly reduced the stimulatory effect of a 15

minute treatment with $1\alpha,25(\text{OH})_2\text{D}_3$ on osteopontin production (Fig. 4.2I) and alkaline phosphatase activity (Fig. 4.2J) at 24 hours.

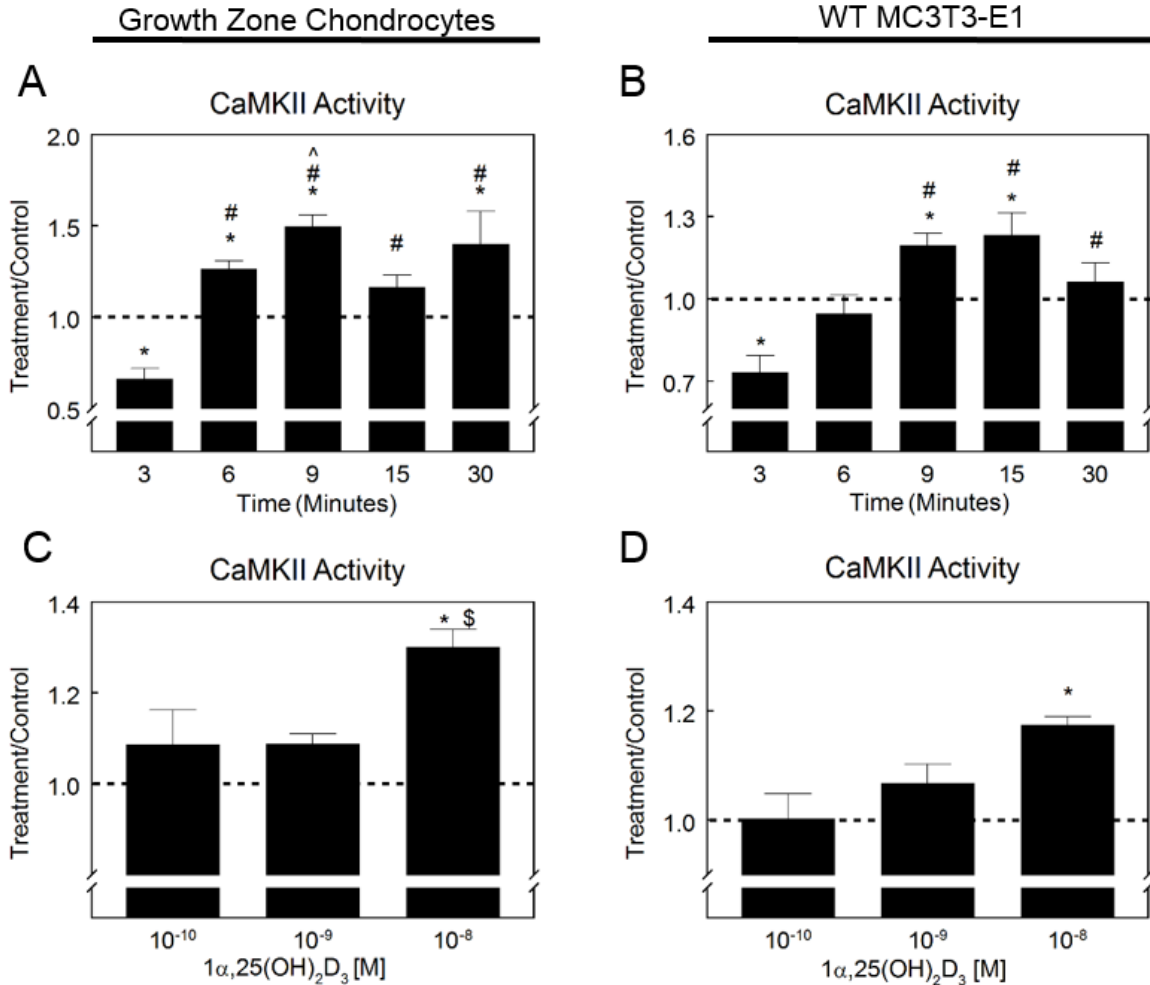


Figure 4.1: Effect of $1\alpha,25(\text{OH})_2\text{D}_3$ on CaMKII activation in growth zone chondrocytes and MC3T3-E1 osteoblasts. Growth zone chondrocytes (A) and MC3T3-E1 osteoblasts (B) were treated with $1\alpha,25(\text{OH})_2\text{D}_3$ for 3, 6, 9, 15 and 30 minutes. CaMKII activity was measured as described and normalized to total protein level. Growth zone chondrocytes (C) were treated for 9 minutes and MC3T3-E1 osteoblasts (D) were treated for 15 minutes with 10^{-10} , 10^{-9} and 10^{-8} M $1\alpha,25(\text{OH})_2\text{D}_3$. CaMKII activity was measured as described and normalized to total protein level. Treatment over control ratios were calculated for each parameter. The dashed line represents the value for the control cultures, which was set to 1. * $p < 0.05$, $1\alpha,25(\text{OH})_2\text{D}_3$ treatment vs. control; # $p < 0.05$, versus 3 minutes; ^ $p < 0.05$, versus 6 minutes; § $p < 0.05$, versus 10^{-9} M $1\alpha,25(\text{OH})_2\text{D}_3$. Each figure is a representative experiment repeated three times with similar results.

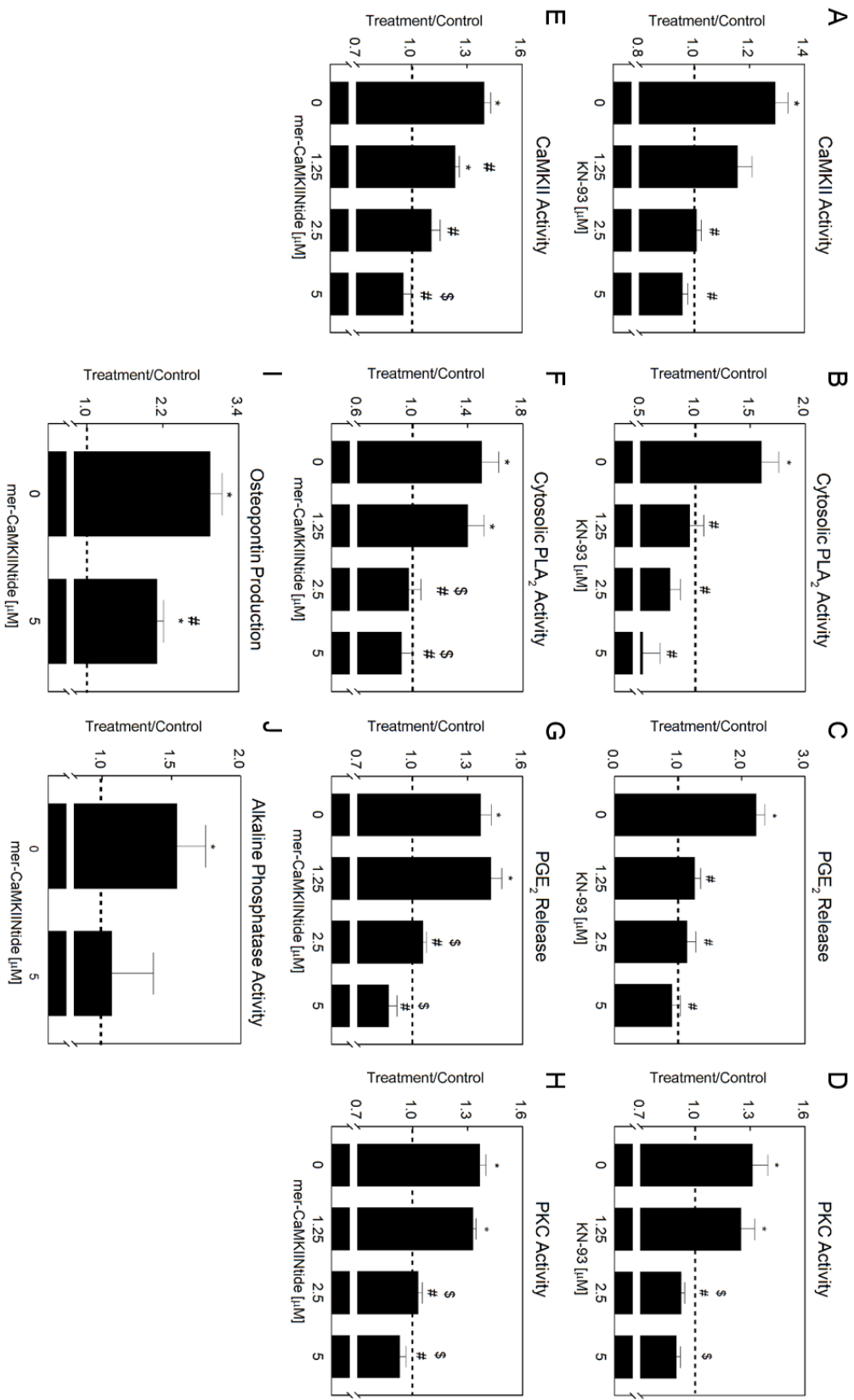


Figure 4.2: Effect of CaMKII inhibition on rapid $1\alpha,25(\text{OH})_2\text{D}_3$ membrane-mediated activation of CaMKII, PLA₂, PKC, and PGE₂ release and downstream physiological effects. GC chondrocytes were treated with 0, 1.25, 2.5, and 5 μM of KN-93 for 30 minutes. CaMKII activity (A), PLA₂ activity (B), PGE₂ release (C) and PKC activity (D) were measured as described and normalized to total protein level. PGE₂ values were normalized to total DNA. * $p < 0.05$, treatment *versus* control; # $p < 0.05$, *versus* 0 μM KN-93; \$ $p < 0.05$, *versus* 1.25 μM KN-93. GC chondrocytes were treated with 0, 1.25, 2.5, and 5 μM of mer-CaMKIINtide for 30 minutes. CaMKII activity (E), PLA₂ activity (F), PGE₂ release (G) and PKC activity (H) were measured as described and normalized to total protein level. PGE₂ values were normalized to total DNA. * $p < 0.05$, treatment *versus* control; # $p < 0.05$, *versus* 0 μM mer-CaMKIINtide; \$ $p < 0.05$, *versus* 1.25 μM mer-CaMKIINtide. MC3T3-E1 osteoblasts were treated with 0 or 5 μM of mer-CaMKIINtide for 30 minutes and next they were treated with $1\alpha,25(\text{OH})_2\text{D}_3$ for 15 minutes. The media containing $1\alpha,25(\text{OH})_2\text{D}_3$ were replaced with fresh media. 24 hours later, osteopontin production (I) and alkaline phosphatase activity (J) were measured as described and normalized to total DNA and total protein level, respectively. * $p < 0.05$, treatment *versus* control; # $p < 0.05$, *versus* 0 μM mer-CaMKIINtide. Treatment over control ratios were calculated for each parameter. The dashed line represents the value for the control cultures, which was set to 1. Each figure is a representative experiment repeated three times with similar results.

Effects of *Camk2a* and *Camk2b* Silencing on Rapid Actions of $1\alpha,25(\text{OH})_2\text{D}_3$ and the Downstream Biological Responses

CaMKII- α is the isoform responsible for mediating the effects of $1\alpha,25(\text{OH})_2\text{D}_3$. Unlike wild-type and shCamk2b MC3T3-E1 cells, shCamk2a osteoblasts did not respond to $1\alpha,25(\text{OH})_2\text{D}_3$ with an increase in PLA₂ activity (Fig. 4.3A). Similarly, $1\alpha,25(\text{OH})_2\text{D}_3$ had no effect on PGE₂ release (Fig. 4.3B) and PKC activity (Fig. 4.3C) in shCamk2a MC3T3-E1 cells. These effects were specific to CaMKII- α , since the MC3T3-E1 cells transfected with empty vectors responded to $1\alpha,25(\text{OH})_2\text{D}_3$ like the wild-type cells.

Camk2a silencing significantly reduced the $1\alpha,25(\text{OH})_2\text{D}_3$ -stimulated increase in alkaline phosphatase activity but had no effect on osteopontin production. Treatment of wild-type and shCamk2b MC3T3-E1 cells with $1\alpha,25(\text{OH})_2\text{D}_3$ for 15 minutes led to a significant increase in alkaline phosphatase activity at 24 hours, whereas shCamk2a osteoblasts failed to activate the enzyme (Fig. 4.D). Treatment of wild-type, shCamk2a and shCamk2b MC3T3-E1 cells with

1 α ,25(OH) $_2$ D $_3$ for 15 minutes led to a significant increase in osteopontin production at 24 hours with shCamk2b osteoblasts showing significantly higher levels of osteopontin production compared to the wild-type cells (Fig. 4.3E). We validated the specificity of the knockdown by examining CaMKII activity in the silenced cells. 1 α ,25(OH) $_2$ D $_3$ treatment of wild-type and shCamk2b MC3T3-E1 cells led to a significant increase in CaMKII activity while shCamk2a osteoblasts did not respond to 1 α ,25(OH) $_2$ D $_3$ with an increase in CaMKII activity (Fig. 4.3F).

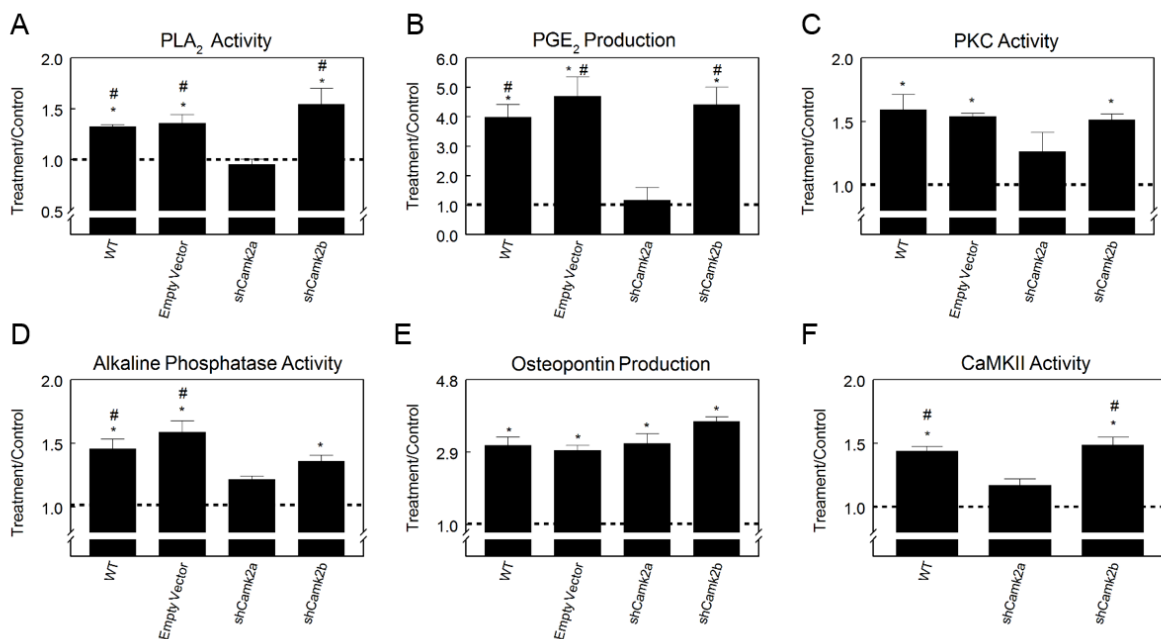


Figure 4.3: Effect of 1 α ,25(OH) $_2$ D $_3$ on PLA $_2$, PKC, CaMKII and alkaline phosphatase activities and PGE $_2$ and osteopontin production in wild type, shCamk2a and shCamk2b MC3T3-E1 cells. 1 α ,25(OH) $_2$ D $_3$ effect on PLA $_2$ activity (A), PGE $_2$ release (B), PKC activity (C), alkaline phosphatase activity (D), osteopontin production (E) and CaMKII activity (F) of WT, shCamk2a and shCamk2b MC3T3-E1 cells. Treatment over control ratios were calculated for each parameter. The dashed line represents the value for the control cultures, which was set to 1. * p <0.05, treatment versus control; # p <0.05, versus shCamk2a; \$ p <0.05, versus Empty Vector. Each figure is a representative experiment repeated three times with similar results.

Roles of Pdia3, Cav-1 and Caveolae in 1 α ,25(OH) $_2$ D $_3$ Membrane-mediated Activation of CaMKII in MC3T3-E1 Osteoblasts

In MC3T3-E1 osteoblasts, $1\alpha,25(\text{OH})_2\text{D}_3$ activation of CaMKII depends on upstream actions of Pdia3, Cav-1 and caveolae microdomains. Anti-Pdia3 antibody significantly reduced the $1\alpha,25(\text{OH})_2\text{D}_3$ -dependent increase in CaMKII activity in MC3T3-E1 osteoblasts (Fig. 4.4A), whereas IgG had no effect. Similarly, shPdia3 osteoblasts failed to rapidly respond to $1\alpha,25(\text{OH})_2\text{D}_3$ with an increase in CaMKII activity (Fig. 4.4B). In contrast to shPdia3 osteoblasts, shVdr cells rapidly activated CaMKII in response to $1\alpha,25(\text{OH})_2\text{D}_3$ within 15 minutes (Fig. 4.4C). Unlike wild-type cells, shCav-1 osteoblasts failed to rapidly activate CaMKII in response to $1\alpha,25(\text{OH})_2\text{D}_3$ (Fig. 4.4D). In addition, treatment of osteoblasts with β -CD altered the response of cells to $1\alpha,25(\text{OH})_2\text{D}_3$. Pretreatment with β -CD abrogated the $1\alpha,25(\text{OH})_2\text{D}_3$ -dependent increase in CaMKII activity in MC3T3-E1 osteoblasts (Fig. 4.4E).

Western blots of whole cell lysates demonstrated that MC3T3-E1 osteoblasts possess CaMKII- β , CaMKII- α and cPLA₂, and $1\alpha,25(\text{OH})_2\text{D}_3$ treatment alters the abundance of these proteins in the plasma membrane. Comparison of the intensity of CaMKII- β bands on the Western blot relative to cadherin loading bands, showed that $1\alpha,25(\text{OH})_2\text{D}_3$ reduced the intensity of CaMKII- β bands by 29% compared to the control group (Fig. 4.4F). Comparison of the intensity of CaMKII- α bands on the Western blot relative to cadherin bands, showed nearly a 19% reduction in the intensity of CaMKII- α bands compared to the control group (Fig. 4.4F). Similarly, comparison of the intensity of cPLA₂ bands on the Western blot relative to cadherin bands, showed almost a 29% reduction in the intensity of cPLA₂ bands compared to the control cells (Fig. 4.4F). Western blots of the plasma membrane fractions of MC3T3-E1 cells indicated that CaMKII- β and CaMKII- α were not present in fraction 3, which represents caveolae microdomains (Fig. 4.4G), and $1\alpha,25(\text{OH})_2\text{D}_3$ did not stimulate their recruitment to caveolae (Fig. 4G).

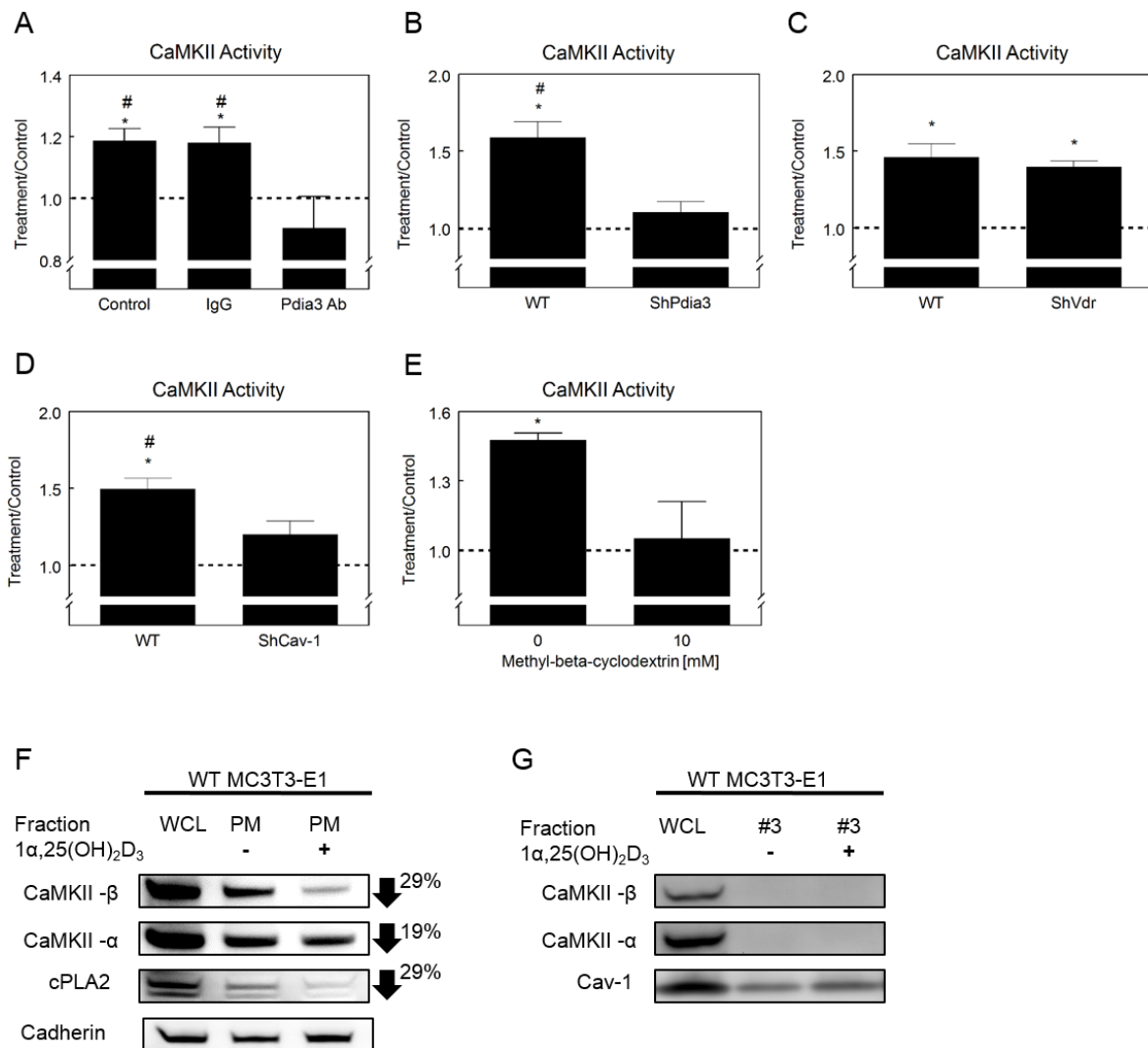


Figure 4.4: Effects of Pdia3 blocking, Pdia3, Vdr and Cav1 silencing, and β -CD on $1\alpha,25(\text{OH})_2\text{D}_3$ -dependent rapid activation of CaMKII in MC3T3-E1 cells. (A) MC3T3-E1 osteoblasts were pretreated with Pdia3-antibody for 30 minutes, and next they were treated with $1\alpha,25(\text{OH})_2\text{D}_3$ for 15 minutes. CaMKII activity was measured and normalized to total protein level. * $p < 0.05$, treatment versus control; # $p < 0.05$, versus Pdia3 Ab. (B) $1\alpha,25(\text{OH})_2\text{D}_3$ effect on CaMKII activity of WT and shPdia3 MC3T3-E1 cells. WT and shPdia3 osteoblasts were treated with $1\alpha,25(\text{OH})_2\text{D}_3$ for 15 minutes. CaMKII activity was measured and normalized to total protein level. * $p < 0.05$, treatment versus control; # $p < 0.05$, versus shPdia3. (C) $1\alpha,25(\text{OH})_2\text{D}_3$ effect on CaMKII activity of WT and shVdr MC3T3-E1 cells. WT and shVdr osteoblasts were treated with $1\alpha,25(\text{OH})_2\text{D}_3$ for 15 minutes. CaMKII activity was measured and normalized to total protein level * $p < 0.05$, treatment versus control. (D) $1\alpha,25(\text{OH})_2\text{D}_3$ effect on CaMKII activity of WT and shCav-1 MC3T3-E1 cells. WT and shCav-1 osteoblasts were treated with $1\alpha,25(\text{OH})_2\text{D}_3$ for 15 minutes. CaMKII activity was measured and normalized to total protein level. * $p < 0.05$, treatment versus control; # $p < 0.05$, versus shCav-1. (E) MC3T3-E1 osteoblasts were pretreated with β -CD for 30 minutes, and next they were treated with $1\alpha,25(\text{OH})_2\text{D}_3$ for 15

minutes. CaMKII activity was measured and normalized to total protein level. * $p < 0.05$, treatment *versus* control. Treatment over control ratios were calculated for each parameter. The dashed line represents the value for the control cultures, which was set to 1. Each figure is a representative experiment repeated three times with similar results. (F) Effect of $1\alpha,25(\text{OH})_2\text{D}_3$ on plasma membrane localization of CaMKII- β , CaMKII- α , cPLA₂. MC3T3-E1 cells were treated with $1\alpha,25(\text{OH})_2\text{D}_3$ for 15 minutes. Plasma membranes were isolated. Presence of CaMKII- β , CaMKII- α , cPLA₂ and Cadherin (loading control) in the plasma membranes were examined by Western blot. Intensity analysis of CaMKII- β , CaMKII- α , cPLA₂ bands relative to Cadherin were calculated and shown at the right corner of each figure. (G) Effect of $1\alpha,25(\text{OH})_2\text{D}_3$ on caveolae localization of CaMKII- β , CaMKII- α . MC3T3-E1 cells were treated with $1\alpha,25(\text{OH})_2\text{D}_3$ for 15 minutes. Caveolae fractions were isolated as described. Presence of CaMKII- β , CaMKII- α , cPLA₂ and Cav-1 (loading control) in the caveolae fractions were examined by Western blot.

Role of PLAA in $1\alpha,25(\text{OH})_2\text{D}_3$ Membrane-mediated Activation of CaMKII in MC3T3-E1

Osteoblasts

In MC3T3-E1 osteoblasts, $1\alpha,25(\text{OH})_2\text{D}_3$ activation of CaMKII depends on upstream actions of PLAA. Anti-PLAA antibody significantly reduced the $1\alpha,25(\text{OH})_2\text{D}_3$ -dependent increase in CaMKII activity in MC3T3-E1 osteoblasts (Fig. 5A), whereas IgG had no effect. Similarly, shPlaa osteoblasts did not respond to $1\alpha,25(\text{OH})_2\text{D}_3$ with an increase in CaMKII activity (Fig. 5B). PLAA peptide caused a significant increase in CaMKII activity in osteoblasts (Fig. 5C) at 10^{-7} M and 10^{-6} M. Treatment of cells with β -CD altered the response of the cells to PLAA. Pretreatment with β -CD abrogated the PLAA-stimulated increase in CaMKII activity in MC3T3-E1 osteoblasts (Fig. 5D).

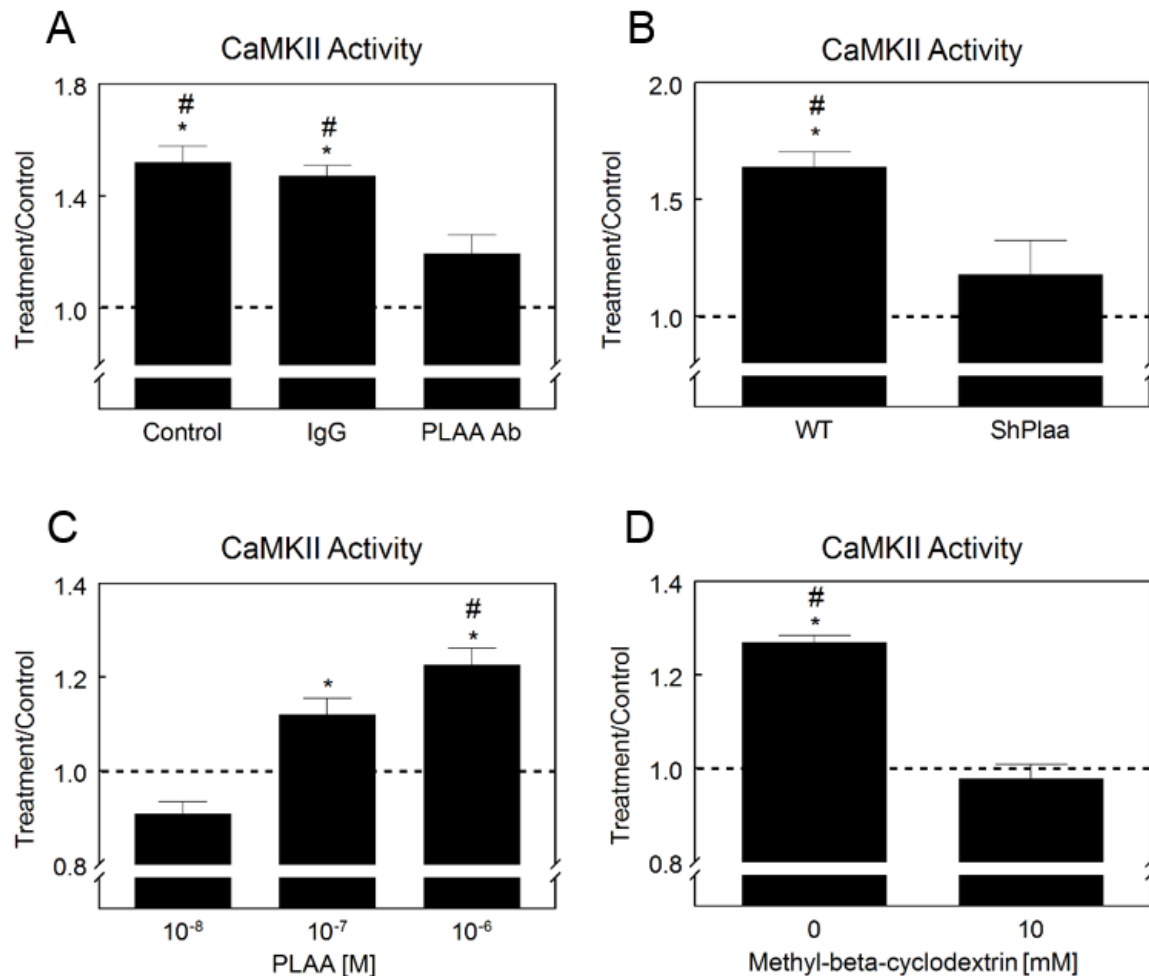


Figure 4.5: Role of PLAA on rapid activation of CaMKII in MC3T3-E1 osteoblasts. (A) MC3T3-E1 osteoblasts pretreated with PLAA-antibody for 30 minutes, and next they were treated with $1\alpha,25(\text{OH})_2\text{D}_3$ for 15 minutes. CaMKII activity was measured and normalized to total protein level. * $p < 0.05$, treatment versus control; # $p < 0.05$, versus PLAA Ab. (B) $1\alpha,25(\text{OH})_2\text{D}_3$ effect on CaMKII activity of WT and shPlaa MC3T3-E1 cells. WT and shPlaa osteoblasts were treated with $1\alpha,25(\text{OH})_2\text{D}_3$ for 15 minutes. CaMKII activity was measured and normalized to total protein level. * $p < 0.05$, treatment versus control; # $p < 0.05$, versus shPlaa. (C) MC3T3-E1 osteoblasts were treated with 10^{-8} , 10^{-7} , 10^{-6} M PLAA peptide for 15 minutes. CaMKII activity was measured and normalized to total protein level. * $p < 0.05$, treatment versus control, # $p < 0.05$, versus 10^{-8} M PLAA. (D) MC3T3-E1 osteoblasts were pretreated with β -CD for 30 minutes, and next they were treated with PLAA peptide for 15 minutes. CaMKII activity was measured and normalized to total protein level. * $p < 0.05$, treatment versus control. Treatment over control ratios were calculated for each parameter. The dashed line represents the value for the control cultures, which was set to 1. Each figure is a representative experiment repeated three times with similar results.

Roles of Pdia3, Cav-1, Caveolae and PLAA in $1\alpha,25(\text{OH})_2\text{D}_3$ Membrane-mediated Activation of CaMKII in GC Chondrocytes

In GC chondrocytes, $1\alpha,25(\text{OH})_2\text{D}_3$ activation of CaMKII depends on upstream actions of Pdia3 and caveolae microdomains. Anti-Pdia3 antibody significantly reduced the $1\alpha,25(\text{OH})_2\text{D}_3$ -dependent increase in CaMKII activity in GC chondrocytes (Fig. 4.6A), whereas, IgG had no effect. Pretreatment with β -CD abrogated the $1\alpha,25(\text{OH})_2\text{D}_3$ -dependent increase in CaMKII activity in GC chondrocytes (Fig. 4.6B).

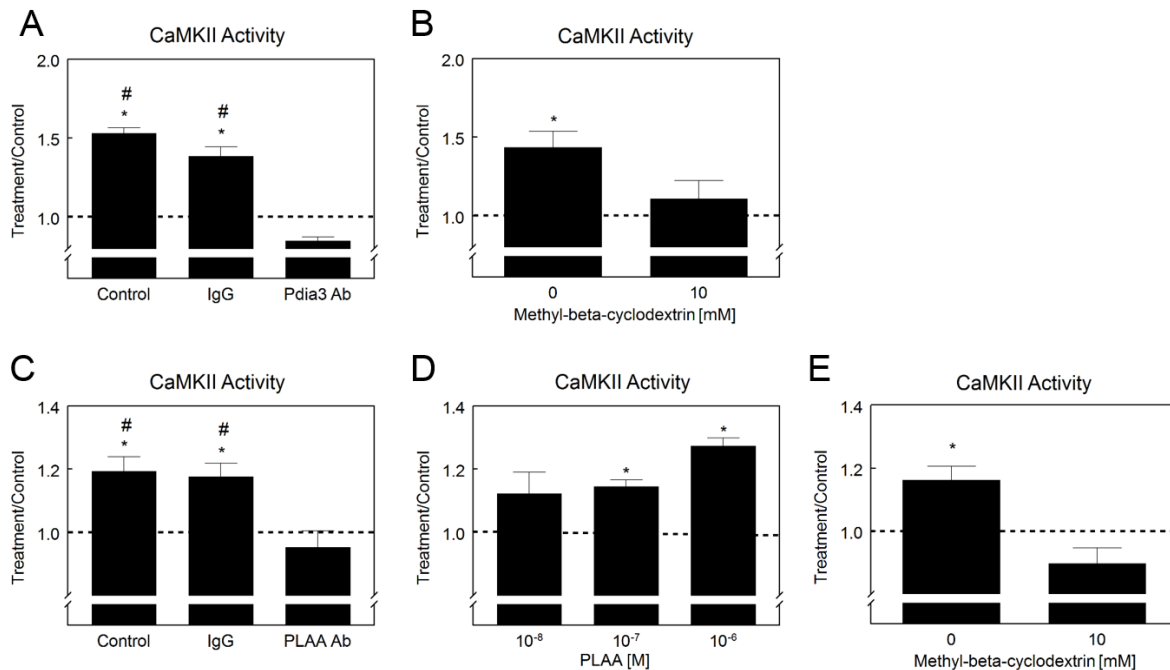


Figure 4.6: Effects of Pdia3 and PLAA blocking and β -CD on $1\alpha,25(\text{OH})_2\text{D}_3$ -mediated rapid activation of CaMKII. (A) GC chondrocytes were pretreated with Pdia3-antibody for 30 minutes, and next they were treated with $1\alpha,25(\text{OH})_2\text{D}_3$ for 9 minutes. CaMKII activity was measured as described and normalized to total protein level. *, $p < 0.05$, treatment *versus* control; #, $p < 0.05$, *versus* Pdia3 Ab. (B) GC cells were pretreated with β -CD for 30 minutes, and next they were treated with $1\alpha,25(\text{OH})_2\text{D}_3$ for 9 minutes. CaMKII activity was normalized to total protein level. *, $p < 0.05$, treatment *versus* control. (C) GC cells were pretreated with PLAA-antibody for 30 minutes, and next they were treated with $1\alpha,25(\text{OH})_2\text{D}_3$ for 9 minutes. CaMKII activity was measured as described and normalized to total protein level. *, $p < 0.05$, treatment *versus* control; #, $p < 0.05$, *versus* PLAA Ab (D) GC cells were treated with 10^{-8} , 10^{-7} , 10^{-6} M PLAA peptide for 9 minutes. CaMKII activity was measured as described and normalized to total protein level. *, $p < 0.05$, treatment *versus* control. (E) GC cells were pretreated with β -CD

for 30 minutes, and next they were treated with PLAA peptide for 9 minutes. CaMKII activity was measured as described and normalized to total protein level. *, $p < 0.05$, treatment *versus* control. Treatment over control ratios were calculated for each parameter. The dashed line represents the value for the control cultures, which was set to 1.

In GC chondrocytes, $1\alpha,25(\text{OH})_2\text{D}_3$ activation of CaMKII depends on upstream actions of PLAA. Anti-PLAA antibody abolished the $1\alpha,25(\text{OH})_2\text{D}_3$ -dependent increase in CaMKII activity (Fig. 4.6C), whereas, IgG had no effect. PLAA peptide caused a significant increase in CaMKII activity (Fig. 4.6D) at 10^{-7} M and 10^{-6} M. Treatment of cells with β -CD altered the response of the cells to PLAA peptide. Pretreatment with β -CD abolished the PLAA-stimulated increase in CaMKII activity (Fig. 4.6E).

Role of CaM in $1\alpha,25(\text{OH})_2\text{D}_3$ Membrane-mediated Rapid Activation of CaMKII

CaM mediated the rapid activation of CaMKII in response to $1\alpha,25(\text{OH})_2\text{D}_3$. The $1\alpha,25(\text{OH})_2\text{D}_3$ -stimulated increase in CaMKII activity was significantly reduced by the CaM inhibitor W-7 in a dose-dependent manner (Fig. 4.7A). W-7 completely blocked $1\alpha,25(\text{OH})_2\text{D}_3$ -dependent increase in PGE₂ release (Fig. 4.7B) and PKC activity (Fig. 4.7C) compared to the control.

The effects of $1\alpha,25(\text{OH})_2\text{D}_3$ on osteopontin and alkaline phosphatase were mediated through a mechanism involving CaM. While treatment of wild-type MC3T3-E1 cells with $1\alpha,25(\text{OH})_2\text{D}_3$ for 15 minutes led to a significant increase in osteopontin production and alkaline phosphatase activity at 24 hours, W-7 pretreatment significantly reduced osteopontin production (Fig. 4.7D) and blocked alkaline phosphatase activation (Fig. 4.7E) in response to $1\alpha,25(\text{OH})_2\text{D}_3$ treatment.

Western blots of the plasma membrane fractions of GC chondrocytes indicated that CaM was present in the plasma membranes with its greatest concentration in fraction 3, which

represents caveolae microdomains (Fig. 4.7F). Comparison of the intensity of CaM bands relative to Cav-1 loading control, showed that $1\alpha,25(\text{OH})_2\text{D}_3$ treatment reduced the levels of CaM in caveolae (Fig. 4.7G). Comparison of the intensity of CaM bands relative to cadherin loading control, showed that $1\alpha,25(\text{OH})_2\text{D}_3$ treatment reduced the levels of CaM in the plasma membrane of GC chondrocytes (Fig. 4.7H). Protein interaction studies indicated when cells were treated with $1\alpha,25(\text{OH})_2\text{D}_3$, PLAA and CaM appeared to increase their interaction in immunoprecipitates of GC cell lysates using anti-PLAA antibodies (Fig. 4.7I).

Western blots of the plasma membrane fractions of MC3T3-E1 cells indicated that CaM was present in the plasma membranes with its greatest concentration in fraction 3, which represents caveolae microdomains (Fig. 4.7J). Comparison of the intensity of CaM bands on the Western blot relative to Cav-1 loading control, showed that $1\alpha,25(\text{OH})_2\text{D}_3$ treatment reduced the levels of CaM in caveolae of MC3T3-E1 osteoblasts by 40% (Fig. 4.7K). Comparison of the intensity of CaM bands relative to cadherin loading control, showed that $1\alpha,25(\text{OH})_2\text{D}_3$ treatment reduced the levels of CaM in the plasma membrane of MC3T3-E1 osteoblasts by 34% (Fig. 4.7L).

Protein interaction studies indicated that when cells were treated with $1\alpha,25(\text{OH})_2\text{D}_3$, PLAA and CaM appeared to increase their interaction in immunoprecipitates of MC3T3-E1 cell lysates using anti-PLAA antibodies (Fig. 4.7M). Pdia3 was not present in anti-CaM antibody immunoprecipitates of osteoblasts treated with either vehicle or $1\alpha,25(\text{OH})_2\text{D}_3$ for 15 minutes (Fig. 4.7N). Likewise, Cav-1 was also not present in anti-CaM antibody immunoprecipitates of osteoblasts treated with either vehicle or $1\alpha,25(\text{OH})_2\text{D}_3$ for 15 minutes (Fig. 4.7O).

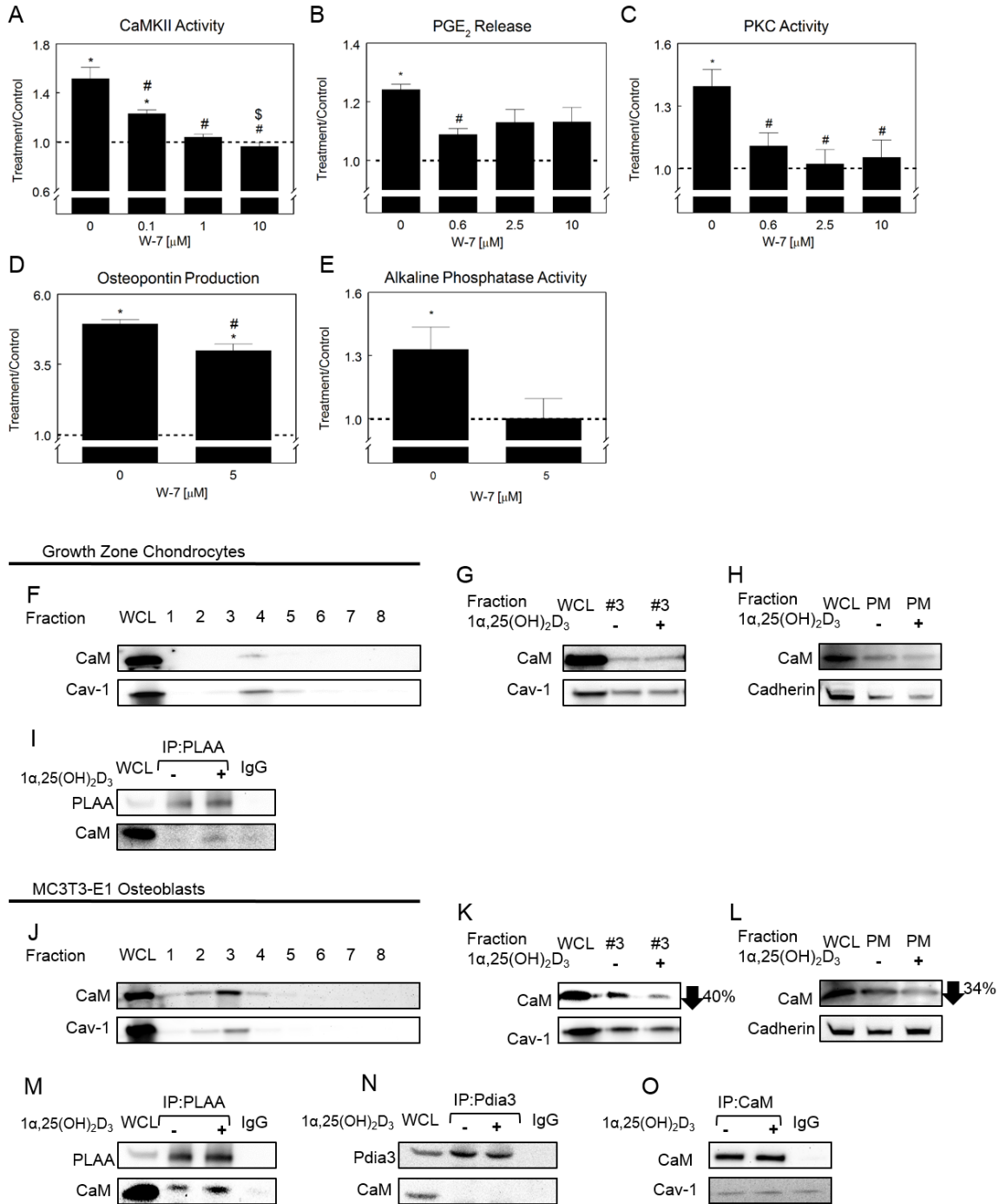


Figure 4.7: Role of CaM on the rapid 1 α ,25(OH)₂D₃-mediated pathway and the downstream physiological effects. GC chondrocytes were pretreated with 0, 0.1, 1 and 10 μ M W-7 for 30 minutes, and next they were treated with 1 α ,25(OH)₂D₃ for 15 minutes. CaMKII activity (A), PGE₂ release (B) and PKC activity (C) were measured as described. **p*<0.05, treatment versus control; #*p*<0.05, versus 0 μ M W-7; \$*p*<0.05, versus 0.1 μ M W-7. MC3T3-E1 osteoblasts were treated with 0 or 5 μ M of W-7 for 30 minutes and next they were treated with 1 α ,25(OH)₂D₃ for 15 minutes. The media containing 1 α ,25(OH)₂D₃ were replaced with fresh media. 24 hours later,

osteopontin production (D) and alkaline phosphatase activity (E) were measured as described and normalized to total DNA and total protein level, respectively. * $p < 0.05$, treatment *versus* control; # $p < 0.05$, *versus* 0 μM W-7. Treatment over control ratios were calculated for each parameter. The dashed line represents the value for the control cultures, which was set to 1. Each figure is a representative experiment repeated three times with similar results. (F) Plasma membrane localization of CaM in GC chondrocytes. (G) The effect of $1\alpha,25(\text{OH})_2\text{D}_3$ treatment on caveolae localization of CaM. GC cells were treated with $1\alpha,25(\text{OH})_2\text{D}_3$ for 9 minutes. Caveolae fractions were isolated as described. Presence of CaM and Cav-1 (loading control) in the caveolae fractions were examined by Western blot. (H) The effect of $1\alpha,25(\text{OH})_2\text{D}_3$ treatment on plasma membrane localization of CaM. GC cells were treated with $1\alpha,25(\text{OH})_2\text{D}_3$ for 9 minutes. Plasma membranes were isolated as described. Presence of CaM and Cadherin (loading control) in plasma membranes was examined by Western blot. (I) The effect of $1\alpha,25(\text{OH})_2\text{D}_3$ on PLAA's interaction with CaM in GC chondrocytes. PLAA was immunoprecipitated and subjected to Western blot. The membranes were incubated with the anti-CaM and anti-PLAA antibodies. (J) Subcellular localization of CaM in MC3T3-E1 cells. (K) The effect of $1\alpha,25(\text{OH})_2\text{D}_3$ treatment on caveolae localization of CaM. MC3T3-E1 cells were treated with $1\alpha,25(\text{OH})_2\text{D}_3$ for 15 minutes. Caveolae fractions were isolated as described. Presence of CaM and Cav-1 (loading control) in the caveolae fractions were examined by Western blot. Relative intensity analysis of CaM bands to Cav-1 were calculated and shown at the right corner of each figure. (L) The effect of $1\alpha,25(\text{OH})_2\text{D}_3$ treatment on plasma membrane localization of CaM. MC3T3-E1 cells were treated with $1\alpha,25(\text{OH})_2\text{D}_3$ for 15 minutes. Plasma membranes were isolated as described. Presence of CaM and Cadherin (loading control) in plasma membranes was examined by Western blot. Relative intensity analysis of CaM bands to Cadherin were calculated and shown at the right corner of each figure. (M) The effect of $1\alpha,25(\text{OH})_2\text{D}_3$ on PLAA's interaction with CaM in MC3T3-E1 osteoblasts. PLAA was immunoprecipitated and subjected to Western blot. The membranes were incubated with the anti-CaM and anti-PLAA antibodies. (N) The effect of $1\alpha,25(\text{OH})_2\text{D}_3$ on Pdia3's interaction with CaM in MC3T3-E1 osteoblasts. Pdia3 was immunoprecipitated and subjected to Western blot. The membranes were incubated with the anti-CaM and anti-Pdia3 antibodies. (O) The effect of $1\alpha,25(\text{OH})_2\text{D}_3$ on CaM's interaction with Cav-1 in MC3T3-E1 osteoblasts. CaM was immunoprecipitated and subjected to Western blot. The membranes were incubated with the anti-Cav-1 and anti-CaM antibodies. Each figure is a representative experiment repeated three times with similar results.

DISCUSSION

Little is known about the role of CaMKII in $1\alpha,25(\text{OH})_2\text{D}_3$ membrane-mediated signaling and its role in the physiological consequences of $1\alpha,25(\text{OH})_2\text{D}_3$ rapid actions. In the present study, we demonstrate that $1\alpha,25(\text{OH})_2\text{D}_3$ stimulates CaMKII activity in MC3T3-E1 osteoblasts and GC chondrocytes, and that CaMKII is required for mediating the rapid effects of $1\alpha,25(\text{OH})_2\text{D}_3$ on these cells, including PLA_2 activation, PGE_2 release, and PKC activation, and

downstream biological responses such as alkaline phosphatase activity and osteopontin production. These findings confirm the pivotal role CaMKII plays in the $1\alpha,25(\text{OH})_2\text{D}_3$ rapid signaling pathway. Our results are also supported by previous studies showing that estradiol and progesterone induce a rapid increase in CaMKII activity (181,182).

The time course of $1\alpha,25(\text{OH})_2\text{D}_3$ -dependent rapid activation of CaMKII indicates a significant increase in the kinase activity within 6-9 minutes of treatment in GC cells and within 9 to 15 minutes of treatment in MC3T3-E1 osteoblasts. This is later than the initial release of arachidonic acid (AA) observed within 15 seconds in our analysis of fatty acid turnover (183), which suggests that the first burst of AA may be due to another mechanism. It is of interest that we also observed a significant reduction in CaMKII at 3 minutes of treatment in both GC and MC3T3-E1 cells. This can be attributable to a rapid decrease in available co-factors, particularly Ca^{2+} (184). Whether the effect observed at 3 minutes is the consequence of an earlier $1\alpha,25(\text{OH})_2\text{D}_3$ -stimulated response that involves a rapid activation and inhibition of CaMKII, or is triggered by only a very rapid inhibition of CaMKII by $1\alpha,25(\text{OH})_2\text{D}_3$, is still not known and requires further investigation.

The time course of CaMKII activation observed in the present study is in concert with the increase in PLA₂ and PKC in response to either $1\alpha,25(\text{OH})_2\text{D}_3$ or PLAA. Moreover, the data strongly support a role for CaMKII in the mechanism by which PLAA mediates its signal from Pdia3 to PLA₂. CaMKII inhibitors, KN-93 and mer-CaMKIINtide, significantly reduce $1\alpha,25(\text{OH})_2\text{D}_3$ -stimulated rapid responses in GC chondrocytes, supporting the hypothesis that CaMKII is a critical member of the $1\alpha,25(\text{OH})_2\text{D}_3$ rapid pathway. Furthermore, silencing of Camk2a isoforms in MC3T3-E1 osteoblasts inhibits the $1\alpha,25(\text{OH})_2\text{D}_3$ membrane-mediated

pathway, confirming the key role the α isoform of CaMKII plays in $1\alpha,25(\text{OH})_2\text{D}_3$ rapid signaling.

While our studies show that CaMKII can mediate the rapid effects of $1\alpha,25(\text{OH})_2\text{D}_3$, they also demonstrate that CaMKII is important for downstream biological responses including alkaline phosphatase activity and osteopontin production. The CaMKII inhibitor, mer-CaMKIINtide, blocks $1\alpha,25(\text{OH})_2\text{D}_3$ -stimulated increase in alkaline phosphatase activity in osteoblasts, suggesting that CaMKII activation is required for downstream activation of this enzyme. Also, mer-CaMKIINtide reduced the $1\alpha,25(\text{OH})_2\text{D}_3$ -dependent osteopontin production by 50%, suggesting that osteopontin production is regulated partially through actions of CaMKII. Previous studies have shown that MAPK activation was involved in Ang II-stimulated osteopontin expression in adventitial fibroblasts (185). Our results also confirmed a similar mechanism for controlling osteopontin production in which $1\alpha,25(\text{OH})_2\text{D}_3$ -stimulated CaMKII activation is upstream of MAPK, and CaMKII inhibition blocks $1\alpha,25(\text{OH})_2\text{D}_3$ -dependent PKC activation and partially inhibits downstream osteopontin production. Our lab previously reported that Pdia3 silencing did not completely block the $1\alpha,25(\text{OH})_2\text{D}_3$ -induced osteopontin gene expression (10). Our results also showed that CaMKII inhibition only partially blocked $1\alpha,25(\text{OH})_2\text{D}_3$ -stimulated osteopontin production suggesting that cross-talk with other pathways may be involved in regulation of osteopontin protein production.

Immunoprecipitation studies demonstrated that CaM only interacts with PLAA in the presence of $1\alpha,25(\text{OH})_2\text{D}_3$. This suggests that CaM serves as a mediator to transfer the signal from the PLAA protein complex to CaMKII and causes downstream activation of PLA_2 . Whether CaMKII directly binds to PLA_2 and triggers its activation or it stimulates PLA_2

activation through activation of other protein kinases is still unknown and has yet to be elucidated.

The present study supports the hypothesis that CaMKII and CaM play crucial roles in mediating rapid $1\alpha,25(\text{OH})_2\text{D}_3$ membrane-associated signaling via PLA_2 and PKC. $1\alpha,25(\text{OH})_2\text{D}_3$ failed to activate rapid responses in shCamk2a osteoblasts, inhibitors against CaM and CaMKII blocked $1\alpha,25(\text{OH})_2\text{D}_3$ membrane-mediated signaling, and CaM associated with PLAA in the presence of $1\alpha,25(\text{OH})_2\text{D}_3$. Moreover, in shPlaa, shPdia3 and shCav-1 osteoblasts, $1\alpha,25(\text{OH})_2\text{D}_3$ failed to activate CaMKII, supporting the hypothesis that the Pdia3 receptor complex proteins in caveolae are required for the rapid activation of CaMKII. Overall, the results of this study suggest that CaMKII and CaM could pose as potential therapeutic targets in conditions associated with aberrations in $1\alpha,25(\text{OH})_2\text{D}_3$ membrane-mediated signaling.

Taken together with previous published studies (10,92,125), the results suggest the following pathway (Fig. 4.8): $1\alpha,25(\text{OH})_2\text{D}_3$ binds its membrane associated protein, Pdia3 in caveolae, triggering binding of PLAA to Pdia3. CaM binds to PLAA, leaves caveolae and activates CaMKII. Next, PLA_2 is activated resulting in production of AA and lysophospholipid LPL (89). AA can either increase $\text{PKC}\alpha$ activity directly (90), or it is further metabolized via Cox-1 to PGE_2 , which acts via its EP1 receptor to contribute to PKC activation (91). Phosphatidylinositol-specific $\text{PLC}\beta$ is activated via $\text{G}\alpha_q$ and lysophospholipid, generating DAG and IP3 (89,92). DAG binds $\text{PKC}\alpha$ and triggers its recruitment to the plasma membrane (93). IP3 activates the release of Ca^{2+} ions from the endoplasmic reticulum, required for $\text{PKC}\alpha$ activation, which subsequently leads to the activation of ERK1/2 (10).

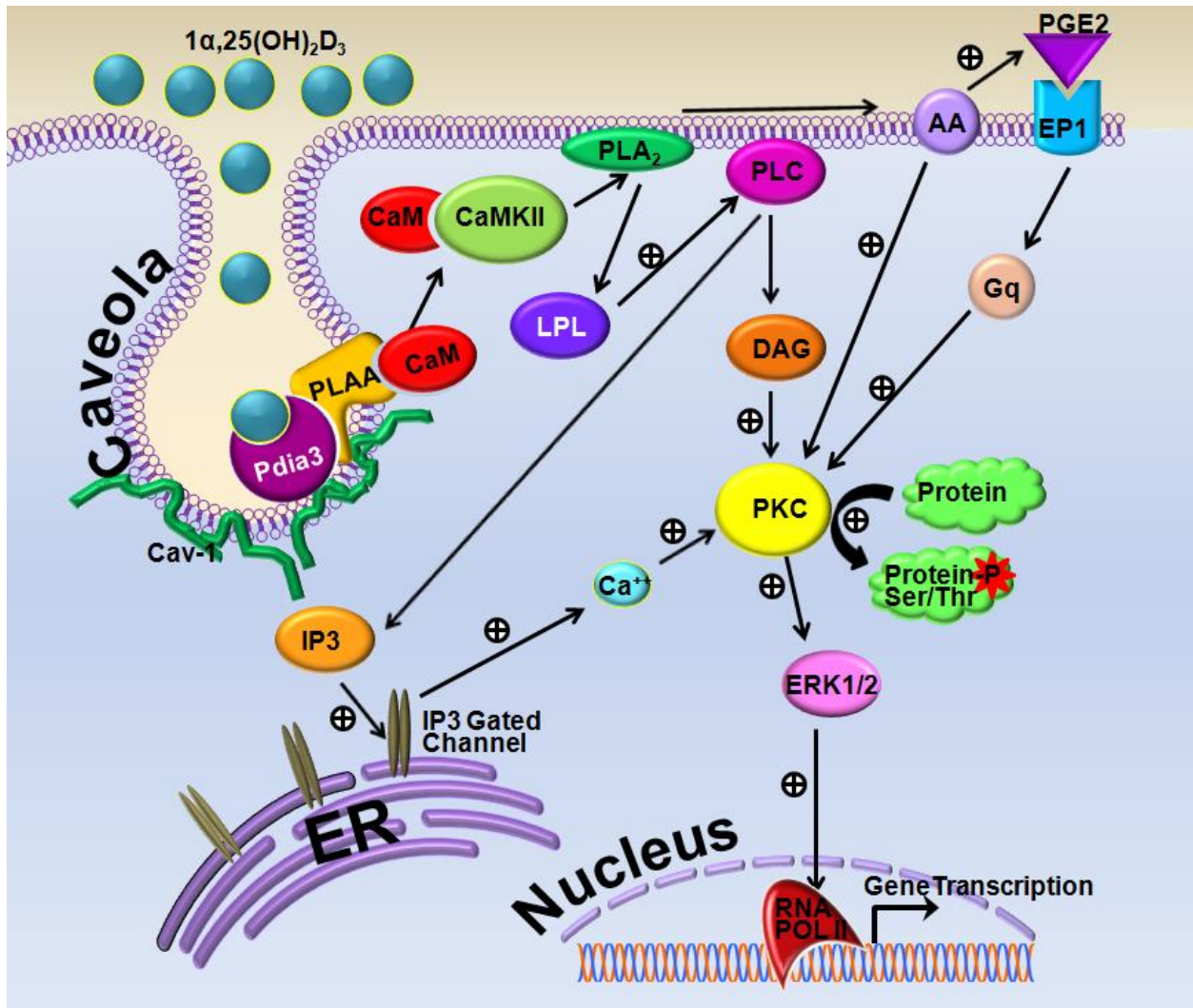


Figure 4.8: Proposed mechanism of $1\alpha,25(\text{OH})_2\text{D}_3$ stimulated rapid response in osteoblasts and chondrocytes.

CONCLUSION

In conclusion, we found a detailed mechanism of $1\alpha,25(\text{OH})_2\text{D}_3$ -stimulated rapid activation of PKC via CaM and CaMKII in chondrocytes and osteoblasts. CaM is required for mediating the Pdia3-dependent actions of $1\alpha,25(\text{OH})_2\text{D}_3$ on GC chondrocytes and MC3T3-E1 osteoblasts. CaM is localized with Pdia3 and PLAA in caveolae domains of the plasma

membrane, and it interacts with PLAA in the presence of $1\alpha,25(\text{OH})_2\text{D}_3$ suggesting it serves as one of the mediators of the rapid pathway. When MC3T3-E1 osteoblasts and GC chondrocytes were treated with $1\alpha,25(\text{OH})_2\text{D}_3$, CaMKII was rapidly activated. Inhibitors against CaM and CaMKII blocked $1\alpha,25(\text{OH})_2\text{D}_3$ -stimulated rapid activation of PLA₂, PKC and PGE₂ release. In agreement with inhibition studies, *Camk2a* silencing was able to block the effect of $1\alpha,25(\text{OH})_2\text{D}_3$ on rapid activation of PLA₂, PKC and PGE₂ release.

CHAPTER 5

SIGNALING COMPONENTS OF THE $1\alpha,25(\text{OH})_2\text{D}_3$ -DEPENDENT Pdia3 RECEPTOR COMPLEX ARE REQUIRED FOR Wnt5a CALCIUM- DEPENDENT SIGNALING

INTRODUCTION

Endochondral ossification encompasses multiple events during which the embryonic cartilaginous template of long bones is gradually calcified and replaced by bone (65). Previous reports by our lab and other groups have suggested that a complex network of interacting signaling pathways induced by hormones and growth factors regulate growth plate chondrocytes and endochondral bone ossification (19,66-68). However, limited information is available on the molecular basis of these interactions.

In the present study, we focus on inter-relation between two pathways involved in regulation of growth plate cartilage and osteoblast maturation: $1\alpha,25$ -dihydroxyvitamin D₃ [$1\alpha,25(\text{OH})_2\text{D}_3$] membrane-mediated signaling and non-canonical Wnt calcium-dependent signaling. $1\alpha,25(\text{OH})_2\text{D}_3$ induces its effects via two mechanisms: classical vitamin D receptor (VDR) signaling and the more recently described calcium-dependent membrane-mediated pathway (6-8). In the membrane-mediated pathway, $1\alpha,25(\text{OH})_2\text{D}_3$ initiates its effects via its specific membrane-associated receptor protein disulfide isomerase family A, member 3 (Pdia3) (10) located in caveolae, which are 50-100 nm lipid rafts highly enriched with cholesterol and glycosphingolipids (186). Caveolae are characterized by caveolin coat proteins (Cav-1, Cav-2, Cav-3) that serve as signaling platforms for several steroid hormones (186). Upon binding to Pdia3, $1\alpha,25(\text{OH})_2\text{D}_3$ induces interactions between Pdia3 and phospholipase-A₂ (PLA₂)-

activating protein (PLAA) (125), stimulating increased calcium/calmodulin-dependent protein kinase II (CaMKII) activity in costochondral growth zone chondrocytes (GC) and MC3T3-E1 osteoblasts (187). PLA₂ is activated (92), producing lysophospholipid and releasing arachidonic acid (AA) (89) that is further processed into prostaglandin E₂ (PGE₂), which acts via its EP1 receptor to increase cyclic AMP (91). Together with G α q, lysophospholipid activates phosphatidylinositol-specific phospholipase C beta (PLC β), generating diacylglycerol (DAG) and inositol 1,4,5-trisphosphate (IP₃) (89,92). DAG binds PKC α , recruiting it to the plasma membrane (93). IP₃ activates the release of calcium ions required for PKC α activation from the endoplasmic reticulum.

1 α ,25(OH)₂D₃ stimulates differentiation of growth zone chondrocytes and osteoblasts, increasing alkaline phosphatase specific activity (91) and in the case of osteoblasts by increasing production of osteopontin (10). While the VDR mediates many of the effects of 1 α ,25(OH)₂D₃ on these cells, Pdia3-dependent signaling has been shown to mediate the effects of the vitamin D metabolite on these two markers of osteoblast differentiation. Pdia3 gene knockout results in embryonic lethality (188,189) and as a result, a definitive demonstration of its role has not been possible. However, conditional knockout of Pdia3 in the intestinal epithelium results in severely blunted Ca²⁺ uptake in response to 1 α ,25(OH)₂D₃ (190), confirming its involvement in 1 α ,25(OH)₂D₃ dependent actions. Moreover, Pdia3^{+/-} mice exhibit a long bone phenotype (188), further demonstrating the importance of this 1 α ,25(OH)₂D₃ receptor in skeletal development.

Wnts are signaling molecules that also regulate skeletal development and maintenance (191,192). In particular, *Wnt5a* is expressed in GC chondrocytes (149), which are isolated from the prehypertrophic and upper hypertrophic zones of the growth plate, and plays an important role in transition of chondrocytes between growth plate zones. *Wnt5a* is also expressed by

osteoblasts at the interface between calcified cartilage and metaphyseal bone and it has been shown to promote osteoblast maturation in vitro (19,20). Osteoblasts isolated from *Wnt5a*^{-/-} mice exhibit down-regulation of osteoblastic differentiation markers including runt related transcription factor 2, osterix and alkaline phosphatase (21) compared to wild type cells, suggesting *Wnt5a* regulates bone formation. This is supported by histological analysis of long bones of *Wnt5a*^{-/-} mice, which exhibit significantly delayed chondrocyte hypertrophy and skeletal ossification compared to wild type mice (153). *Wnt5a* induces its effects via several known receptors and co-receptors including Frizzled2 (FZD2), Frizzled5 (FZD5), and receptor tyrosine kinase-like orphan receptor 2 (ROR2), activating intracellular release of calcium, thereby activating PLC, PKC, CaMKII and calcineurin (24,193-196).

Although $1\alpha,25(\text{OH})_2\text{D}_3$ and *Wnt5a* both regulate osteoblast and chondrocyte maturation and signal via calcium-dependent mechanisms, little is known about the role of components of the $1\alpha,25(\text{OH})_2\text{D}_3$ membrane-associated receptor complex in *Wnt5a* calcium-dependent signaling. The purpose of this study was to determine if the same receptor complex and pathway signaling proteins that are critical for the $1\alpha,25(\text{OH})_2\text{D}_3$ membrane-mediated pathway via *Pdia3* are also important for *Wnt5a* calcium-dependent signaling. To address this question, we first verified *Wnt5a*-dependent activation of CaMKII, PLA₂, PKC, and PGE₂ release in MC3T3-E1 osteoblasts and GC cells. Next, we determined the role of the $1\alpha,25(\text{OH})_2\text{D}_3$ membrane receptor complex and its downstream signaling proteins in *Wnt5a*-stimulated PKC activation using the MC3T3-E1 cell model. Finally, we determined the interactions between the $1\alpha,25(\text{OH})_2\text{D}_3$ membrane-receptor complex and *Wnt5a* receptors with or without $1\alpha,25(\text{OH})_2\text{D}_3$ or *Wnt5a* treatment in MC3T3-E1 osteoblasts.

MATERIALS AND METHODS

Reagents

Recombinant human/mouse Wnt5a was purchased from R&D Systems (Minneapolis, MN). $1\alpha,25(\text{OH})_2\text{D}_3$ and PLAA were purchased from Enzo Life Sciences (Plymouth Meeting, PA). The anti-PLAA polyclonal antibody was designed and developed by Strategic Diagnostics Inc. (Newark, DE) (125). Rabbit antiserum against the N-terminal peptide of Pdia3 was purchased from Alpha Diagnostic International (San Antonio, TX) (165). A polyclonal antibody to Cav-1 was purchased from Santa Cruz Biotechnology (Santa Cruz, CA). ROR2 polyclonal antibody was from Cell Signaling Technology (Danvers, MA). Frizzled2 polyclonal antibody and Frizzled5 polyclonal antibody were from Abcam (San Francisco, CA). Monoclonal antibody to CaM was from Millipore (Billerica, MA). Myristoylated calmodulin kinase IINtide (mer-CaMKIINtide) peptide was from EMD Biosciences (Billerica, MA) and arachidonyl trifluoromethyl ketone (AACOCF₃) was from Abcam. All other reagents were purchased from Sigma Aldrich (St. Louis, MO) unless specified.

Cell Culture

Wild type (WT) mouse MC3T3-E1 subclone 4 osteoblast-like cells (CRL-2593) were purchased from ATCC (Manassas, VA, USA). Stably silenced MC3T3-E1 cell lines for Pdia3 (shPdia3), PLAA (shPlaa), Cav-1 (shCav-1), VDR (shVdr), CaMKII- α (shCamk2a), and CaMKII- β (shCamk2b) were generated and characterized by our lab previously (10,125,178). Cells were plated at 10,000 cells/cm² and cultured in Minimum Essential Medium Alpha (α -MEM) (Life Technologies, Carlsbad, CA) containing 10% fetal bovine serum (FBS) (Hyclone, Waltham, MA) and 1% penicillin-streptomycin (P/S), (Life Technologies). Osteoblastic differentiation of MC3T3-E1 cells was induced by culture in α -MEM supplemented with 10%

FBS, 1% P/S and 50 µg/ml ascorbic acid 24 hours after plating, and then every 48 hours thereafter (86).

GC cells were isolated from costochondral cartilage of 100-125g male Sprague-Dawley rats (Harlan, Indianapolis, IN). Rats were at the end of their adolescent growth spurt; therefore, their long bones were growing at a reduced rate. The culture system used in this study was described previously in detail (11,166). Briefly, fourth passage cultures of GC chondrocytes were plated at 10,000 cells/cm² and cultured in Dulbecco's modified Eagle's medium (Mediatech) containing 10% FBS, 1% P/S, and 50 µg/ml ascorbic acid.

All cells were cultured at 37°C with 5% CO₂ and 100% humidity. Confluent cultures were treated for experiments as described below.

Time Course and Dose Response of PKC Activity to Wnt5a

To assess the dose-dependent effects of Wnt5a on PKC, GC cells were treated for 9 minutes and MC3T3-E1 cells were treated for 15 minutes with 50, 125 and 200 ng/ml Wnt5a (20,197), time points previously demonstrated to be optimal for activation of PKC by 1 α ,25(OH)₂D₃ in these cell types (9,125). After treatment, cell layers were washed with phosphate buffered saline (PBS) and then were lysed in RIPA buffer (20 mM Tris-HCl, 150 mM NaCl, 5 mM disodium EDTA, 1% Nonidet P-40). PKC activity was measured in cell layer lysates using a commercially available kit following manufacturer's instructions (GE Healthcare, Piscataway, NJ) and data were normalized to total protein (Pierce BCA Protein Assay, Thermo Fisher Scientific, Waltham, MA).

Next, the time course of PKC activation by Wnt5a was examined. GC cells and MC3T3-E1 cells were treated with 125 ng/ml (20,197) Wnt5a for 6, 9, 15, or 30 minutes. PKC activity was measured as described above.

Time Course of Wnt5a Effect on CaMKII Activity

GC and MC3T3-E1 cells were treated for 6, 9, 15, and 30 minutes with 125 ng/ml Wnt5a and cell layer lysates were assayed for CaMKII activity. CaMKII activity was measured using a commercially available assay following manufacturer's instructions (SignaTECT® Calcium/Calmodulin-Dependent Protein Kinase Assay System, Promega, Madison, WI). CaMKII activity was normalized to total protein in the cell lysate.

Time Course of Wnt5a Effect on PLA₂ Activity

GC and MC3T3-E1 cells were treated for 6, 9, 15, or 30 minutes with 125 ng/ml Wnt5a. After washing the cell layers with PBS, the cell layers were lysed and assayed for PLA₂ activity using a commercially available kit (cPLA₂ Assay kit, 765021, Cayman Chemical, Ann Arbor, MI). PLA₂ data were normalized to total protein.

Time Course of Wnt5a Effect on PGE₂ Release

GC and MC3T3-E1 cells were treated for 6, 9, 15, and 30 minutes with 125 ng/ml Wnt5a. At the end of incubation, conditioned media were acidified and PGE₂ was measured using a commercially available kit (Prostaglandin E₂ [¹²⁵I]-RIA kit, Perkin Elmer, Waltham, MA). PGE₂ levels were normalized to total DNA (Quant-iT™ PicoGreen® dsDNA Assay kit, Life Technologies).

Role of Vitamin D Signaling Components on Wnt5a-induced PKC Activity

Based on the results of time-course and dose-response studies, the treatment conditions resulting in the highest PKC activity (125 ng/ml Wnt5a for 9 minutes in GC cells and 125 ng/ml Wnt5a for 15 minutes in MC3T3-E1 osteoblasts) were selected for subsequent experiments unless specified in the text.

To determine the effects of Pdia3, Vdr, and Cav-1 silencing on Wnt5a-induced PKC activity, wild type (WT), shPdia3, shVdr, and shCav-1 cells were treated with Wnt5a and PKC measured. These results were confirmed using Pdia3 and VDR blocking antibodies in GC chondrocytes and MC3T3-E1 osteoblasts. Cells were pretreated with either anti-Pdia3 or anti-VDR antibodies for 30 minutes, and PKC activity measured after Wnt5a treatment.

Methyl-beta-cyclodextrin (β -CD) disrupts lipids rafts and caveolae by binding cholesterol and removing it from the plasma membranes. To determine the effects of caveolae destruction on PKC activation, MC3T3-E1 cells were treated with 10 mM of β -CD for 30 minutes in serum-free media, as described previously (12). At the end of incubation, cell layers were rinsed with serum free media. Cells were then treated with Wnt5a and cell layer lysates were assayed for PKC activity.

Role of Calmodulin on Wnt5a-induced PKC Activity

MC3T3-E1 cells were pre-treated with 0.1, 1, or 10 μ M of calmodulin inhibitor W-7 for 30 minutes (198), then cells were treated with Wnt5a for 15 minutes and cell layer lysates were assayed for PKC activity. To investigate the effect of CaMKII inhibition on $1\alpha,25(\text{OH})_2\text{D}_3$ -dependent PKC activation, MC3T3-E1 cells were treated for 30 minutes with 1.25, 2.5, and 5 μ M CaMKII peptide-inhibitor mer-CaMKIINtide (180) followed by Wnt5a. Cell layer lysates were assayed for PKC activity. To investigate the effects of Camk2a and Camk2b silencing on Wnt5a-stimulated PKC activation, confluent WT, shCamk2a, and shCamk2a MC3T3-E1 cells were treated with Wnt5a. Cell layer lysates were assayed for PKC.

Role of PLAA on Wnt5a-induced PKC Activity

Cells were pretreated with anti-PLAA antibody (PLAA Ab) for 30 minutes followed by Wnt5a for 15 minutes. Cell layer lysates were assayed for PKC activity. To confirm these findings,

PKC activity was measured in WT and shPlaa MC3T3-E1 cells after Wnt5a treatment. To investigate the effects of PLA₂ inhibition on PKC activity, MC3T3-E1 osteoblasts were pretreated with 0.1, 1, and 10 μM AACOCF3 for 30 minutes followed by Wnt5a. PKC activity was measured in cell layer lysates. AACOCF3 has been shown in other studies to inhibit PLA₂ in these cells (199).

Effects of Wnt5a and 1 α ,25(OH)₂D₃ Co-treatment on Regulation of PKC Activity

MC3T3-E1 cells were treated with 10⁻¹⁰, 10⁻⁹, or 10⁻⁸ M 1 α ,25(OH)₂D₃. Wnt5a was added to one-half of the cultures at the concentration of 125 ng/ml. At the end of 15 minute incubation, cell layer lysates were assayed for PKC. To assess the effects of Wnt5a in 1 α ,25(OH)₂D₃ regulation of PKC activity, MC3T3-E1 cells were treated with 10⁻⁸ M 1 α ,25(OH)₂D₃ and 0, 50, 87.5 or 125 ng/ml Wnt5a for 15 minutes. At the end of the incubation, the cell layer lysates were assayed for PKC.

Roles of ROR2, FZD2 and FZD5 on 1 α ,25(OH)₂D₃-induced PKC Activity

MC3T3-E1 osteoblasts were pretreated with anti-Frizzled2 (FZD2 Ab), anti-Frizzled5 (FZD5 Ab), or anti-ROR2 (ROR2 Ab) antibodies for 30 minutes, then were treated with 10⁻⁸ M 1 α ,25(OH)₂D₃ for 15 minutes. PKC activity was measured in cell layer lysates.

Role of ROR2 on 1 α ,25(OH)₂D₃-induced CaMKII Activity

MC3T3-E1 osteoblasts, cells were pretreated with anti-ROR2 antibodies for 30 minutes, then were treated with 10⁻⁸ M 1 α ,25(OH)₂D₃ for 15 minutes. CaMKII activity was measured in cell layer lysates.

Role of ROR2 on PLAA-induced CaMKII Activity

MC3T3-E1 osteoblasts were pretreated with anti-ROR2 antibodies for 30 minutes, then were treated with 10⁻⁶ M PLAA peptide for 15 minutes. CaMKII activity was measured in cell layer lysates.

Caveolae Isolation

Pdia3 exists in plasma membrane caveolae of osteoblasts (10). To determine the plasma membrane localization of FZD2, FZD5 and ROR2, plasma membranes and caveolae were isolated using a detergent-free method as described previously (121). Briefly, confluent MC3T3-E1 cultures were harvested by scraping while in isolation buffer (0.25 M sucrose, 1 mM EDTA, 20 mM Tricine, pH 7.8) and were homogenized using a tissue grinder (20 strokes; 10 strokes clockwise and 10 strokes counter-clockwise). Homogenates were centrifuged at 20,000 g for 10 minutes. The supernatant was collected and layered on top of isolation buffer containing 30% Percoll® (GE Healthcare, Piscataway, NJ). The pellet, including nucleus, mitochondria, and endoplasmic reticulum, was discarded. Samples were centrifuged at 84,000 g for 30 minutes. Syringe needles (18G) were used to collect the plasma membrane fraction from the gradient column. The isolated fraction was layered over a 10-20% OptiPrep gradient (Sigma Aldrich, St. Louis, MO), then centrifuged at 52,000 g for another 4 hours. Plasma membrane sub-fractions were collected from the tube, resulting in isolation of thirteen fractions. Caveolae were observed as an opaque band that was collected in fraction 3.

Western Blots

Whole cell layer lysates and plasma membrane fractions (50µg protein) were loaded onto 4–20% Mini-PROTEAN® TGX™ precast polyacrylamide gels (Bio-Rad, Hercules, CA). Proteins were transferred to low-fluorescence PVDF membranes (Bio-Rad) using a Trans-Blot® Turbo™ Transfer System (Bio-Rad). Membranes were incubated with blocking buffer (LI-COR, Lincoln, NE) for 1 hour. Subsequently, the membranes were incubated with antibodies against Cav-1, FZD2, FZD5, and ROR2 overnight. The next day, the membranes were incubated for one hour with IRDye 800CW conjugated goat anti-rabbit IgG secondary antibodies (LI-COR) in

blocking buffer containing 0.2% Tween-20, and 0.01% SDS. Following three washes with PBS containing 0.05% Tween-20 membranes were imaged using the LI-COR Odyssey® CLx Infrared Imaging System.

Effects of $1\alpha,25(\text{OH})_2\text{D}_3$ and Wnt5a on Receptor Complex Interactions

MC3T3-E1 osteoblasts were treated with 10^{-8} M $1\alpha,25(\text{OH})_2\text{D}_3$ or its vehicle (ethanol), or 125 ng/ml Wnt5a or its vehicle (cell culture medium) for 15 minutes. At the end of treatment, cell layers were washed with PBS and lysed in RIPA buffer containing 100 mM sodium fluoride, protease inhibitor cocktail, and 1 mM phenylmethylsulfonyl fluoride. Protein samples (500 μg) were precleared by incubation in 5 μg of rabbit IgG conjugated to Dynabeads® Protein A (Life Technologies) at 4°C for 1 hour. The beads were separated from solution using a magnet. To immunoprecipitate Pdia3, PLAA, Cav-1 and CaM protein complexes, anti-Pdia3, anti-PLAA, anti-Cav-1, and anti-CaM antibodies were covalently coupled to the Dynabeads Protein A according to the manufacturer's protocol. Pre-cleared protein samples were mixed with antibody coated Dynabeads and incubated at 4°C overnight with continuous agitation. Dynabeads were recovered using a magnet and were washed three times with 0.05% Tween-20 in PBS. Precipitated proteins were eluted in elution buffer, then diluted in Tris-glycine SDS sample loading buffer (Bio-Rad) and boiled for 5 minutes. Immunoprecipitated samples were examined by Western blot (ONE-HOUR Western™ Fluorescent Kit, Genscript, Piscataway, NJ).

Statistical Analysis

For each experiment, data points represent the mean \pm standard error of the mean (SEM) of six individual cultures, per variable. Each experiment was repeated at least three times to ensure validity of the data. Statistical significance was assessed by analysis of variance and post hoc testing performed using Bonferroni's modification of Student's t-test for multiple

comparisons (GraphPad Prism, GraphPad Software, Inc., San Diego, CA). P-values <0.05 were considered significant.

RESULTS

Rapid Effects of Wnt5a on PKC, CaMKII, PLA₂ Activations, and PGE₂ Release

Wnt5a regulated the activity of PKC in GC and MC3T3-E1 cells in a dose- and time-dependent manner. Similarly, the effects of Wnt5a on CaMKII and PLA₂ activities and PGE₂ release were time-dependent and rapid. Wnt5a protein increased PKC-specific activity in a dose-dependent manner in GC cells with the highest stimulatory effects of the peptide observed at 125 ng/ml concentration (Fig. 5.1A). Wnt5a activated PKC in a dose-dependent manner in MC3T3-E1 cells, with the highest stimulatory effect observed at 125 ng/ml (Fig. 5.1B). Wnt5a activated PKC in GC cells within 9 minutes of treatment, and PKC remained significantly higher than control at 15 and 30 minutes after treatment (Fig. 5.1C). We further assessed whether Wnt5a acts on cells by a mechanism similar to that used by 1 α ,25(OH)₂D₃. Wnt5a increased CaMKII activity at 9 and 15 minutes after treatment in GC chondrocytes (Fig. 5.1D). Wnt5a increased PLA₂ activity (Fig. 5.1E) and PGE₂ release (Fig. 5.1F) in GC cells at both 9 minutes and 30 minutes after treatment. Similarly, Wnt5a caused a rapid increase in PKC activity in MC3T3-E1 cells at 9 minutes that remained elevated until 30 minutes, with a peak at 15 minutes (Fig. 5.1G). Wnt5a increased CaMKII activity at 6, 9, and 30 minutes in MC3T3-E1 osteoblasts (Fig. 5.1H). Similarly, the effect of Wnt5a on PLA₂ activity (Fig. 5.1I) and PGE₂ release (Fig. 5.1J) was time-dependent and significant increases were observed at 9 and 30 minutes after the treatment.

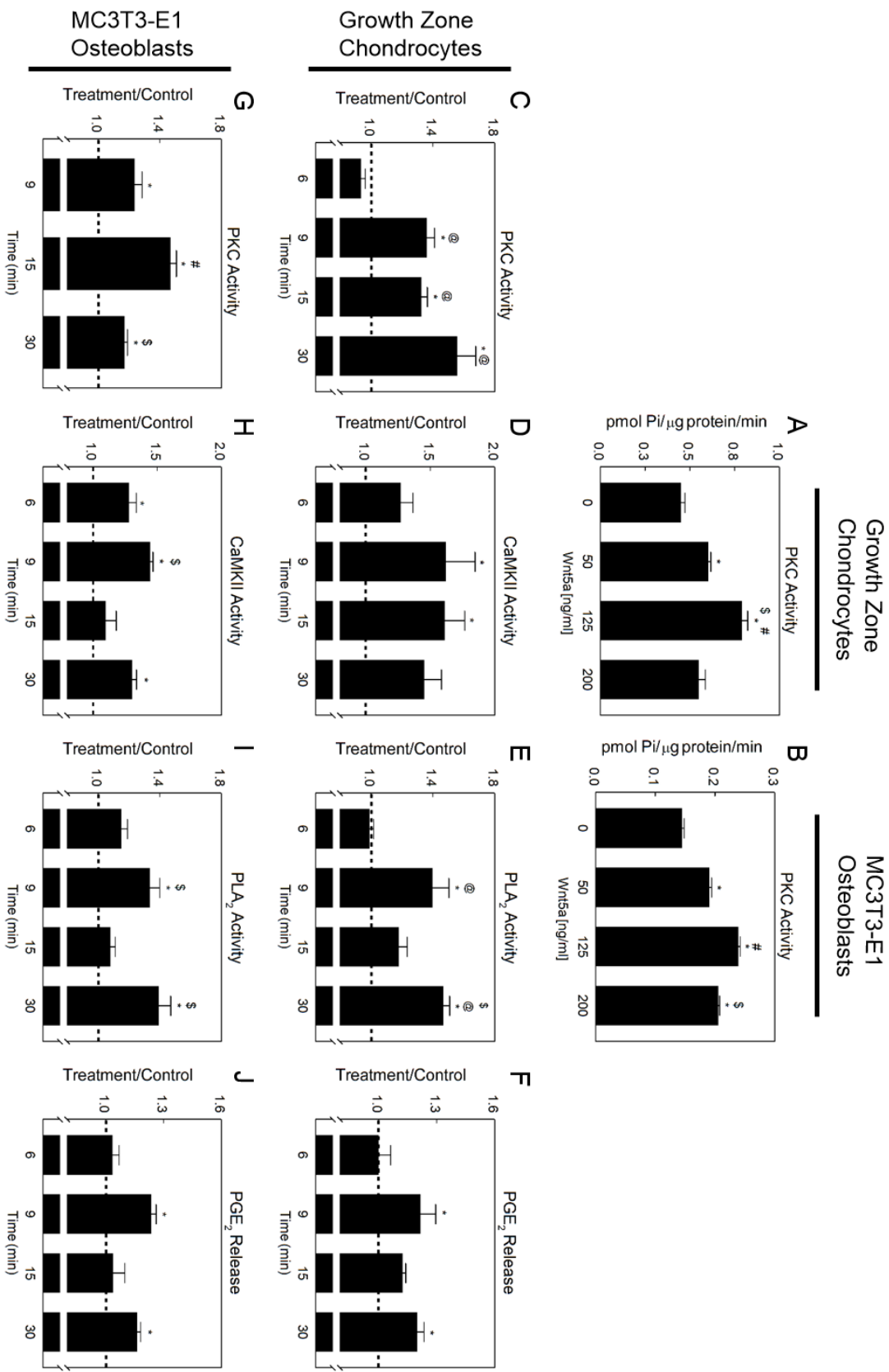


Figure 5.1: Effects of Wnt5a treatment on PKC, CaMKII, PLA₂ activations, and PGE₂ release. Growth zone chondrocytes (GC) were treated for 9 minutes (A) and MC3T3-E1 osteoblasts were treated for 15 minutes (B) with 0, 50, 125, and 200 ng/ml Wnt5a. PKC activity was measured as described and normalized to total protein level. .^{*}*p*<0.05, *versus* 0 ng/ml Wnt5a; #*p*<0.05, *versus* 50 ng/ml Wnt5a; \$*p*<0.05, *versus* 50 ng/ml Wnt5a. Growth zone chondrocytes (C-F) and MC3T3-E1 (G-J) were treated with 125 ng/ml Wnt5a for 6, 9, 15, and 30 minutes. PKC (C,G), CaMKII (D,H) and PLA₂ (E,I) activations were measured as described and normalized to total protein. PGE₂ release (F,J) was measured and normalized to total DNA. Treatment over control ratios were calculated for each parameter. The dashed line represents the value for the control cultures, which was set to 1. ^{*}*p*<0.05, 1 α ,25(OH)₂D₃ treatment *versus* control; [@]*p*<0.05, *versus* 6 minutes; #*p*<0.05, *versus* 9 minutes; \$*p*<0.05, *versus* 6 minutes.

Roles of Pdia3, VDR, Cav-1, and Lipid Rafts in Wnt5a-mediated Rapid Activation of PKC

Pdia3, VDR, and plasma membrane lipids rafts structures were involved in Wnt5a-stimulated rapid activation of PKC in MC3T3-E1 osteoblasts, while Cav-1 was not required. Unlike WT cells, shPdia3 osteoblasts did not increase in PKC activity in response to Wnt5a (Fig. 5.2A). Wnt5a stimulated PKC activity in shVdr cells was significantly lower than in WT cells (Fig. 5.2B). However, Wnt5a activated PKC in shCav-1 osteoblasts (Fig. 5.2C). Likewise, Pdia3 antibody (Fig. 5.2D) and VDR antibody (Fig. 5.2E) significantly reduced the Wnt5a-induced increase in PKC activity in MC3T3-E1 cells. Although Wnt5a stimulated PKC activity in cells pretreated with lipid raft disruptor β -CD, the increase was significantly lower when compared to the β -CD untreated group (Fig. 5.2F).

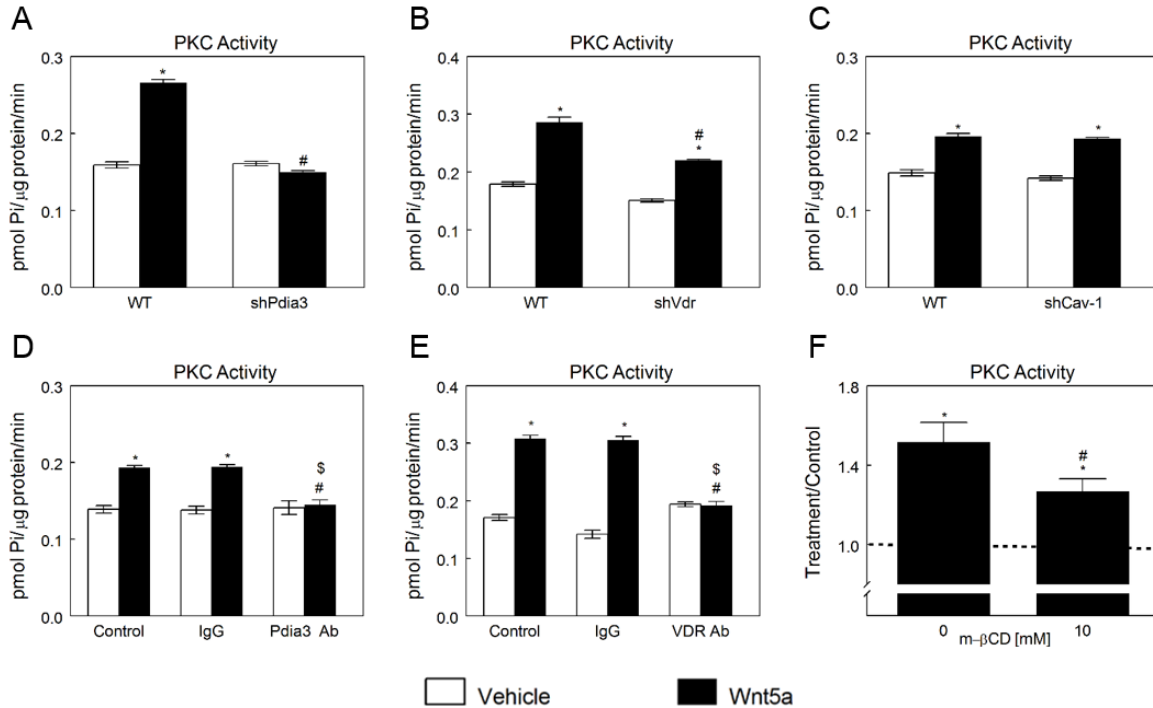


Figure 5.2: Effects of Pdia3, VDR and Cav-1 silencing or blocking and β -CD on Wnt5a-mediated activation of PKC in MC3T3-E1 cells. Wild type (WT), shPdia3 (A), shVdr (B) and shCav-1 (C) MC3T3-E1 cells were treated with Wnt5a for 15 minutes. PKC activity was measured as described and normalized to total protein level. * $p < 0.05$, treatment versus control; # $p < 0.05$, versus Wnt5a treated WT. MC3T3-E1 osteoblasts were pretreated with either anti-Pdia3 (D) or anti-VDR (E) antibodies for 30 minutes, and next they were treated with Wnt5a for 15 minutes. PKC activity was measured as described and normalized to total protein level. * $p < 0.05$, treatment versus control; # $p < 0.05$, versus Wnt5a treated control group; \$ $p < 0.05$, versus Wnt5a treated IgG group. (F) MC3T3-E1 osteoblasts were pretreated with β -CD for 30 minutes, and next they were treated with Wnt5a for 15 minutes. PKC activity was measured as described and normalized to total protein level. Treatment over control ratios were calculated for each parameter. The dashed line represents the value for the control cultures, which was set to 1. * $p < 0.05$, treatment versus control.

Roles of CaM, CaMKII- α , CaMKII- β , PLAA, and PLA₂ in Wnt5a-mediated Rapid Activation of PKC

In MC3T3-E1 cells, Wnt5a-mediated activation of PKC depends on upstream actions of CaM, CaMKII- α , PLAA, and PLA₂. Calmodulin inhibitor W-7 blocked activation of PKC in response to Wnt5a at 1 and 10 μ M, but not at 0.1 μ M (Fig. 5.3A). mer-CaMKIINtide inhibited

the Wnt5a induced increase in PKC activity in a comparable manner to W-7. mer-CaMKIIntide significantly reduced stimulatory effects of Wnt5a on PKC activation at 1.25 μ M, and completely blocked the effect at 2.5 and 5 μ M (Fig. 5.3B). Wnt5a significantly increased PKC activity in WT and shCamk2b MC3T3-E1 cells, but this effect was prevented in shCamk2a cells (Fig. 5.3C). PLAA antibody significantly reduced the Wnt5a-induced increase in PKC activity in MC3T3-E1 cells, whereas IgG had no effect (Fig. 5.3D). Similarly, Wnt5a increased PKC activity in MC3T3-E1 cells, and effect was blocked in shPlaa cells (Fig. 5.3E). PLA₂ inhibitor AACOCF3 significantly reduced stimulatory effects of Wnt5a on PKC activation at 0.1 μ M, and completely blocked the effect at 1 and 10 μ M (Fig. 5.3F).

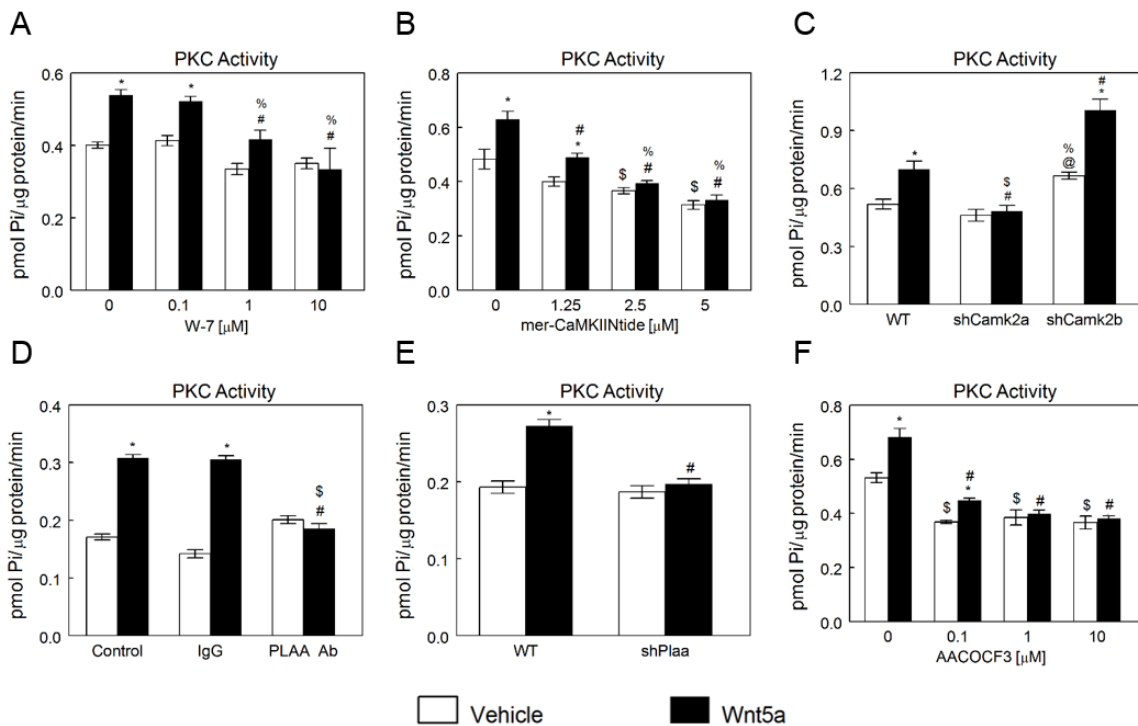


Figure 5.3: Effects of CaM, CaMKII, PLAA, and PLA₂ inhibition, and Plaa, Camk2a, and Camk2b silencing on Wnt5a-mediated activation of PKC in MC3T3-E1 cells. (A) MC3T3-E1 osteoblasts were pretreated with 0, 0.1, 1 and 10 μ M W-7 for 30 minutes, and next they were treated with Wnt5a for 15 minutes. PKC activity was measured as described and normalized to total protein level. * p <0.05, treatment versus control; # p <0.05, versus 0 μ M W-7 + Wnt5a; % p <0.05, versus 0.1 μ M W-7 + Wnt5a. (B) MC3T3-E1 osteoblasts were pretreated with 0, 1.25,

2.5, and 5 μM mer-CaMKIINtide for 30 minutes, and next they were treated with Wnt5a for 15 minutes. PKC activity was measured as described and normalized to total protein level. * $p < 0.05$, treatment *versus* control; # $p < 0.05$, *versus* 0 μM mer-CaMKIINtide + Wnt5a; \$ $p < 0.05$, *versus* 0.1 μM mer-CaMKIINtide + vehicle; % $p < 0.05$, *versus* 1.25 μM mer-CaMKIINtide + Wnt5a. (C) Wild type (WT), shCamk2a, and shCamk2b MC3T3-E1 cells were treated with Wnt5a for 15 minutes. PKC activity was measured as described and normalized to total protein level. * $p < 0.05$, treatment *versus* control; # $p < 0.05$, *versus* Wnt5a-treated WT; \$ $p < 0.05$, *versus* Wnt5a treated shCamk2b; @ $p < 0.05$, *versus* vehicle treated WT; % $p < 0.05$, *versus* vehicle treated shCamk2a. (D) MC3T3-E1 osteoblasts were pretreated with anti-PLAA antibody for 30 minutes, and next they were treated with Wnt5a for 15 minutes. PKC activity was measured as described and normalized to total protein level. * $p < 0.05$, treatment *versus* control; # $p < 0.05$, *versus* Wnt5a treated control group; \$ $p < 0.05$, *versus* Wnt5a treated IgG group. (E) Wild type (WT) and shPlaa MC3T3-E1 cells were treated with Wnt5a for 15 minutes. PKC activity was measured as described and normalized to total protein level. * $p < 0.05$, treatment *versus* control; # $p < 0.05$, *versus* Wnt5a-treated WT cells. (F) MC3T3-E1 cells were pretreated with 0, 0.1, 1, and 10 μM AACOCF3 for 30 minutes, and next they were treated with Wnt5a for 15 minutes. PKC activity was measured as described and normalized to total protein level. * $p < 0.05$, treatment *versus* control; # $p < 0.05$, *versus* 0 μM AACOCF3 + Wnt5a; \$ $p < 0.05$, 0 μM AACOCF3 + vehicle *versus* 0.1 μM AACOCF3 + Wnt5a.

Wnt5a and $1\alpha,25(\text{OH})_2\text{D}_3$ Co-treatment Studies

Given that both $1\alpha,25(\text{OH})_2\text{D}_3$ and Wnt5a promote maturation of osteoblasts and use Pdia3 to induce their effects, we tested the effects of their co-treatment on the induction of their signaling pathways in MC3T3-E1 osteoblasts, specifically examining PKC activation. In MC3T3-E1 osteoblasts, $1\alpha,25(\text{OH})_2\text{D}_3$ caused a dose-dependent increase in PKC activity in control cultures (Fig. 5.4A). When 10^{-10} - 10^{-8} M $1\alpha,25(\text{OH})_2\text{D}_3$ and 125 ng/ml Wnt5a were added to MC3T3-E1 cell together, the increase in PKC activity was reduced in a $1\alpha,25(\text{OH})_2\text{D}_3$ dose-dependent manner, and returned to control levels at the highest concentration of $1\alpha,25(\text{OH})_2\text{D}_3$ tested. Furthermore, Wnt5a increased PKC activity in a dose-dependent manner (Fig. 5.4B). Co-treatment with 50 ng/ml Wnt5a caused a 2-fold increase in $1\alpha,25(\text{OH})_2\text{D}_3$ stimulated PKC activity compared to cultures treated with only $1\alpha,25(\text{OH})_2\text{D}_3$. However, as the concentration of Wnt5a increased, $1\alpha,25(\text{OH})_2\text{D}_3$ -stimulated PKC activation was suppressed.

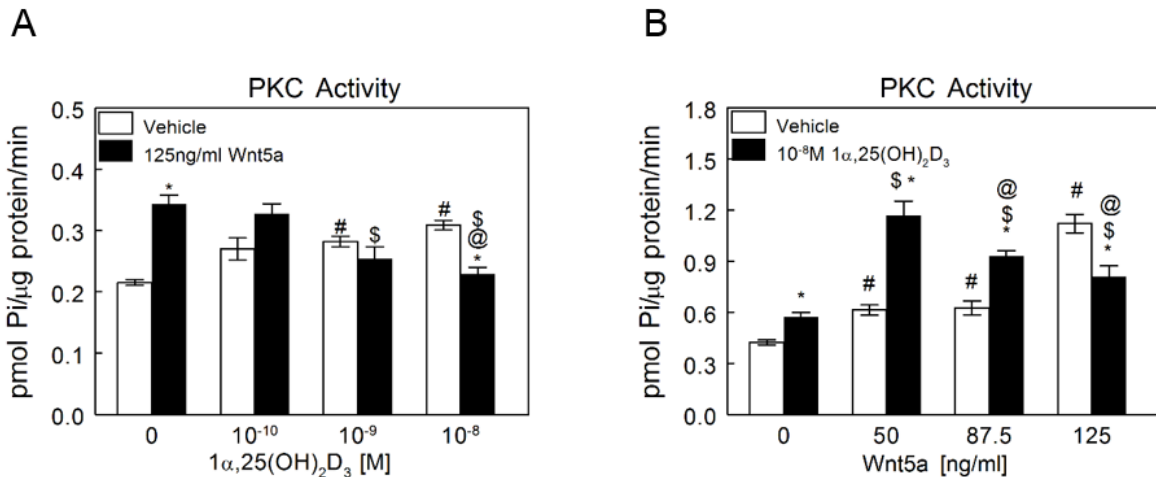


Figure 5.4: Effect of $1\alpha,25(\text{OH})_2\text{D}_3$ in Wnt5a-dependent PKC activation and effect of Wnt5a in $1\alpha,25(\text{OH})_2\text{D}_3$ regulation of PKC activity. (A) MC3T3-E1 cells were treated for 15 minutes with 10^{-10} , 10^{-9} and 10^{-8} M $1\alpha,25(\text{OH})_2\text{D}_3$. Wnt5a was added to one-half of the cultures at the concentration of 125 ng/ml, at the time of the treatment. At the end of incubation, cell layers were collected for PKC assay. PKC values were normalized to total protein. * $p < 0.05$, treatment versus control; # $p < 0.05$, versus 0 M $1\alpha,25(\text{OH})_2\text{D}_3$ + vehicle; \$ $p < 0.05$, versus 0 M $1\alpha,25(\text{OH})_2\text{D}_3$ + Wnt5a; @ $p < 0.05$ versus 10^{-10} M $1\alpha,25(\text{OH})_2\text{D}_3$ + Wnt5a. (B) MC3T3-E1 cells were treated with 10^{-8} M $1\alpha,25(\text{OH})_2\text{D}_3$ in the presence and absence of 50, 87.5 and 125 ng/ml Wnt5a. At the end of the incubation, the cell layers were collected for PKC assay. PKC values were normalized to total protein. * $p < 0.05$, treatment versus control; # $p < 0.05$, versus 0 ng/ml Wnt5a + vehicle; \$ $p < 0.05$, versus $1\alpha,25(\text{OH})_2\text{D}_3$ + 0 ng/ml Wnt5a; @ $p < 0.05$ versus $1\alpha,25(\text{OH})_2\text{D}_3$ + 5 ng/ml Wnt5a.

Roles of ROR2, FZD2, and FZD5 in $1\alpha,25(\text{OH})_2\text{D}_3$ -mediated PKC Activation and Their Subcellular Localization

Given, the key roles ROR2, FZD2 and FZD5 play in Wnt5a signaling, we assessed their role on $1\alpha,25(\text{OH})_2\text{D}_3$ stimulated rapid activation of PKC and CaMKII. ROR2, but not FZD2 and FZD5 mediated the $1\alpha,25(\text{OH})_2\text{D}_3$ stimulated rapid activation of PKC and CaMKII in MC3T3-E1 osteoblasts. Anti-ROR2 antibody abolished the $1\alpha,25(\text{OH})_2\text{D}_3$ -dependent increase in PKC activity in MC3T3-E1 cells (Fig. 5.5A), whereas, IgG had no effect. Conversely, blocking FZD2 and FZD5 receptors had no effect on activation of PKC in response to $1\alpha,25(\text{OH})_2\text{D}_3$ treatment. Similarly, anti-ROR2 antibody abolished the $1\alpha,25(\text{OH})_2\text{D}_3$ -dependent increase in

CaMKII activity in MC3T3-E1 cells (Fig. 5.5B). Furthermore, anti-ROR2 antibody had no effect on PLAA-induced CaMKII activation (Fig. 5.5C). Western blots of the plasma membrane fractions of MC3T3-E1 cells indicated that ROR2, FZD2, and FZD5 were present in the plasma membranes with their greatest concentration in fraction 3, which represents caveolae microdomains (Fig. 5.5D).

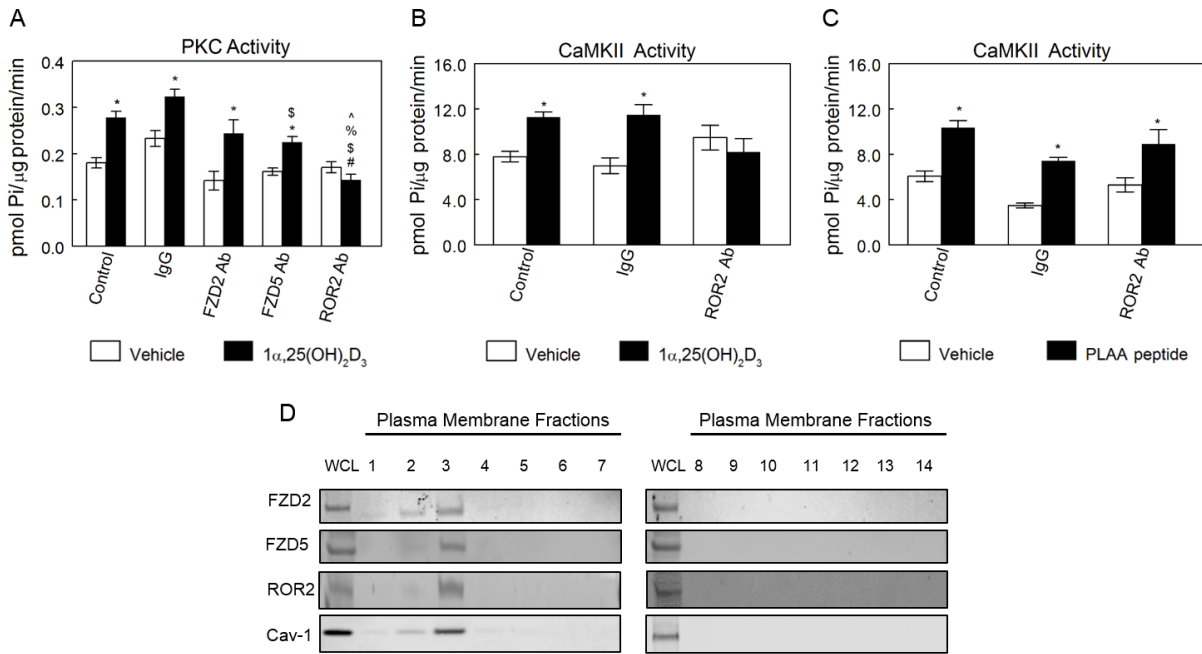


Figure 5.5: Role of FZD2, FZD5 and ROR2 in 1 α ,25(OH) $_2$ D $_3$ -dependent PKC activation and their plasma membrane localization. (A) MC3T3-E1 osteoblasts were pretreated with either anti-FZD2, anti-FZD5 or anti-ROR2 antibodies for 30 minutes, and next they were treated with 1 α ,25(OH) $_2$ D $_3$ for 15 minutes. PKC activity was measured as described and normalized to total protein level. * p <0.05, treatment versus control; [#] p <0.05, versus vehicle treated Control group; [§] p <0.05, versus IgG + 1 α ,25(OH) $_2$ D $_3$; [¶] p <0.05 versus FZD2 Ab + 1 α ,25(OH) $_2$ D $_3$; [^] p <0.05 versus ROR2 Ab + 1 α ,25(OH) $_2$ D $_3$. (B) MC3T3-E1 osteoblasts were pretreated with anti-ROR2 antibodies for 30 minutes, and next they were treated with 1 α ,25(OH) $_2$ D $_3$ for 15 minutes. CaMKII activity was measured and normalized to total protein level. * p <0.05, treatment versus control. (C) MC3T3-E1 osteoblasts were pretreated with anti-ROR2 antibodies for 30 minutes, and next they were treated with PLAA peptide for 15 minutes. CaMKII activity was measured and normalized to total protein level. * p <0.05, treatment versus control. (D) Plasma membrane localization of FZD2, FZD5 and ROR2. Plasma membrane fractions were isolated as described. Presence of FZD2, FZD5, ROR2 and Cav-1 in fractions were examined by Western blot. Each figure is a representative experiment repeated three times with similar results.

Effects of $1\alpha,25(\text{OH})_2\text{D}_3$ Treatment on $1\alpha,25(\text{OH})_2\text{D}_3$ Receptor Complex and Wnt5a Receptors Interactions

Immunoprecipitation studies confirmed the interaction between components of $1\alpha,25(\text{OH})_2\text{D}_3$ receptor complex and Wnt5a receptors. $1\alpha,25(\text{OH})_2\text{D}_3$ treatment altered some of these interactions. Samples of MC3T3-E1 whole cell lysates immunoprecipitated using antibodies to Pdia3 (IP:Pdia3) were positive for FZD2, FZD5, and ROR2 (Fig. 5.6A). Treatment with $1\alpha,25(\text{OH})_2\text{D}_3$ for 15 minutes had no effect on Pdia3:FRZ5 but increased Pdia3:FZD2 and Pdia3:ROR2. Western blots of whole cell lysates immunoprecipitated with antibodies to PLAA (IP:PLAA) demonstrated an increase in FZD2-associated PLAA after addition of $1\alpha,25(\text{OH})_2\text{D}_3$ (Fig. 5.6B). FZD5 and ROR2 interacted with PLAA, but $1\alpha,25(\text{OH})_2\text{D}_3$ treatment had no effect on these interactions. Cav-1 (IP:Cav-1) interacted with FZD2, FZD5, and ROR2 (Fig. 5.6C). Treatment with $1\alpha,25(\text{OH})_2\text{D}_3$ for 15 minutes had no effect on FZD2 and FZD5 but reduced ROR2. Immunoprecipitation of CaM (IP:CaM) demonstrated interaction with FZD5 with or without $1\alpha,25(\text{OH})_2\text{D}_3$ treatment (Fig. 5.6D). FZD2 and ROR2 also interacted with CaM and $1\alpha,25(\text{OH})_2\text{D}_3$ treatment reduced their interactions with CaM.

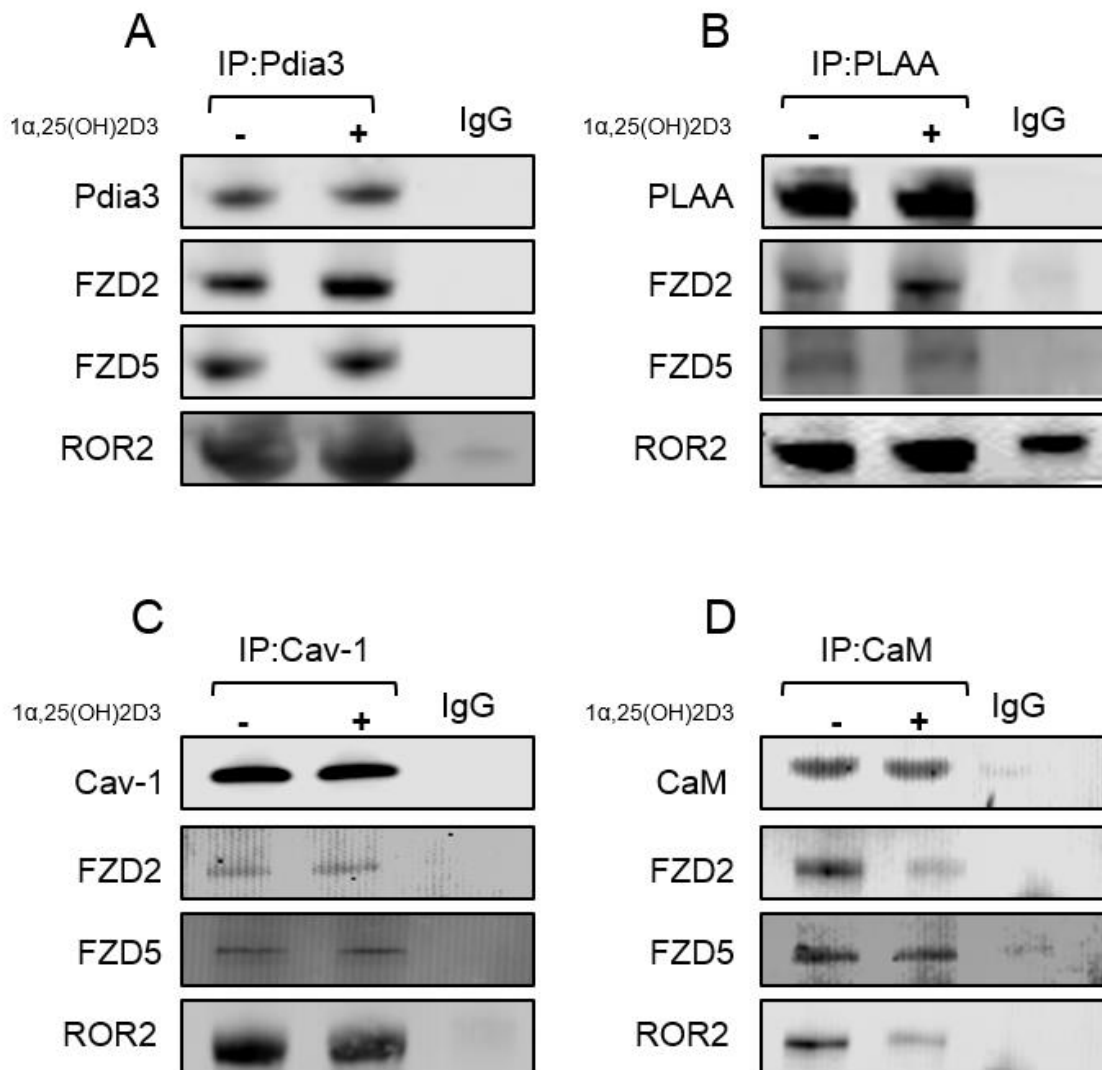


Figure 5.6: Effect of $1\alpha,25(\text{OH})_2\text{D}_3$ treatment on interactions between $1\alpha,25(\text{OH})_2\text{D}_3$ receptor complex and Wnt5a receptors. MC3T3-E1 cells were treated with $1\alpha,25(\text{OH})_2\text{D}_3$ for 15 minutes. Whole cell lysates were isolated as described. (A) Pdia3 was immunoprecipitated and subjected to Western blot. The membranes were incubated with Ab Pdia3, Ab FZD2, anti-FZD5, and anti-ROR2 antibodies. (B) PLAA was immunoprecipitated and subjected to Western blot. The membranes were incubated with the anti-PLAA, anti-FZD2, anti-FZD5, and anti-ROR2 antibodies. (C) Cav-1 was immunoprecipitated and subjected to Western blot. The membranes were incubated with the anti-Cav-1, anti-FZD2, anti-FZD5, and anti-ROR2 antibodies. (D) CaM was immunoprecipitated and subjected to Western blot. The membranes were incubated with the anti-CaM, anti-FZD2, anti-FZD5, and anti-ROR2 antibodies. Each figure is a representative experiment repeated three times with similar results.

Effects of Wnt5a Treatment on Interactions between $1\alpha,25(\text{OH})_2\text{D}_3$ Receptor Complex and Wnt5a Receptors

Immunoprecipitates of MC3T3-E1 whole cell lysates using antibodies to Pdia3 (IP:Pdia3) were positive for FZD2 and FZD5 (Fig. 5.7A). Treatment with Wnt5a for 15 minutes had no effect on FZD2's interaction with Pdia3 but increased FZD5. Western blots of whole cell lysates immunoprecipitated with antibodies to PLAA (IP:PLAA) demonstrated interaction with FZD2 and FZD5 with and without $1\alpha,25(\text{OH})_2\text{D}_3$ treatment (Fig. 5.7B). ROR2 also interacted with PLAA, and Wnt5a treatment reduced its interaction with PLAA. Immunoprecipitation of Cav-1 (IP:Cav-1) demonstrated interactions with FZD2, FZD5 and ROR2 (Fig. 5.7C). While Wnt5a treatment reduced FZD2 and ROR2 interactions with Cav-1, it had no effect on FZD5 interactions with Cav-1. Immunoprecipitation of CaM (IP:CaM) demonstrated interaction with FZD5 with or without Wnt5a treatment (Fig. 5.7D). FZD2 and ROR2 also interacted with CaM. $1\alpha,25(\text{OH})_2\text{D}_3$ treatment increased FZD2 and CaM interaction and decreased ROR2 and CaM interaction.

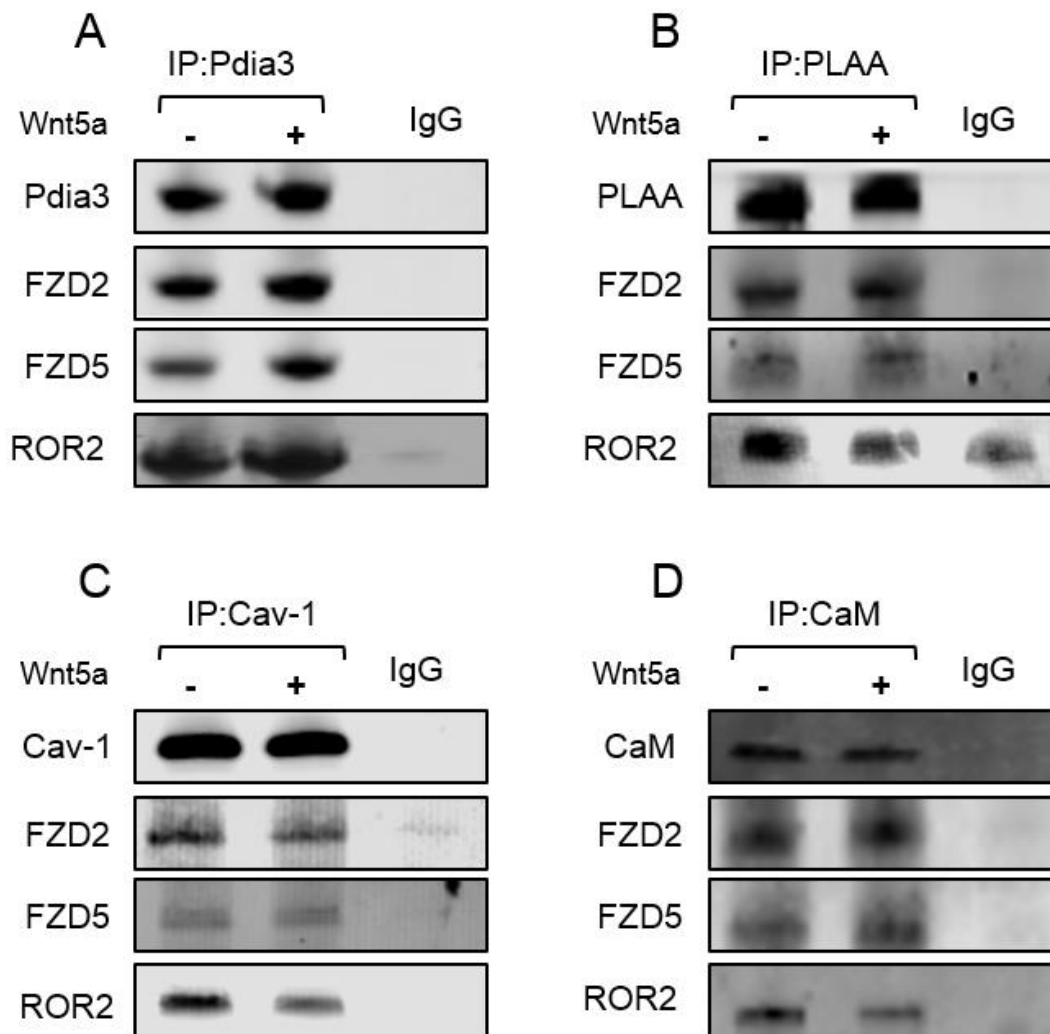


Figure 5.7: Effect of Wnt5a treatment on interactions between $1\alpha,25(\text{OH})_2\text{D}_3$ receptor complex and Wnt5a receptors. MC3T3-E1 cells were treated with Wnt5a for 15 minutes. Whole cell lysates were isolated as described. (A) Pdia3 was immunoprecipitated and subjected to Western blot. The membranes were incubated with the anti-Pdia3, anti-FZD2 and anti-FZD5 antibodies. (B) PLAA was immunoprecipitated and subjected to Western blot. The membranes were incubated with the anti-PLAA, anti-FZD2, anti-FZD5 and anti-ROR2 antibodies. (C) Cav-1 was immunoprecipitated and subjected to Western blot. The membranes were incubated with the anti-Cav-1, anti-FZD2, anti-FZD5 and anti-ROR2 antibodies. (D) CaM was immunoprecipitated and subjected to Western blot. The membranes were incubated with the anti-CaM, anti-FZD2, anti-FZD5 and anti-ROR2 antibodies. Each figure is a representative experiment repeated three times with similar results.

DISCUSSION

This study demonstrates that signaling proteins critical for the $1\alpha,25(\text{OH})_2\text{D}_3$ membrane-mediated pathway are also crucial for Wnt5a calcium-dependent signaling. Events at the signaling level indicated that Wnt5a calcium-dependent signaling works through a mechanism involving the CaMKII/PLA₂/PGE₂/PKC pathway. Moreover, silencing or blocking of Pdia3, PLAA and VDR and inhibition of CaM, CaMKII and PLA₂ affected the activity of PKC in response to Wnt5a treatment. In contrast, PKC activity was unaffected in Cav-1 silenced cells, but the stimulatory effect of Wnt5a was decreased in cells treated with β -CD. Furthermore, Western blots of plasma membrane fractions indicated that ROR2, FZD2, and FZD5 are localized in caveolae fraction. Blocking of ROR2 abolished the stimulatory effects of $1\alpha,25(\text{OH})_2\text{D}_3$ on PKC and CaMKII activations. This study also provides mechanistic information by showing that the $1\alpha,25(\text{OH})_2\text{D}_3$ receptor complex and its downstream mediators form complexes with Wnt5a receptors, and these complexes respond to both $1\alpha,25(\text{OH})_2\text{D}_3$ and Wnt5a treatment by altering some of their protein-protein interactions.

Similar to $1\alpha,25(\text{OH})_2\text{D}_3$ signaling, Wnt5a time course studies indicate a rapid increase in CaMKII, PLA₂ and PKC activities and PGE₂ release in GC chondrocytes and MC3T3-E1 osteoblasts. While the profiles of time points at which Wnt5a activated PLA₂ and triggered PGE₂ release were similar between GC and MC3T3-E1 cells, differences were observed in PKC and CaMKII activities. One reason that may contribute to such a difference is that while GC cells are primary cartilage cells isolated from rat costochondral cartilage growth zone, MC3T3-E1 osteoblasts are a cell line derived from mouse calvaria. The second potential reason for such an observation is that growth zone chondrocytes used in these experiments were isolated from 100-

125 g male Sprague-Dawley rats, and these rats were at the end of their adolescent growth spurt while the mouse osteoblastic MC3T3-E1 cell line was derived from a newborn mouse.

Previously, we reported that Pdia3, PLAA, VDR, Cav-1 and caveolae are critical for $1\alpha,25(\text{OH})_2\text{D}_3$ membrane-mediated signaling (10,12,87,125). Similar to $1\alpha,25(\text{OH})_2\text{D}_3$ membrane-mediated signaling, our results indicated that Pdia3, PLAA, and VDR are critical for Wnt5a calcium-dependent pathway. However, to our surprise, silenced Cav-1 osteoblasts activated PKC in response to Wnt5a treatment, suggesting that Cav-1 is not necessary for the Wnt5a calcium-dependent pathway. To further investigate the role of lipid rafts in Wnt5a calcium-dependent pathway, we subjected the cells to β -CD. PKC activity increased in cells pretreated with β -CD but the increase was significantly lower than the β -CD-untreated group. Collectively, these studies indicate that Wnt5a induces its effects partially via lipid rafts and caveolae are not required to mediate Wnt5a effects. Previously, FZD5 and FZD2 proteins have been reported to be found in clathrin coated pits, suggesting Wnt5a regulates its pathway via this group of lipid rafts (200).

Our inhibitor study indicates that CaM, CaMKII, and PLA₂ are critical for Wnt5a stimulated PKC activation. We previously reported that CaM plays a critical role in $1\alpha,25(\text{OH})_2\text{D}_3$ membrane-mediated pathway and its inhibition blocks $1\alpha,25(\text{OH})_2\text{D}_3$ stimulated rapid activation of PKC (187). In the present study, we found that CaM inhibition by W-7 abolished Wnt5a stimulated activation of PKC in a dose-dependent manner. Our hypothesis that CaM is required for Wnt5a stimulated activation of PKC is also supported by the observation that CaM inhibition suppresses PKC translocation in response to phorbol 12-myristate 13-acetate (PMA) treatment in the rat aorta (201). In our previous work, we reported that CaMKII, isoform α , is necessary for $1\alpha,25(\text{OH})_2\text{D}_3$ membrane stimulated activation of PLA₂, PKC and PGE₂

release (187). Using mer-CaMKIINtide to inhibit the effect of CaMKII, we tested the role of CaMKII in Wnt5a induced PKC activation. In the current study, we found that CaMKII inhibition abolished Wnt5a stimulated activation of PKC in a dose-dependent manner. Our hypothesis that CaMKII is required for Wnt5a induced activation of PKC is also supported by the observation that CaMKII regulates PLA₂ activity (18). PLA₂ is known to act upstream of PKC in several signaling pathways, including 1 α ,25(OH)₂D₃ and dihydrotestosterone (92,202), hence CaMKII influences PKC activity in a PLA₂-dependent mechanism. Additionally, in agreement with previous findings (92,202), we found that PLA₂ inhibition abolished Wnt5a induced activation of PKC in a dose-dependent manner.

MC3T3-E1 osteoblasts respond to 125 ng/ml Wnt5a with a rapid increase in PKC activity. Here we report that co-treatment with 10⁻¹⁰-10⁻⁸ M 1 α ,25(OH)₂D₃ abrogates the increase in PKC activation seen with exogenous 125 ng/ml Wnt5a treatment alone, in a dose dependent manner. Co-treatment of osteoblasts with 125 ng/ml Wnt5a and 10⁻⁸ M 1 α ,25(OH)₂D₃, returned PKC activity to the control level. Previously, we reported that MC3T3-E1 osteoblasts respond to 10⁻⁸ M 1 α ,25(OH)₂D₃ with a rapid increase in PKC activity (10). However, co-treatment with 50-125ng/ml Wnt5a leads to a strong increase in PKC activity. Surprisingly, we observed that co-treatment with Wnt5a induces enhanced effects on 1 α ,25(OH)₂D₃ stimulated PKC activation at low dose of Wnt5a and repressive effects at high dose of Wnt5a. These results may suggest that Wnt5a and 1 α ,25(OH)₂D₃ pathways compete at their receptor complex or downstream pathway mediators levels.

Previously, we reported that 1 α ,25(OH)₂D₃ membrane associated receptor, Pdia3, is present in plasma membrane compartments called caveolae (203). We also showed that PLAA and CaM are present in caveolae, where their interaction with Pdia3 receptor complex is critical

for transducing the $1\alpha,25(\text{OH})_2\text{D}_3$ signal (125,187). In the present study, our plasma membrane fractionation experiment indicates that ROR2, FZD2, and FZD5 are localized in fraction 3. Furthermore, our receptor antibody blocking experiments shows that blocking ROR2 abolishes $1\alpha,25(\text{OH})_2\text{D}_3$ stimulated PKC activation while blocking FZD2 and FZD5 receptors has no effect on activation of PKC in response to $1\alpha,25(\text{OH})_2\text{D}_3$ treatment. These results indicate that Wnt5a co-receptor, ROR2, is part of $1\alpha,25(\text{OH})_2\text{D}_3$ membrane-associated receptor complex in caveolae. In agreement with our findings, another group has detected ROR2 in Cav-1- α positive cholesterol-rich, detergent-resistant microdomains (DRMs) of the plasma membrane in (204). Furthermore, they showed that ROR2 forms a complex with bone morphogenetic protein receptor type 1B (BMPR1B) in a ligand-independent manner and it inhibited the growth and differentiation factor 5 (GDF5)/BMPR1B induced Smad 1/5 signaling pathway in ATDC5 cells (205). Collectively, these findings suggest that ROR2 participates in multiple signaling pathways including Wnt5a, BMP and $1\alpha,25(\text{OH})_2\text{D}_3$.

Wnt5a induces its non-canonical signaling via several receptors. ROR2 is a transmembrane receptor, previously identified to mediate Wnt5a actions (206). Wnt5a increases *ROR2* expression, and knockdown of *WNT5A* dramatically decreases expression of *ROR2* (195). ROR2 has regions of cysteine-rich domain that serve as its Wnt binding domain (157,158). Several conditions, including brachydactyly type B and autosomal recessive Robinow syndrome, which display severe skeletal dysplasia, are due to mutations in the *ROR2* gene (207,208). Additionally, ROR2 is critically required for Wnt5a-induced migration of osteoblasts (209). Wnt5a can also act via the Frizzled family of receptors. In human cells, FZD2 and FZD5 are known to act as Wnt5a receptors and activate its non-canonical signaling cascades (155,156). Our immunoprecipitation study indicates that Pdia3 forms complexes with ROR2, FZD2, and

FZD5. While Wnt5a treatment increases the interactions between Pdia3-FZD5, the interactions between Pdia3-FZD2 remains unchanged. $1\alpha,25(\text{OH})_2\text{D}_3$ reduces the interactions between Pdia3-FZD2 whereas the interaction between Pdia3-FZD5 and Pdia3:ROR2 are not altered. Our PLAA immunoprecipitation shows that PLAA forms a complex with ROR2, FZD2, and FZD5. Our studies indicate that $1\alpha,25(\text{OH})_2\text{D}_3$ and Wnt5a trigger an increase in interaction between PLAA-FZD2 and a reduction in interaction between PLAA-FZD5. While Wnt5a treatment decreases the interaction between PLAA-ROR2, $1\alpha,25(\text{OH})_2\text{D}_3$ treatment does not change the interaction between PLAA-ROR2. To our surprise, Cav-1 immunoprecipitation studies indicate that Cav-1 forms a complex with ROR2, FZD2, and FZD5. Cav-1 immunoprecipitation studies show no change in Cav-1-FZD2 and Cav-1-FZD-5, while a reduction is observed between Cav-1-ROR2. Furthermore, we show that Wnt5a does not alter the interactions between Cav-1-FZD5 while, but it stimulates a reduction between Cav-1-FZD2 and Cav-1-ROR2. While Cav-1 silencing does not alter the response of osteoblasts to Wnt5a, our immunoprecipitation studies suggest Wnt5a treatment changes the interactions between Cav-1 and its receptors. Others have reported that while most of the FZD5 co-localizes with clathrin, a small amount of FZD5 has been observed to co-localize with Cav-1 in HeLaS3 cells (200).

Our CaM immunoprecipitation studies suggest that CaM forms a complex with ROR2, FZD2, and FZD5. Wnt5a treatment does not alter the interactions between CaM-FZD2 and CaM-FZD5, while it reduces the interaction between CaM-ROR2. $1\alpha,25(\text{OH})_2\text{D}_3$ treatment decreases the interactions between CaM-FZD2 and CaM-ROR2; however, it does not alter the interactions between CaM-FZD5. These results indicates that CaM serves as a mediator in both $1\alpha,25(\text{OH})_2\text{D}_3$ and Wnt5a pathways; suggesting its potential role to mediate the cross-talk between these two pathways.

The results of this study suggest that Wnt5a and $1\alpha,25(\text{OH})_2\text{D}_3$ mediate their effects via a network of interacting mediators rather than through a secluded linear pathway. In co-treatment studies, we speculate that $1\alpha,25(\text{OH})_2\text{D}_3$ receptor competes with Wnt5a receptors for binding of PLAA, CaM and Cav-1, thus inhibiting downstream PKC signaling. Previously, similar $1\alpha,25(\text{OH})_2\text{D}_3$ -induced mechanisms in which one hormone can modulate the activity of a second, by competing for a shared mediator site, have been identified. Work from the Ross lab has shown that retinoid X receptor (RXR)-vitamin D receptor (VDR) and retinoid acid receptor (RAR)-RXR heterodimers compete for a novel steroid hormone response element containing elements responding to retinoid acid and $1\alpha,25(\text{OH})_2\text{D}_3$ in the promoter region of the avian $\beta 3$ integrin gene (210). Co-treatment with retinoid acid and $1\alpha,25(\text{OH})_2\text{D}_3$ resulted in a response equal to that of retinoid acid alone (210). Furthermore, their results indicated RAR-RXR had a greater affinity for the shared promoter region than RXR-VDR, hence co-addition of retinoid acid and $1\alpha,25(\text{OH})_2\text{D}_3$ resulted in preferred binding of RAR-RXR to the promoter and inhibition of $1\alpha,25(\text{OH})_2\text{D}_3$ induced transcription (210). Similar to this finding, our results also indicated that Wnt5a and $1\alpha,25(\text{OH})_2\text{D}_3$ compete for similar signaling mediators and co-treatment antagonizes the immunological effects of $1\alpha,25(\text{OH})_2\text{D}_3$. $1\alpha,25(\text{OH})_2\text{D}_3$ is known to stimulate alkaline phosphatase activity (91) and osteopontin production (10), markers of osteoblast maturation, via its membrane-mediated events. Wnt5a has also been shown to promote osteoblasts differentiation and maturation. Wnt5a treatment increases osteocalcin and osteoprotegerin levels and alkaline phosphatase specific activity (20), while its knockout down regulates osteoblastic differentiation markers including runt related transcription factor 2, osterix and alkaline phosphatase (21). Future studies should focus on the *in vivo* consequences of the regulation of growth plate chondrocytes growth and differentiation by Wnt5a and $1\alpha,25(\text{OH})_2\text{D}_3$.

CONCLUSION

In conclusion, this study investigated the requirement for components of $1\alpha,25(\text{OH})_2\text{D}_3$ membrane-associated receptor complex in Wnt5a calcium-dependent signaling. We found that Wnt5a stimulates its calcium-dependent actions via Pdia3 receptor complex. In time course studies, GC chondrocytes and MC3T3-E1 osteoblasts treated with Wnt5a exhibited a time-dependent increase in activation of CaMKII, PLA₂, PKC, and PGE₂ release. Silencing Pdia3, PLAA, VDR, and inhibition of CaM, CaMKII, and PLA₂ suppressed the activation of PKC in response to Wnt5a treatment. Silencing Cav-1 had no effect on Wnt5a-mediated PKC activation, which reveals one of the differences between the mediators of $1\alpha,25(\text{OH})_2\text{D}_3$ and Wnt5a calcium-dependent pathways. Our results also showed that ROR2, one of the receptors of Wnt5a, plays an important role in $1\alpha,25(\text{OH})_2\text{D}_3$ membrane mediated signaling. Blocking ROR2 abolished $1\alpha,25(\text{OH})_2\text{D}_3$ induced PKC and CaMKII activations. Moreover, immunoprecipitation studies showed that $1\alpha,25(\text{OH})_2\text{D}_3$ membrane receptor complex (Pdia3, PLAA, Cav-1 and CaM) interacts with Wnt5a receptors (ROR2, FZD2 and FZD5). While most of their protein-protein interactions were independent of either $1\alpha,25(\text{OH})_2\text{D}_3$ or Wnt5a treatment, a few of the interactions changed with ligands treatments. In co-treatment study, addition of $1\alpha,25(\text{OH})_2\text{D}_3$ induced repressive effects on Wnt5a mediated PKC activation in a dose-dependent manner. We found that co-treatment with $1\alpha,25(\text{OH})_2\text{D}_3$ repressed Wnt5a-mediated PKC activation in a dose-dependent manner, and was most inhibited at 10^{-8} M. Furthermore, co-treatment with 50 ng/ml Wnt5a caused a 2-fold increase in $1\alpha,25(\text{OH})_2\text{D}_3$ stimulated PKC activity compared to cultures treated with only $1\alpha,25(\text{OH})_2\text{D}_3$. However, as the concentration of Wnt5a increased, it induced repressive effects on $1\alpha,25(\text{OH})_2\text{D}_3$ -mediated PKC activation. The results of this study suggest that signaling components of Pdia3 receptor complex are required for mediating the calcium-

dependent actions of Wnt5a and $1\alpha,25(\text{OH})_2\text{D}_3$ may modulate the response of Wnt5a by competing for similar signaling mediators.

CHAPTER 6

CONCLUSIONS AND FUTURE DIRECTIONS

Considering the complexity of signal transduction pathways, occasional errors in cell signaling may result in pathological or disease states. $1\alpha,25(\text{OH})_2\text{D}_3$ and its receptors play key roles in the regulation of growth plate chondrocytes and bone mineralization. Successful development of therapeutic agents that mimic the effects of $1\alpha,25(\text{OH})_2\text{D}_3$ requires a comprehensive understanding of the signaling mechanisms involved in the actions of this secosteroid hormone. The objective of this thesis was to examine the roles of PLAA protein and CaMKII in $1\alpha,25(\text{OH})_2\text{D}_3$ rapid membrane-mediated signaling, and to determine the receptor complex interactions between the $1\alpha,25(\text{OH})_2\text{D}_3$ and Wnt5a receptor complex. The results of our study confirm that PLAA and CaMKII are crucial for mediating the rapid actions of $1\alpha,25(\text{OH})_2\text{D}_3$, and $1\alpha,25(\text{OH})_2\text{D}_3$ and Wnt5a calcium-dependent pathways are mediated by similar signaling components, which suggest the two pathways may interact.

PLAA is produced in many $1\alpha,25(\text{OH})_2\text{D}_3$ -responsive cells including growth zone chondrocytes and osteoblasts. PLAA peptide treatment mimicked the effects of $1\alpha,25(\text{OH})_2\text{D}_3$ on growth zone chondrocytes and MC3T3-E1 osteoblasts, and was found to be necessary for $1\alpha,25(\text{OH})_2\text{D}_3$ rapid membrane-mediated signaling. This protein was detected in plasma membranes and caveolae, and crosslinking studies confirmed the localization of PLAA on the extracellular face of the membrane. $1\alpha,25(\text{OH})_2\text{D}_3$ increased the interaction between Pdia3 and PLAA, and it failed to activate PLA₂ and PKC or cause PGE₂ release when PLAA was knocked down. The results of this study suggest that PLAA is the likely candidate aiding in transducing the $1\alpha,25(\text{OH})_2\text{D}_3$ signal from the Pdia3 receptor complex. Moreover, the strong link between

PLAA and $1\alpha,25(\text{OH})_2\text{D}_3$ rapid signaling may have implications on normal skeletal development, which requires further investigation. Our results suggest that PLAA is exposed to the extracellular membrane region, which makes it an attractive candidate as a potential therapeutic target for conditions that are resistant to conventional vitamin D therapy. Small-molecule drugs can be designed to activate PLAA at the extracellular face of the plasma membrane, thereby reducing the cytotoxicity caused by entrance of these molecules inside of the cells. Developing a novel small-molecule drug that stimulates rapid actions of $1\alpha,25(\text{OH})_2\text{D}_3$ via activation of PLAA may take decades before it is clinically available to patients. Alternatively, delivering the full-length PLAA protein or its peptide, which contains a region of homology with melittin, via molecular targeted nanocarriers, may lead to the next big clinical breakthrough for treating disorders that are resistant to vitamin D therapy.

In the growth plate, CaMKII is an important regulator of chondrocyte hypertrophy, and chemical inhibition of CaMKII disrupts the growth plate architecture. The data demonstrated that $1\alpha,25(\text{OH})_2\text{D}_3$ and PLAA peptide rapidly increased CaMKII activity, and knockdown of members of $1\alpha,25(\text{OH})_2\text{D}_3$ receptor complex inhibited $1\alpha,25(\text{OH})_2\text{D}_3$ -induced CaMKII activation. $1\alpha,25(\text{OH})_2\text{D}_3$ increased the interaction between CaM and PLAA. Knockdown of CaMKII- α and inhibition of CaM reduced cPLA₂ and PKC activities, PGE₂ release and osteoblast maturation markers in response to $1\alpha,25(\text{OH})_2\text{D}_3$. Collectively, these findings suggest $1\alpha,25(\text{OH})_2\text{D}_3$ mediates its signal from PLAA to PLA₂ via a mechanism involving CaM and CaMKII. Aberrations in $1\alpha,25(\text{OH})_2\text{D}_3$ membrane-mediated signaling due to the loss of activated CaMKII may have adverse effects on skeletal development, which remains to be elucidated in future studies. It is possible that in clinical cases where complications arise with inactivation of CaMKII isoform(s), including Alzheimer's disease, the response to $1\alpha,25(\text{OH})_2\text{D}_3$ and other

activators of the calcium-dependent pathway is less robust than the response in individuals carrying functional CaMKII. This deregulation of calcium-dependent pathways may possibly affect bone and cartilage.

Wnt5a and $1\alpha,25(\text{OH})_2\text{D}_3$ play critical roles in promoting osteoblast maturation. This study demonstrated that signaling proteins critical for $1\alpha,25(\text{OH})_2\text{D}_3$ membrane mediated pathway are also important for Wnt5a calcium-dependent signaling, and suggests a novel mechanism by which Pdia3 receptor complex modulates the calcium-dependent actions of Wnt5a. The results of this study indicated that Wnt5a signal is transduced via a mechanism involving the rapid activation of CaMKII/PLA₂/PGE₂/PKC pathway in growth zone chondrocytes and MC3T3-E1 osteoblasts. Pdia3, PLAA, CaM, CaMKII and PLA₂ were essential for mediating rapid actions of Wnt5a. Moreover, Wnt5a receptors were found to be localized in caveolae, where they interacted with the $1\alpha,25(\text{OH})_2\text{D}_3$ receptor complex. Co-treatment with $1\alpha,25(\text{OH})_2\text{D}_3$ repressed Wnt5a-mediated PKC activation in a dose-dependent manner, and was most inhibited at 10^{-8} M. Furthermore, co-treatment with 50 ng/ml Wnt5a caused a 2-fold increase in $1\alpha,25(\text{OH})_2\text{D}_3$ stimulated PKC activity compared to cultures treated with only $1\alpha,25(\text{OH})_2\text{D}_3$. However, as the concentration of Wnt5a increased, it induced repressive effects on $1\alpha,25(\text{OH})_2\text{D}_3$ -mediated PKC activation. These results demonstrate that $1\alpha,25(\text{OH})_2\text{D}_3$ and Wnt5a calcium-dependent pathways are mediated by similar signaling components, which suggest the two pathways may interact. Aberrations in $1\alpha,25(\text{OH})_2\text{D}_3$ membrane-mediated signaling may affect those signaling orchestrated by Wnt5a and their regulation of skeletal development, which remains to be elucidated in future studies. It is possible that in disorders arising due to inactivation of $1\alpha,25(\text{OH})_2\text{D}_3$ membrane-mediated signaling, the response to Wnt5a is reduced, leading to deregulation of skeletal development. *In vivo* animal studies examining the

role of interactions between the two pathways in growth plate development are needed to confirm this hypothesis. Biochemically, the endochondral fracture healing process is similar to that of growth plate calcification. It is probable that the interaction between $1\alpha,25(\text{OH})_2\text{D}_3$ and Wnt5a calcium-dependent pathways may regulate bone fracture healing.

Caveolae are plasma membrane domains enriched in cholesterol and sphingolipids. These special types of lipid rafts are involved in signal transduction processes, and trafficking and sorting of proteins (211,212). $1\alpha,25(\text{OH})_2\text{D}_3$ stimulates the rapid Pdia3-mediated signaling via caveolae microdomains of the plasma membrane. The Pdia3 receptor complex is localized in caveolae and the disruption of these membranes using methyl-beta-cyclodextrin (β -CD) abolishes $1\alpha,25(\text{OH})_2\text{D}_3$ -dependent PKC and CaMKII activation.

β -CD is well known to bind and sequester cholesterol in its hydrophobic core (213,214). In addition to cholesterol binding, several other studies reported that cyclodextrins can form complexes with sphingolipid monomers (215,216). “Stringent” treatment conditions, 10mM β -CD for 30 minutes, significantly reduce phosphatidylcholine (PC), cholesterol and sphingolipid content of low-density detergent-insoluble membrane fractions, which include caveolae (217). Recent studies have also indicated a role for sphingolipid signaling in rapid actions induced by $1\alpha,25(\text{OH})_2\text{D}_3$ (218,219). $1\alpha,25(\text{OH})_2\text{D}_3$ activates sphingomyelinase, leading to hydrolysis of sphingomyelin and ceramide production at 15 minutes after treatment in ROS17/2.8 osteosarcoma cells. Ceramide is known to directly bind to the calcium/lipid-binding domain (CaLB) of cPLA₂, stimulating its translocation to the plasma membrane and subsequent activation (220). Moreover, ceramide-1-phosphate has also been shown to bind to the C2 domain of group IV cPLA₂ stimulating its activation (221). Thus, another possible mechanism by which β -CD abolishes $1\alpha,25(\text{OH})_2\text{D}_3$ -dependent PKC and CaMKII activation can be explained via

depletion of sphingolipids from caveolae, which indicates a need for further investigation. Additionally, although our data are not sufficient to establish $1\alpha,25(\text{OH})_2\text{D}_3$ -activated ceramide-mediated PLA_2 activation in osteoblasts and chondrocytes, it is highly probable that sphingolipid signaling may contribute to activation of PLA_2 in response to $1\alpha,25(\text{OH})_2\text{D}_3$ treatment. Effects of ceramide on $1\alpha,25(\text{OH})_2\text{D}_3$ -dependent activation of PLA_2 should be considered in future studies.

Furthermore, recent studies investigating the cholesterol-independent effects of β -CD on membrane protein mobility have suggested a role for cyclodextrins (222). These studies indicate that both β -CD and α -cyclodextrin (which does not extract cholesterol) reduce mobility of membrane proteins independent of their cholesterol binding properties. It is quite possible that β -CD treatment reduces mobility of Pdia3 receptor complex; hence, reducing its ability to mediate the $1\alpha,25(\text{OH})_2\text{D}_3$ signal, although our data are not sufficient to confirm this mechanism. Future studies are required to explicitly test for the effect of β -CD on $1\alpha,25(\text{OH})_2\text{D}_3$ -activated Pdia3 receptor complex proteins mobility.

Previously, we reported that Pdia3, PLAA, VDR, Cav-1 and caveolae are critical for $1\alpha,25(\text{OH})_2\text{D}_3$ membrane-mediated signaling (10,12,87,125). Similar to $1\alpha,25(\text{OH})_2\text{D}_3$ membrane-mediated signaling, our results indicated that Pdia3, PLAA, and VDR are critical for Wnt5a calcium-dependent pathway. However, to our surprise, silenced Cav-1 osteoblasts activated PKC in response to Wnt5a treatment, suggesting that Cav-1 is not necessary for the Wnt5a calcium-dependent pathway. To further investigate the role of lipid rafts in the Wnt5a calcium-dependent pathway, we subjected the cells to β -CD. PKC activity increased in cells pretreated with β -CD but the increase was significantly lower than the β -CD-untreated group. Collectively, these studies suggest that caveolae are not required to mediate Wnt5a effects, however the cholesterol-depleting agent significantly reduced Wnt5a-dependent PKC activity

indicating that the lipid domains of the plasma membrane are important to mediate the Wnt5a signal. Additionally, recent studies have demonstrated that after 30 minutes treatment with 10 mM β -CD, the amount of cholesterol lost by cells was higher than the amount of sphingolipids lost in the same treatment (217). It is quite possible that Wnt5a induces its effects via a predominantly sphingolipid signaling-dependent pathway. β -CD treatment reduces the abundance of sphingolipids in lipid rafts, but since its reduction is not as great as cholesterol depletion, Wnt5a is still able to activate its pathway. Role of sphingolipid signaling in Wnt5a pathway should be considered in future studies.

REFERENCES

1. Panda, D. K., Miao, D., Tremblay, M. L., Sirois, J., Farookhi, R., Hendy, G. N., and Goltzman, D. (2001) Targeted ablation of the 25-hydroxyvitamin D 1alpha -hydroxylase enzyme: evidence for skeletal, reproductive, and immune dysfunction. *Proc Natl Acad Sci U S A* **98**, 7498-7503
2. Li, Y. C., Pirro, A. E., Amling, M., Dellling, G., Baron, R., Bronson, R., and Demay, M. B. (1997) Targeted ablation of the vitamin D receptor: an animal model of vitamin D-dependent rickets type II with alopecia. *Proc Natl Acad Sci U S A* **94**, 9831-9835
3. van Leeuwen, J. P., van Driel, M., van den Bemd, G. J., and Pols, H. A. (2001) Vitamin D control of osteoblast function and bone extracellular matrix mineralization. *Crit Rev Eukaryot Gene Expr* **11**, 199-226
4. van Driel, M., Pols, H. A., and van Leeuwen, J. P. (2004) Osteoblast differentiation and control by vitamin D and vitamin D metabolites. *Curr Pharm Des* **10**, 2535-2555
5. Hendy, G. N., Hruska, K. A., Mathew, S., and Goltzman, D. (2006) New insights into mineral and skeletal regulation by active forms of vitamin D. *Kidney Int* **69**, 218-223
6. Nemere, I., and Norman, A. W. (1987) The rapid, hormonally stimulated transport of calcium (transcaltachia). *J Bone Miner Res* **2**, 167-169

7. Boyan, B. D., Schwartz, Z., Swain, L. D., Bonewald, L. F., and Khare, A. (1989) Regulation of matrix vesicle metabolism by vitamin D metabolites. *Connect Tissue Res* **22**, 3-16; discussion 53-61
8. Khanal, R. C., and Nemere, I. (2007) The ERp57/GRp58/1,25D3-MARRS receptor: multiple functional roles in diverse cell systems. *Curr Med Chem* **14**, 1087-1093
9. Schwartz, Z., Ehland, H., Sylvia, V. L., Larsson, D., Hardin, R. R., Bingham, V., Lopez, D., Dean, D. D., and Boyan, B. D. (2002) 1 α ,25-dihydroxyvitamin D(3) and 24R,25-dihydroxyvitamin D(3) modulate growth plate chondrocyte physiology via protein kinase C-dependent phosphorylation of extracellular signal-regulated kinase 1/2 mitogen-activated protein kinase. *Endocrinology* **143**, 2775-2786
10. Chen, J., Olivares-Navarrete, R., Wang, Y., Herman, T. R., Boyan, B. D., and Schwartz, Z. (2010) Protein-disulfide isomerase-associated 3 (Pdia3) mediates the membrane response to 1,25-dihydroxyvitamin D3 in osteoblasts. *J Biol Chem* **285**, 37041-37050
11. Schwartz, Z., Graham, E. J., Wang, L., Lossdorfer, S., Gay, I., Johnson-Pais, T. L., Carnes, D. L., Sylvia, V. L., and Boyan, B. D. (2005) Phospholipase A2 activating protein (PLAA) is required for 1 α ,25(OH)₂D₃ signaling in growth plate chondrocytes. *J Cell Physiol* **203**, 54-70

12. Boyan, B. D., Wong, K. L., Wang, L., Yao, H., Guldborg, R. E., Drab, M., Jo, H., and Schwartz, Z. (2006) Regulation of growth plate chondrocytes by 1,25-dihydroxyvitamin D3 requires caveolae and caveolin-1. *J Bone Miner Res* **21**, 1637-1647
13. Buitrago, C., and Boland, R. (2010) Caveolae and caveolin-1 are implicated in 1alpha,25(OH)2-vitamin D3-dependent modulation of Src, MAPK cascades and VDR localization in skeletal muscle cells. *J Steroid Biochem Mol Biol* **121**, 169-175
14. Boyan, B. D., Wang, L., Wong, K. L., Jo, H., and Schwartz, Z. (2006) Plasma membrane requirements for 1alpha,25(OH)2D3 dependent PKC signaling in chondrocytes and osteoblasts. *Steroids* **71**, 286-290
15. Boyan, B. D., Sylvia, V. L., Dean, D. D., Pedrozo, H., Del Toro, F., Nemere, I., Posner, G. H., and Schwartz, Z. (1999) 1,25-(OH)2D3 modulates growth plate chondrocytes via membrane receptor-mediated protein kinase C by a mechanism that involves changes in phospholipid metabolism and the action of arachidonic acid and PGE2. *Steroids* **64**, 129-136
16. Chen, J., Olivares-Navarrete, R., Wang, Y., Herman, T. R., Boyan, B. D., and Schwartz, Z. (2010) Protein disulfide isomerase associated 3 (Pdia3) mediates the membrane response to 1,25-dihydroxy vitamin D3 in osteoblasts. *J Biol Chem*

17. Bergh, J. J., Xu, Y., and Farach-Carson, M. C. (2004) Osteoprotegerin expression and secretion are regulated by calcium influx through the L-type voltage-sensitive calcium channel. *Endocrinology* **145**, 426-436
18. Muthalif, M. M., Benter, I. F., Uddin, M. R., and Malik, K. U. (1996) Calcium/calmodulin-dependent protein kinase IIalpha mediates activation of mitogen-activated protein kinase and cytosolic phospholipase A2 in norepinephrine-induced arachidonic acid release in rabbit aortic smooth muscle cells. *J Biol Chem* **271**, 30149-30157
19. Nemoto, E., Ebe, Y., Kanaya, S., Tsuchiya, M., Nakamura, T., Tamura, M., and Shimauchi, H. (2012) Wnt5a signaling is a substantial constituent in bone morphogenetic protein-2-mediated osteoblastogenesis. *Biochem Biophys Res Commun* **422**, 627-632
20. Olivares-Navarrete, R., Hyzy, S. L., Hutton, D. L., Dunn, G. R., Appert, C., Boyan, B. D., and Schwartz, Z. (2011) Role of non-canonical Wnt signaling in osteoblast maturation on microstructured titanium surfaces. *Acta Biomater* **7**, 2740-2750
21. Guo, J., Jin, J., and Cooper, L. F. (2008) Dissection of sets of genes that control the character of wnt5a-deficient mouse calvarial cells. *Bone* **43**, 961-971
22. Wan, M., Li, J., Herbst, K., Zhang, J., Yu, B., Wu, X., Qiu, T., Lei, W., Lindvall, C., Williams, B. O., Ma, H., Zhang, F., and Cao, X. (2011) LRP6 mediates cAMP generation

by G protein-coupled receptors through regulating the membrane targeting of Galpha(s).
Sci Signal **4**, ra15

23. Ma, L., and Wang, H. Y. (2006) Suppression of cyclic GMP-dependent protein kinase is essential to the Wnt/cGMP/Ca²⁺ pathway. *J Biol Chem* **281**, 30990-31001
24. Kuhl, M., Sheldahl, L. C., Malbon, C. C., and Moon, R. T. (2000) Ca²⁺/calmodulin-dependent protein kinase II is stimulated by Wnt and Frizzled homologs and promotes ventral cell fates in *Xenopus*. *J Biol Chem* **275**, 12701-12711
25. Kuhl, M., Sheldahl, L. C., Park, M., Miller, J. R., and Moon, R. T. (2000) The Wnt/Ca²⁺ pathway: a new vertebrate Wnt signaling pathway takes shape. *Trends Genet* **16**, 279-283
26. Kohn, A. D., and Moon, R. T. (2005) Wnt and calcium signaling: beta-catenin-independent pathways. *Cell Calcium* **38**, 439-446
27. DeLuca, H. F. (1982) Metabolism and molecular mechanism of action of vitamin D: 1981. *Biochemical Society transactions* **10**, 147-158
28. Holick, M. F. (2008) The vitamin D deficiency pandemic and consequences for nonskeletal health: mechanisms of action. *Mol Aspects Med* **29**, 361-368
29. Haussler, M. R., Whitfield, G. K., Haussler, C. A., Hsieh, J. C., Thompson, P. D., Selznick, S. H., Dominguez, C. E., and Jurutka, P. W. (1998) The nuclear vitamin D

- receptor: biological and molecular regulatory properties revealed. *J Bone Miner Res* **13**, 325-349
30. Barbour, G. L., Coburn, J. W., Slatopolsky, E., Norman, A. W., and Horst, R. L. (1981) Hypercalcemia in an anephric patient with sarcoidosis: evidence for extrarenal generation of 1,25-dihydroxyvitamin D. *The New England journal of medicine* **305**, 440-443
31. Koeffler, H. P., Reichel, H., Bishop, J. E., and Norman, A. W. (1985) gamma-Interferon stimulates production of 1,25-dihydroxyvitamin D₃ by normal human macrophages. *Biochem Biophys Res Commun* **127**, 596-603
32. Lambert, P. W., Stern, P. H., Avioli, R. C., Brackett, N. C., Turner, R. T., Greene, A., Fu, I. Y., and Bell, N. H. (1982) Evidence for extrarenal production of 1 alpha ,25-dihydroxyvitamin D in man. *J Clin Invest* **69**, 722-725
33. Zehnder, D., Bland, R., Williams, M. C., McNinch, R. W., Howie, A. J., Stewart, P. M., and Hewison, M. (2001) Extrarenal expression of 25-hydroxyvitamin d(3)-1 alpha-hydroxylase. *J Clin Endocrinol Metab* **86**, 888-894
34. DeLuca, H. F. (1986) The metabolism and functions of vitamin D. *Advances in experimental medicine and biology* **196**, 361-375

35. Buentig, N., Stoerkel, S., Richter, E., Dallmann, I., Reitz, M., and Atzpodien, J. (2004) Predictive impact of retinoid X receptor-alpha-expression in renal-cell carcinoma. *Cancer biotherapy & radiopharmaceuticals* **19**, 331-342
36. Urbschat, A., Paulus, P., von Quernheim, Q. F., Bruck, P., Badenhoop, K., Zeuzem, S., and Ramos-Lopez, E. (2013) Vitamin D hydroxylases CYP2R1, CYP27B1 and CYP24A1 in renal cell carcinoma. *European journal of clinical investigation* **43**, 1282-1290
37. DeLuca, H. F. (1988) The vitamin D story: a collaborative effort of basic science and clinical medicine. *FASEB journal : official publication of the Federation of American Societies for Experimental Biology* **2**, 224-236
38. Norman, A. W., Henry, H. L., and Malluche, H. H. (1980) 24R,25-Dihydroxyvitamin D₃ and 1 alpha,25-dihydroxyvitamin D₃ are both indispensable for calcium and phosphorus homeostasis. *Life sciences* **27**, 229-237
39. Donnelly, E., Boskey, A.L. (2011) Mineralization. in *Vitamin D* (Feldman, D., Pike, J.W., Adams, J.S. ed.), 3 Ed., Elsevier pp 381-401
40. Manolagas, S. C., Provvedini, D. M., and Tsoukas, C. D. (1985) Interactions of 1,25-dihydroxyvitamin D₃ and the immune system. *Mol Cell Endocrinol* **43**, 113-122

41. Provvedini, D. M., Tsoukas, C. D., Deftos, L. J., and Manolagas, S. C. (1983) 1,25-dihydroxyvitamin D3 receptors in human leukocytes. *Science* **221**, 1181-1183
42. Nelson, C. D., Reinhardt, T. A., Beitz, D. C., and Lippolis, J. D. (2010) In vivo activation of the intracrine vitamin D pathway in innate immune cells and mammary tissue during a bacterial infection. *PLoS One* **5**, e15469
43. Amento, E. P., Bhalla, A. K., Kurnick, J. T., Kradin, R. L., Clemens, T. L., Holick, S. A., Holick, M. F., and Krane, S. M. (1984) 1 alpha,25-dihydroxyvitamin D3 induces maturation of the human monocyte cell line U937, and, in association with a factor from human T lymphocytes, augments production of the monokine, mononuclear cell factor. *J Clin Invest* **73**, 731-739
44. Min, B. (2013) Effects of Vitamin D on Blood Pressure and Endothelial Function. *The Korean journal of physiology & pharmacology : official journal of the Korean Physiological Society and the Korean Society of Pharmacology* **17**, 385-392
45. Tukaj, S., Trzonkowski, P., and Tukaj, C. (2012) Regulatory effects of 1,25-dihydroxyvitamin D3 on vascular smooth muscle cells. *Acta biochimica Polonica* **59**, 395-400
46. Temmerman, J. C. (2011) Vitamin D and cardiovascular disease. *J Am Coll Nutr* **30**, 167-170

47. Summerday, N. M., Brown, S. J., Allington, D. R., and Rivey, M. P. (2011) Vitamin D and Multiple Sclerosis: Review of a Possible Association. *J Pharm Pract*
48. Ma, Y., Zhang, P., Wang, F., Yang, J., Liu, Z., and Qin, H. (2011) Association between vitamin d and risk of colorectal cancer: a systematic review of prospective studies. *J Clin Oncol* **29**, 3775-3782
49. Gonzalez-Parra, E., Rojas-Rivera, J., Tunon, J., Praga, M., Ortiz, A., and Egido, J. (2012) Vitamin D receptor activation and cardiovascular disease. *Nephrology, dialysis, transplantation : official publication of the European Dialysis and Transplant Association - European Renal Association* **27 Suppl 4**, iv17-21
50. DeLuca, H. F., and Schnoes, H. K. (1983) Vitamin D: recent advances. *Annual review of biochemistry* **52**, 411-439
51. Deeb, K. K., Trump, D. L., and Johnson, C. S. (2007) Vitamin D signalling pathways in cancer: potential for anticancer therapeutics. *Nature reviews. Cancer* **7**, 684-700
52. Gallagher, J. C., Jernbak, C. M., Jee, W. S., Johnson, K. A., DeLuca, H. F., and Riggs, B. L. (1982) 1,25-Dihydroxyvitamin D₃: short- and long-term effects on bone and calcium metabolism in patients with postmenopausal osteoporosis. *Proc Natl Acad Sci U S A* **79**, 3325-3329

53. Reid, I. R., Bolland, M. J., and Grey, A. (2014) Effects of vitamin D supplements on bone mineral density: a systematic review and meta-analysis. *Lancet* **383**, 146-155
54. Franceschi, R. T., Li, Y. (2011) Vitamin D Regulation of Osteoblast Function in *Vitamin D* (Feldman, D., Pike, J.W., Adams, J.S. ed.), 3 Ed., Elsevier pp 321-333
55. Hsu, H., Lacey, D. L., Dunstan, C. R., Solovyev, I., Colombero, A., Timms, E., Tan, H. L., Elliott, G., Kelley, M. J., Sarosi, I., Wang, L., Xia, X. Z., Elliott, R., Chiu, L., Black, T., Scully, S., Capparelli, C., Morony, S., Shimamoto, G., Bass, M. B., and Boyle, W. J. (1999) Tumor necrosis factor receptor family member RANK mediates osteoclast differentiation and activation induced by osteoprotegerin ligand. *Proc Natl Acad Sci U S A* **96**, 3540-3545
56. Kong, Y. Y., Yoshida, H., Sarosi, I., Tan, H. L., Timms, E., Capparelli, C., Morony, S., Oliveira-dos-Santos, A. J., Van, G., Itie, A., Khoo, W., Wakeham, A., Dunstan, C. R., Lacey, D. L., Mak, T. W., Boyle, W. J., and Penninger, J. M. (1999) OPGL is a key regulator of osteoclastogenesis, lymphocyte development and lymph-node organogenesis. *Nature* **397**, 315-323
57. Kitazawa, S., Kajimoto, K., Kondo, T., and Kitazawa, R. (2003) Vitamin D3 supports osteoclastogenesis via functional vitamin D response element of human RANKL gene promoter. *J Cell Biochem* **89**, 771-777

58. Kitazawa, R., and Kitazawa, S. (2002) Vitamin D(3) augments osteoclastogenesis via vitamin D-responsive element of mouse RANKL gene promoter. *Biochem Biophys Res Commun* **290**, 650-655
59. Kim, S., Yamazaki, M., Zella, L. A., Meyer, M. B., Fretz, J. A., Shevde, N. K., and Pike, J. W. (2007) Multiple enhancer regions located at significant distances upstream of the transcriptional start site mediate RANKL gene expression in response to 1,25-dihydroxyvitamin D3. *J Steroid Biochem Mol Biol* **103**, 430-434
60. Hofbauer, L. C., Dunstan, C. R., Spelsberg, T. C., Riggs, B. L., and Khosla, S. (1998) Osteoprotegerin production by human osteoblast lineage cells is stimulated by vitamin D, bone morphogenetic protein-2, and cytokines. *Biochem Biophys Res Commun* **250**, 776-781
61. Kondo, T., Kitazawa, R., Maeda, S., and Kitazawa, S. (2004) 1 alpha,25 dihydroxyvitamin D3 rapidly regulates the mouse osteoprotegerin gene through dual pathways. *J Bone Miner Res* **19**, 1411-1419
62. Baldock, P. A., Thomas, G. P., Hodge, J. M., Baker, S. U., Dressel, U., O'Loughlin, P. D., Nicholson, G. C., Briffa, K. H., Eisman, J. A., and Gardiner, E. M. (2006) Vitamin D action and regulation of bone remodeling: suppression of osteoclastogenesis by the mature osteoblast. *J Bone Miner Res* **21**, 1618-1626

63. Owen, T. A., Aronow, M. S., Barone, L. M., Bettencourt, B., Stein, G. S., and Lian, J. B. (1991) Pleiotropic effects of vitamin D on osteoblast gene expression are related to the proliferative and differentiated state of the bone cell phenotype: dependency upon basal levels of gene expression, duration of exposure, and bone matrix competency in normal rat osteoblast cultures. *Endocrinology* **128**, 1496-1504
64. Thomas, G. P., Baker, S. U., Eisman, J. A., and Gardiner, E. M. (2001) Changing RANKL/OPG mRNA expression in differentiating murine primary osteoblasts. *The Journal of endocrinology* **170**, 451-460
65. Howell DS, D. D. (1992) Biology, Chemistry and Biochemistry of the Mammalian Growth Plate. in *Disorders of Bone and Mineral Metabolism* (Coe FL, F. M. ed.), Raven, New York. pp 313-353
66. Gurlek, A., and Kumar, R. (2001) Regulation of osteoblast growth by interactions between transforming growth factor-beta and 1alpha,25-dihydroxyvitamin D3. *Crit Rev Eukaryot Gene Expr* **11**, 299-317
67. Pedrozo, H. A., Schwartz, Z., Mokeyev, T., Ornoy, A., Xin-Sheng, W., Bonewald, L. F., Dean, D. D., and Boyan, B. D. (1999) Vitamin D3 metabolites regulate LTBP1 and latent TGF-beta1 expression and latent TGF-beta1 incorporation in the extracellular matrix of chondrocytes. *J Cell Biochem* **72**, 151-165

68. Alvarez, J., Sohn, P., Zeng, X., Doetschman, T., Robbins, D. J., and Serra, R. (2002) TGFbeta2 mediates the effects of hedgehog on hypertrophic differentiation and PTHrP expression. *Development* **129**, 1913-1924
69. Vanhooke, J. L., Prah, J. M., Kimmel-Jehan, C., Mendelsohn, M., Danielson, E. W., Healy, K. D., and DeLuca, H. F. (2006) CYP27B1 null mice with LacZreporter gene display no 25-hydroxyvitamin D3-1alpha-hydroxylase promoter activity in the skin. *Proc Natl Acad Sci U S A* **103**, 75-80
70. Christakos, S., and DeLuca, H. F. (2011) Minireview: Vitamin D: is there a role in extraskeletal health? *Endocrinology* **152**, 2930-2936
71. DeLucia, M. C., Mitnick, M. E., and Carpenter, T. O. (2003) Nutritional rickets with normal circulating 25-hydroxyvitamin D: a call for reexamining the role of dietary calcium intake in North American infants. *J Clin Endocrinol Metab* **88**, 3539-3545
72. Muller, S. A., Posner, A. S., and Firschein, H. E. (1966) Effect of vitamin D deficiency on the crystal chemistry of bone mineral. *Proc Soc Exp Biol Med* **121**, 844-846
73. Chen, C. H., Sakai, Y., and Demay, M. B. (2001) Targeting expression of the human vitamin D receptor to the keratinocytes of vitamin D receptor null mice prevents alopecia. *Endocrinology* **142**, 5386-5389

74. Kato, S. (1999) Genetic mutation in the human 25-hydroxyvitamin D3 1alpha-hydroxylase gene causes vitamin D-dependent rickets type I. *Mol Cell Endocrinol* **156**, 7-12
75. Dean, D. D., Muniz, O. E., Berman, I., Pita, J. C., Carreno, M. R., Woessner, J. F., Jr., and Howell, D. S. (1985) Localization of collagenase in the growth plate of rachitic rats. *J Clin Invest* **76**, 716-722
76. Reinholt, F. P., Engfeldt, B., Heinegard, D., and Hjerpe, A. (1985) Proteoglycans and glycosaminoglycans of epiphyseal cartilage in florid and healing low phosphate, vitamin D deficiency rickets. *Coll Relat Res* **5**, 55-64
77. Idelevich, A., Kerschnitzki, M., Shahar, R., and Monsonego-Ornan, E. (2011) 1,25(OH)2D3 alters growth plate maturation and bone architecture in young rats with normal renal function. *PLoS One* **6**, e20772
78. Gerstenfeld, L. C., Kelly, C. M., Von Deck, M., and Lian, J. B. (1990) Comparative morphological and biochemical analysis of hypertrophic, non-hypertrophic and 1,25(OH)2D3 treated non-hypertrophic chondrocytes. *Connect Tissue Res* **24**, 29-39
79. Boyan, B. D., and Schwartz, Z. (2009) 1,25-Dihydroxy vitamin D3 is an autocrine regulator of extracellular matrix turnover and growth factor release via ERp60-activated matrix vesicle matrix metalloproteinases. *Cells Tissues Organs* **189**, 70-74

80. Maeda, S., Dean, D. D., Sylvia, V. L., Boyan, B. D., and Schwartz, Z. (2001) Metalloproteinase activity in growth plate chondrocyte cultures is regulated by 1,25-(OH)₂D₃ and 24,25-(OH)₂D₃ and mediated through protein kinase C. *Matrix Biol* **20**, 87-97
81. Dean, D. D., Boyan, B. D., Schwartz, Z., Muniz, O. E., Carreno, M. R., Maeda, S., and Howell, D. S. (2001) Effect of 1α,25-dihydroxyvitamin D₃ and 24R,25-dihydroxyvitamin D₃ on metalloproteinase activity and cell maturation in growth plate cartilage in vivo. *Endocrine* **14**, 311-323
82. Boyan, B. D., Hurst-Kennedy, J., Denison, T. A., and Schwartz, Z. (2010) 24R,25-dihydroxyvitamin D₃ [24R,25(OH)₂D₃] controls growth plate development by inhibiting apoptosis in the reserve zone and stimulating response to 1α,25(OH)₂D₃ in hypertrophic cells. *J Steroid Biochem Mol Biol* **121**, 212-216
83. Lemon, B. D., and Freedman, L. P. (1996) Selective effects of ligands on vitamin D₃ receptor- and retinoid X receptor-mediated gene activation in vivo. *Molecular and cellular biology* **16**, 1006-1016
84. Nemere, I., Schwartz, Z., Pedrozo, H., Sylvia, V. L., Dean, D. D., and Boyan, B. D. (1998) Identification of a membrane receptor for 1,25-dihydroxyvitamin D₃ which mediates rapid activation of protein kinase C. *J Bone Miner Res* **13**, 1353-1359

85. Nemere, I., Dormanen, M. C., Hammond, M. W., Okamura, W. H., and Norman, A. W. (1994) Identification of a specific binding protein for 1 alpha,25-dihydroxyvitamin D3 in basal-lateral membranes of chick intestinal epithelium and relationship to transcaltachia. *J Biol Chem* **269**, 23750-23756
86. Wang, D., Christensen, K., Chawla, K., Xiao, G., Krebsbach, P. H., and Franceschi, R. T. (1999) Isolation and characterization of MC3T3-E1 preosteoblast subclones with distinct in vitro and in vivo differentiation/mineralization potential. *J Bone Miner Res* **14**, 893-903
87. Chen, J., Doroudi, M., Cheung, J., Grozier, A. L., Schwartz, Z., and Boyan, B. D. (2013) Plasma membrane Pdia3 and VDR interact to elicit rapid responses to 1alpha,25(OH)D. *Cell Signal*
88. Sylvia, V. L., Del Toro, F., Jr., Hardin, R. R., Dean, D. D., Boyan, B. D., and Schwartz, Z. (2001) Characterization of PGE(2) receptors (EP) and their role as mediators of 1alpha,25-(OH)(2)D(3) effects on growth zone chondrocytes. *J Steroid Biochem Mol Biol* **78**, 261-274
89. Schwartz, Z., Shaked, D., Hardin, R. R., Gruwell, S., Dean, D. D., Sylvia, V. L., and Boyan, B. D. (2003) 1alpha,25(OH)2D3 causes a rapid increase in phosphatidylinositol-specific PLC-beta activity via phospholipase A2-dependent production of lysophospholipid. *Steroids* **68**, 423-437

90. Boyan, B. D., Sylvia, V. L., Curry, D., Chang, Z., Dean, D. D., and Schwartz, Z. (1998) Arachidonic acid is an autocoid mediator of the differential action of 1,25-(OH)₂D₃ and 24,25-(OH)₂D₃ on growth plate chondrocytes. *J Cell Physiol* **176**, 516-524
91. Sylvia, V. L., Del Toro, F., Dean, D. D., Hardin, R. R., Schwartz, Z., and Boyan, B. D. (2001) Effects of 1 α ,25-(OH)₂D₃ on rat growth zone chondrocytes are mediated via cyclooxygenase-1 and phospholipase A₂. *J Cell Biochem Suppl* **Suppl 36**, 32-45
92. Sylvia, V. L., Schwartz, Z., Curry, D. B., Chang, Z., Dean, D. D., and Boyan, B. D. (1998) 1,25(OH)₂D₃ regulates protein kinase C activity through two phospholipid-dependent pathways involving phospholipase A₂ and phospholipase C in growth zone chondrocytes. *J Bone Miner Res* **13**, 559-569
93. Kishimoto, A., Takai, Y., Mori, T., Kikkawa, U., and Nishizuka, Y. (1980) Activation of calcium and phospholipid-dependent protein kinase by diacylglycerol, its possible relation to phosphatidylinositol turnover. *J Biol Chem* **255**, 2273-2276
94. Farooqui, A. A., and Horrocks, L. A. (2004) Brain phospholipases A₂: a perspective on the history. *Prostaglandins Leukot Essent Fatty Acids* **71**, 161-169
95. Farooqui, A. A., and Horrocks, L. A. (2006) Phospholipase A₂-generated lipid mediators in the brain: the good, the bad, and the ugly. *Neuroscientist* **12**, 245-260

96. Schaloske, R. H., and Dennis, E. A. (2006) The phospholipase A2 superfamily and its group numbering system. *Biochim Biophys Acta* **1761**, 1246-1259
97. Schwartz, Z., Gilley, R. M., Sylvia, V. L., Dean, D. D., and Boyan, B. D. (1999) Prostaglandins mediate the effects of 1,25-(OH)₂D₃ and 24,25-(OH)₂D₃ on growth plate chondrocytes in a metabolite-specific and cell maturation-dependent manner. *Bone* **24**, 475-484
98. Aepfelbacher, F. C., Weber, P. C., and Aepfelbacher, M. (1995) Activation of phospholipase A2 by 1,25 (OH)₂ vitamin D3 and cell growth in monocytic U937 and Mono Mac 6 cells. *Cell Biochem Funct* **13**, 19-23
99. De Boland, A. R., Morelli, S., and Boland, R. (1995) 1,25(OH)₂-vitamin D-3 stimulates phospholipase A2 activity via a guanine nucleotide-binding protein in chick myoblasts. *Biochim Biophys Acta* **1257**, 274-278
100. Keeting, P. E., Li, C. H., Whipkey, D. L., Thweatt, R., Xu, J., Murty, M., Blaha, J. D., and Graeber, G. M. (1998) 1,25-Dihydroxyvitamin D3 pretreatment limits prostaglandin biosynthesis by cytokine-stimulated adult human osteoblast-like cells. *J Cell Biochem* **68**, 237-246
101. Thomas, W., Coen, N., Faherty, S., Flatharta, C. O., and Harvey, B. J. (2006) Estrogen induces phospholipase A2 activation through ERK1/2 to mobilize intracellular calcium in MCF-7 cells. *Steroids* **71**, 256-265

102. Ribardo, D. A., Kuhl, K. R., Peterson, J. W., and Chopra, A. K. (2002) Role of melittin-like region within phospholipase A(2)-activating protein in biological function. *Toxicon* **40**, 519-526
103. Peitsch, M. C., Borner, C., and Tschopp, J. (1993) Sequence similarity of phospholipase A2 activating protein and the G protein beta-subunits: a new concept of effector protein activation in signal transduction? *Trends Biochem Sci* **18**, 292-293
104. Brown, R. E. (1998) Sphingolipid organization in biomembranes: what physical studies of model membranes reveal. *J Cell Sci* **111 (Pt 1)**, 1-9
105. Rietveld, A., and Simons, K. (1998) The differential miscibility of lipids as the basis for the formation of functional membrane rafts. *Biochim Biophys Acta* **1376**, 467-479
106. Silvius, J. R. (2003) Role of cholesterol in lipid raft formation: lessons from lipid model systems. *Biochim Biophys Acta* **1610**, 174-183
107. Simons, K., and Ikonen, E. (1997) Functional rafts in cell membranes. *Nature* **387**, 569-572
108. Rothberg, K. G., Heuser, J. E., Donzell, W. C., Ying, Y. S., Glenney, J. R., and Anderson, R. G. (1992) Caveolin, a protein component of caveolae membrane coats. *Cell* **68**, 673-682

109. Glenney, J. R., Jr., and Zokas, L. (1989) Novel tyrosine kinase substrates from Rous sarcoma virus-transformed cells are present in the membrane skeleton. *J Cell Biol* **108**, 2401-2408
110. Scherer, P. E., Okamoto, T., Chun, M., Nishimoto, I., Lodish, H. F., and Lisanti, M. P. (1996) Identification, sequence, and expression of caveolin-2 defines a caveolin gene family. *Proc Natl Acad Sci U S A* **93**, 131-135
111. Smart, E. J., Graf, G. A., McNiven, M. A., Sessa, W. C., Engelman, J. A., Scherer, P. E., Okamoto, T., and Lisanti, M. P. (1999) Caveolins, liquid-ordered domains, and signal transduction. *Molecular and cellular biology* **19**, 7289-7304
112. Tang, Z., Scherer, P. E., Okamoto, T., Song, K., Chu, C., Kohtz, D. S., Nishimoto, I., Lodish, H. F., and Lisanti, M. P. (1996) Molecular cloning of caveolin-3, a novel member of the caveolin gene family expressed predominantly in muscle. *J Biol Chem* **271**, 2255-2261
113. Way, M., and Parton, R. G. (1995) M-caveolin, a muscle-specific caveolin-related protein. *FEBS Lett* **376**, 108-112
114. Brown, D. A., and Rose, J. K. (1992) Sorting of GPI-anchored proteins to glycolipid-enriched membrane subdomains during transport to the apical cell surface. *Cell* **68**, 533-544

115. Foster, L. J., De Hoog, C. L., and Mann, M. (2003) Unbiased quantitative proteomics of lipid rafts reveals high specificity for signaling factors. *Proc Natl Acad Sci U S A* **100**, 5813-5818
116. Schroeder, R., London, E., and Brown, D. (1994) Interactions between saturated acyl chains confer detergent resistance on lipids and glycosylphosphatidylinositol (GPI)-anchored proteins: GPI-anchored proteins in liposomes and cells show similar behavior. *Proc Natl Acad Sci U S A* **91**, 12130-12134
117. Schuck, S., Honsho, M., Ekroos, K., Shevchenko, A., and Simons, K. (2003) Resistance of cell membranes to different detergents. *Proc Natl Acad Sci U S A* **100**, 5795-5800
118. Ortegren, U., Karlsson, M., Blazic, N., Blomqvist, M., Nystrom, F. H., Gustavsson, J., Fredman, P., and Stralfors, P. (2004) Lipids and glycosphingolipids in caveolae and surrounding plasma membrane of primary rat adipocytes. *Eur J Biochem* **271**, 2028-2036
119. Pike, L. J., Han, X., Chung, K. N., and Gross, R. W. (2002) Lipid rafts are enriched in arachidonic acid and plasmenylethanolamine and their composition is independent of caveolin-1 expression: a quantitative electrospray ionization/mass spectrometric analysis. *Biochemistry* **41**, 2075-2088
120. Smart, E. J., Ying, Y. S., Mineo, C., and Anderson, R. G. (1995) A detergent-free method for purifying caveolae membrane from tissue culture cells. *Proc Natl Acad Sci U S A* **92**, 10104-10108

121. Huhtakangas, J. A., Olivera, C. J., Bishop, J. E., Zanello, L. P., and Norman, A. W. (2004) The vitamin D receptor is present in caveolae-enriched plasma membranes and binds 1 alpha,25(OH)₂-vitamin D₃ in vivo and in vitro. *Mol Endocrinol* **18**, 2660-2671
122. Chambliss, K. L., Yuhanna, I. S., Mineo, C., Liu, P., German, Z., Sherman, T. S., Mendelsohn, M. E., Anderson, R. G., and Shaul, P. W. (2000) Estrogen receptor alpha and endothelial nitric oxide synthase are organized into a functional signaling module in caveolae. *Circ Res* **87**, E44-52
123. Chambliss, K. L., Yuhanna, I. S., Anderson, R. G., Mendelsohn, M. E., and Shaul, P. W. (2002) ERbeta has nongenomic action in caveolae. *Mol Endocrinol* **16**, 938-946
124. Gilad, L. A., and Schwartz, B. (2007) Association of estrogen receptor beta with plasma-membrane caveola components: implication in control of vitamin D receptor. *J Mol Endocrinol* **38**, 603-618
125. Doroudi, M., Schwartz, Z., and Boyan, B. D. (2012) Phospholipase A(2) activating protein is required for 1alpha,25-dihydroxyvitamin D(3) dependent rapid activation of protein kinase C via Pdia3. *J Steroid Biochem Mol Biol* **132**, 48-56
126. Dupree, P., Parton, R. G., Raposo, G., Kurzchalia, T. V., and Simons, K. (1993) Caveolae and sorting in the trans-Golgi network of epithelial cells. *The EMBO journal* **12**, 1597-1605

127. Glenney, J. R., Jr. (1992) The sequence of human caveolin reveals identity with VIP21, a component of transport vesicles. *FEBS Lett* **314**, 45-48
128. Glenney, J. R., Jr., and Soppet, D. (1992) Sequence and expression of caveolin, a protein component of caveolae plasma membrane domains phosphorylated on tyrosine in Rous sarcoma virus-transformed fibroblasts. *Proc Natl Acad Sci U S A* **89**, 10517-10521
129. Kurzchalia, T. V., Dupree, P., and Monier, S. (1994) VIP21-Caveolin, a protein of the trans-Golgi network and caveolae. *FEBS Lett* **346**, 88-91
130. Kurzchalia, T. V., Dupree, P., Parton, R. G., Kellner, R., Virta, H., Lehnert, M., and Simons, K. (1992) VIP21, a 21-kD membrane protein is an integral component of trans-Golgi-network-derived transport vesicles. *J Cell Biol* **118**, 1003-1014
131. Mora, R., Bonilha, V. L., Marmorstein, A., Scherer, P. E., Brown, D., Lisanti, M. P., and Rodriguez-Boulan, E. (1999) Caveolin-2 localizes to the golgi complex but redistributes to plasma membrane, caveolae, and rafts when co-expressed with caveolin-1. *J Biol Chem* **274**, 25708-25717
132. Scherer, P. E., Lewis, R. Y., Volonte, D., Engelman, J. A., Galbiati, F., Couet, J., Kohtz, D. S., van Donselaar, E., Peters, P., and Lisanti, M. P. (1997) Cell-type and tissue-specific expression of caveolin-2. Caveolins 1 and 2 co-localize and form a stable hetero-oligomeric complex in vivo. *J Biol Chem* **272**, 29337-29346

133. Toni, M., Spisni, E., Griffoni, C., Santi, S., Riccio, M., Lenaz, P., and Tomasi, V. (2006) Cellular prion protein and caveolin-1 interaction in a neuronal cell line precedes Fyn/Erk 1/2 signal transduction. *Journal of biomedicine & biotechnology* **2006**, 69469
134. Joshi, B., Strugnelli, S. S., Goetz, J. G., Kojic, L. D., Cox, M. E., Griffith, O. L., Chan, S. K., Jones, S. J., Leung, S. P., Masoudi, H., Leung, S., Wiseman, S. M., and Nabi, I. R. (2008) Phosphorylated caveolin-1 regulates Rho/ROCK-dependent focal adhesion dynamics and tumor cell migration and invasion. *Cancer research* **68**, 8210-8220
135. Song, Y., Xue, L., Du, S., Sun, M., Hu, J., Hao, L., Gong, L., Yeh, D., Xiong, H., and Shao, S. (2012) Caveolin-1 knockdown is associated with the metastasis and proliferation of human lung cancer cell line NCI-H460. *Biomedicine & pharmacotherapy = Biomedecine & pharmacotherapie* **66**, 439-447
136. Zayzafoon, M. (2006) Calcium/calmodulin signaling controls osteoblast growth and differentiation. *J Cell Biochem* **97**, 56-70
137. Hook, S. S., and Means, A. R. (2001) Ca(2+)/CaM-dependent kinases: from activation to function. *Annu Rev Pharmacol Toxicol* **41**, 471-505
138. Braun, A. P., and Schulman, H. (1995) The multifunctional calcium/calmodulin-dependent protein kinase: from form to function. *Annu Rev Physiol* **57**, 417-445

139. Fink, C. C., and Meyer, T. (2002) Molecular mechanisms of CaMKII activation in neuronal plasticity. *Curr Opin Neurobiol* **12**, 293-299
140. Zayzafoon, M., Fulzele, K., and McDonald, J. M. (2005) Calmodulin and calmodulin-dependent kinase II α regulate osteoblast differentiation by controlling c-fos expression. *J Biol Chem* **280**, 7049-7059
141. Logan, C. Y., and Nusse, R. (2004) The Wnt signaling pathway in development and disease. *Annual review of cell and developmental biology* **20**, 781-810
142. Moon, R. T., Bowerman, B., Boutros, M., and Perrimon, N. (2002) The promise and perils of Wnt signaling through beta-catenin. *Science* **296**, 1644-1646
143. Willert, K., Brown, J. D., Danenberg, E., Duncan, A. W., Weissman, I. L., Reya, T., Yates, J. R., 3rd, and Nusse, R. (2003) Wnt proteins are lipid-modified and can act as stem cell growth factors. *Nature* **423**, 448-452
144. Nusse, R. (2003) Wnts and Hedgehogs: lipid-modified proteins and similarities in signaling mechanisms at the cell surface. *Development* **130**, 5297-5305
145. MacDonald, B. T., Tamai, K., and He, X. (2009) Wnt/beta-catenin signaling: components, mechanisms, and diseases. *Dev Cell* **17**, 9-26

146. Shimizu, K., Sato, M., and Tabata, T. (2011) The Wnt5/planar cell polarity pathway regulates axonal development of the *Drosophila* mushroom body neuron. *J Neurosci* **31**, 4944-4954
147. Bradley, E. W., and Drissi, M. H. (2011) Wnt5b regulates mesenchymal cell aggregation and chondrocyte differentiation through the planar cell polarity pathway. *J Cell Physiol* **226**, 1683-1693
148. Vivancos, V., Chen, P., Spassky, N., Qian, D., Dabdoub, A., Kelley, M., Studer, M., and Guthrie, S. (2009) Wnt activity guides facial branchiomotor neuron migration, and involves the PCP pathway and JNK and ROCK kinases. *Neural Dev* **4**, 7
149. Andrade, A. C., Nilsson, O., Barnes, K. M., and Baron, J. (2007) Wnt gene expression in the post-natal growth plate: regulation with chondrocyte differentiation. *Bone* **40**, 1361-1369
150. Kennerdell, J. R., Fetter, R. D., and Bargmann, C. I. (2009) Wnt-Ror signaling to SIA and SIB neurons directs anterior axon guidance and nerve ring placement in *C. elegans*. *Development* **136**, 3801-3810
151. Katoh, M., and Katoh, M. (2005) Comparative genomics on Wnt5a and Wnt5b genes. *International journal of molecular medicine* **15**, 749-753

152. Kurayoshi, M., Oue, N., Yamamoto, H., Kishida, M., Inoue, A., Asahara, T., Yasui, W., and Kikuchi, A. (2006) Expression of Wnt-5a is correlated with aggressiveness of gastric cancer by stimulating cell migration and invasion. *Cancer research* **66**, 10439-10448
153. Yang, Y., Topol, L., Lee, H., and Wu, J. (2003) Wnt5a and Wnt5b exhibit distinct activities in coordinating chondrocyte proliferation and differentiation. *Development* **130**, 1003-1015
154. Povelones, M., and Nusse, R. (2005) The role of the cysteine-rich domain of Frizzled in Wingless-Armadillo signaling. *The EMBO journal* **24**, 3493-3503
155. Wang, H., Lee, Y., and Malbon, C. C. (2004) PDE6 is an effector for the Wnt/Ca²⁺/cGMP-signalling pathway in development. *Biochemical Society transactions* **32**, 792-796
156. Blumenthal, A., Ehlers, S., Lauber, J., Buer, J., Lange, C., Goldmann, T., Heine, H., Brandt, E., and Reiling, N. (2006) The Wingless homolog WNT5A and its receptor Frizzled-5 regulate inflammatory responses of human mononuclear cells induced by microbial stimulation. *Blood* **108**, 965-973
157. Cheung, R., Kelly, J., and Macleod, R. J. (2011) Regulation of villin by wnt5a/ror2 signaling in human intestinal cells. *Frontiers in physiology* **2**, 58

158. Saldanha, J., Singh, J., and Mahadevan, D. (1998) Identification of a Frizzled-like cysteine rich domain in the extracellular region of developmental receptor tyrosine kinases. *Protein science : a publication of the Protein Society* **7**, 1632-1635
159. DeChiara, T. M., Kimble, R. B., Poueymirou, W. T., Rojas, J., Masiakowski, P., Valenzuela, D. M., and Yancopoulos, G. D. (2000) Ror2, encoding a receptor-like tyrosine kinase, is required for cartilage and growth plate development. *Nat Genet* **24**, 271-274
160. Schwabe, G. C., Trepczik, B., Suring, K., Brieske, N., Tucker, A. S., Sharpe, P. T., Minami, Y., and Mundlos, S. (2004) Ror2 knockout mouse as a model for the developmental pathology of autosomal recessive Robinow syndrome. *Developmental dynamics : an official publication of the American Association of Anatomists* **229**, 400-410
161. Kikuchi, A., and Yamamoto, H. (2008) Tumor formation due to abnormalities in the beta-catenin-independent pathway of Wnt signaling. *Cancer science* **99**, 202-208
162. Kuhl, M., Geis, K., Sheldahl, L. C., Pukrop, T., Moon, R. T., and Wedlich, D. (2001) Antagonistic regulation of convergent extension movements in *Xenopus* by Wnt/beta-catenin and Wnt/Ca²⁺ signaling. *Mechanisms of development* **106**, 61-76
163. Veeman, M. T., Axelrod, J. D., and Moon, R. T. (2003) A second canon. Functions and mechanisms of beta-catenin-independent Wnt signaling. *Dev Cell* **5**, 367-377

164. Westfall, T. A., Brimeyer, R., Twedt, J., Gladon, J., Olberding, A., Furutani-Seiki, M., and Slusarski, D. C. (2003) Wnt-5/pipetail functions in vertebrate axis formation as a negative regulator of Wnt/beta-catenin activity. *J Cell Biol* **162**, 889-898
165. Pedrozo, H. A., Schwartz, Z., Rimes, S., Sylvia, V. L., Nemere, I., Posner, G. H., Dean, D. D., and Boyan, B. D. (1999) Physiological importance of the 1,25(OH)₂D₃ membrane receptor and evidence for a membrane receptor specific for 24,25(OH)₂D₃. *J Bone Miner Res* **14**, 856-867
166. Boyan, B. D., Schwartz, Z., Swain, L. D., Carnes, D. L., Jr., and Zislis, T. (1988) Differential expression of phenotype by resting zone and growth region costochondral chondrocytes in vitro. *Bone* **9**, 185-194
167. Kang, S., Hawkrige, A. M., Johnson, K. L., Muddiman, D. C., and Prevelige, P. E., Jr. (2006) Identification of subunit-subunit interactions in bacteriophage P22 procapsids by chemical cross-linking and mass spectrometry. *J Proteome Res* **5**, 370-377
168. Clark, M. A., Ozgur, L. E., Conway, T. M., Dispoto, J., Crooke, S. T., and Bomalaski, J. S. (1991) Cloning of a phospholipase A₂-activating protein. *Proc Natl Acad Sci U S A* **88**, 5418-5422
169. Raghuraman, H., and Chattopadhyay, A. (2004) Interaction of melittin with membrane cholesterol: a fluorescence approach. *Biophys J* **87**, 2419-2432

170. Sheynis, T., Sykora, J., Benda, A., Kolusheva, S., Hof, M., and Jelinek, R. (2003) Bilayer localization of membrane-active peptides studied in biomimetic vesicles by visible and fluorescence spectroscopies. *Eur J Biochem* **270**, 4478-4487
171. Ghosh, A. K., Rukmini, R., and Chattopadhyay, A. (1997) Modulation of tryptophan environment in membrane-bound melittin by negatively charged phospholipids: implications in membrane organization and function. *Biochemistry* **36**, 14291-14305
172. Beschiaschvili, G., and Seelig, J. (1990) Melittin binding to mixed phosphatidylglycerol/phosphatidylcholine membranes. *Biochemistry* **29**, 52-58
173. Simionescu, N., Lupu, F., and Simionescu, M. (1983) Rings of membrane sterols surround the openings of vesicles and fenestrae, in capillary endothelium. *J Cell Biol* **97**, 1592-1600
174. Allende, D., Simon, S. A., and McIntosh, T. J. (2005) Melittin-induced bilayer leakage depends on lipid material properties: evidence for toroidal pores. *Biophys J* **88**, 1828-1837
175. Steiner, M. R., Bomalaski, J. S., and Clark, M. A. (1993) Responses of purified phospholipases A2 to phospholipase A2 activating protein (PLAP) and melittin. *Biochim Biophys Acta* **1166**, 124-130

176. Buitrago, C., Costabel, M., and Boland, R. (2011) PKC and PTPalpha participate in Src activation by 1alpha,25OH₂ vitamin D₃ in C2C12 skeletal muscle cells. *Mol Cell Endocrinol* **339**, 81-89
177. Buitrago, C. G., Ronda, A. C., de Boland, A. R., and Boland, R. (2006) MAP kinases p38 and JNK are activated by the steroid hormone 1alpha,25(OH)₂-vitamin D₃ in the C2C12 muscle cell line. *J Cell Biochem* **97**, 698-708
178. Chen, J., Doroudi, M., Cheung, J., Grozier, A. L., Schwartz, Z., and Boyan, B. D. (2013) Plasma membrane Pdia3 and VDR interact to elicit rapid responses to 1alpha,25(OH)₂D₃. *Cell Signal* **25**, 2362-2373
179. Sumi, M., Kiuchi, K., Ishikawa, T., Ishii, A., Hagiwara, M., Nagatsu, T., and Hidaka, H. (1991) The newly synthesized selective Ca²⁺/calmodulin dependent protein kinase II inhibitor KN-93 reduces dopamine contents in PC12h cells. *Biochem Biophys Res Commun* **181**, 968-975
180. Chang, B. H., Mukherji, S., and Soderling, T. R. (1998) Characterization of a calmodulin kinase II inhibitor protein in brain. *Proc Natl Acad Sci U S A* **95**, 10890-10895
181. Sawai, T., Bernier, F., Fukushima, T., Hashimoto, T., Ogura, H., and Nishizawa, Y. (2002) Estrogen induces a rapid increase of calcium-calmodulin-dependent protein kinase II activity in the hippocampus. *Brain Res* **950**, 308-311

182. Balasubramanian, B., Portillo, W., Reyna, A., Chen, J. Z., Moore, A. N., Dash, P. K., and Mani, S. K. (2008) Nonclassical mechanisms of progesterone action in the brain: II. Role of calmodulin-dependent protein kinase II in progesterone-mediated signaling in the hypothalamus of female rats. *Endocrinology* **149**, 5518-5526
183. Schwartz, Z., Swain, L. D., Ramirez, V., and Boyan, B. D. (1990) Regulation of arachidonic acid turnover by 1,25-(OH)₂D₃ and 24,25-(OH)₂D₃ in growth zone and resting zone chondrocyte cultures. *Biochim Biophys Acta* **1027**, 278-286
184. Langston, G. G., Swain, L. D., Schwartz, Z., Del Toro, F., Gomez, R., and Boyan, B. D. (1990) Effect of 1,25(OH)₂D₃ and 24,25(OH)₂D₃ on calcium ion fluxes in costochondral chondrocyte cultures. *Calcif Tissue Int* **47**, 230-236
185. Jin, X., Fu, G. X., Li, X. D., Zhu, D. L., and Gao, P. J. (2011) Expression and function of osteopontin in vascular adventitial fibroblasts and pathological vascular remodeling. *PLoS One* **6**, e23558
186. Thomas, C. M., and Smart, E. J. (2008) Caveolae structure and function. *Journal of cellular and molecular medicine* **12**, 796-809
187. Doroudi, M., Plaisance, M.C., Boyan, B.D., Schwartz, Z. (2014) Membrane Actions of 1 α ,25(OH)₂D₃ is Mediated by Ca²⁺/Calmodulin-dependent Protein Kinase II in Bone and Cartilage Cells. **Under Review**

188. Wang, Y., Chen, J., Lee, C. S., Nizkorodov, A., Riemenschneider, K., Martin, D., Hyzy, S., Schwartz, Z., and Boyan, B. D. (2010) Disruption of *Pdia3* gene results in bone abnormality and affects 1 α ,25-dihydroxy-vitamin D₃-induced rapid activation of PKC. *J Steroid Biochem Mol Biol* **121**, 257-260
189. Coe, H., Jung, J., Groenendyk, J., Prins, D., and Michalak, M. (2010) ERp57 modulates STAT3 signaling from the lumen of the endoplasmic reticulum. *J Biol Chem* **285**, 6725-6738
190. Nemere, I., Garbi, N., Hammerling, G. J., and Khanal, R. C. (2010) Intestinal cell calcium uptake and the targeted knockout of the 1,25D₃-MARRS (membrane-associated, rapid response steroid-binding) receptor/PDIA3/Erp57. *J Biol Chem* **285**, 31859-31866
191. Yates, K. E., Shortkroff, S., and Reish, R. G. (2005) Wnt influence on chondrocyte differentiation and cartilage function. *DNA and cell biology* **24**, 446-457
192. Wang, Y., Li, Y. P., Paulson, C., Shao, J. Z., Zhang, X., Wu, M., and Chen, W. (2014) Wnt and the Wnt signaling pathway in bone development and disease. *Frontiers in bioscience* **19**, 379-407
193. He, X., Saint-Jeannet, J. P., Wang, Y., Nathans, J., Dawid, I., and Varmus, H. (1997) A member of the Frizzled protein family mediating axis induction by Wnt-5A. *Science* **275**, 1652-1654

194. Bazhin, A. V., Tambor, V., Dikov, B., Philippov, P. P., Schadendorf, D., and Eichmuller, S. B. (2010) cGMP-phosphodiesterase 6, transducin and Wnt5a/Frizzled-2-signaling control cGMP and Ca(2+) homeostasis in melanoma cells. *Cellular and molecular life sciences : CMLS* **67**, 817-828
195. O'Connell, M. P., Fiori, J. L., Xu, M., Carter, A. D., Frank, B. P., Camilli, T. C., French, A. D., Dissanayake, S. K., Indig, F. E., Bernier, M., Taub, D. D., Hewitt, S. M., and Weeraratna, A. T. (2010) The orphan tyrosine kinase receptor, ROR2, mediates Wnt5A signaling in metastatic melanoma. *Oncogene* **29**, 34-44
196. Kikuchi, A., Yamamoto, H., Sato, A., and Matsumoto, S. (2012) Wnt5a: its signalling, functions and implication in diseases. *Acta physiologica* **204**, 17-33
197. Liu, Y., Rubin, B., Bodine, P. V., and Billiard, J. (2008) Wnt5a induces homodimerization and activation of Ror2 receptor tyrosine kinase. *J Cell Biochem* **105**, 497-502
198. Nebigil, C., and Malik, K. U. (1993) Alpha adrenergic receptor subtypes involved in prostaglandin synthesis are coupled to Ca⁺⁺ channels through a pertussis toxin-sensitive guanine nucleotide-binding protein. *J Pharmacol Exp Ther* **266**, 1113-1124
199. Murakami, M., Kuwata, H., Amakasu, Y., Shimbara, S., Nakatani, Y., Atsumi, G., and Kudo, I. (1997) Prostaglandin E2 amplifies cytosolic phospholipase A2- and

- cyclooxygenase-2-dependent delayed prostaglandin E2 generation in mouse osteoblastic cells. Enhancement by secretory phospholipase A2. *J Biol Chem* **272**, 19891-19897
200. Yamamoto, H., Komekado, H., and Kikuchi, A. (2006) Caveolin is necessary for Wnt-3a-dependent internalization of LRP6 and accumulation of beta-catenin. *Dev Cell* **11**, 213-223
201. Chuprun, J. K., Bazan, E., Chang, K. C., Campbell, A. K., and Rapoport, R. M. (1991) Inhibition of phorbol ester-induced contraction by calmodulin antagonists in rat aorta. *Am J Physiol* **261**, C675-684
202. ElBaradie, K., Wang, Y., Boyan, B. D., and Schwartz, Z. (2012) Rapid membrane responses to dihydrotestosterone are sex dependent in growth plate chondrocytes. *J Steroid Biochem Mol Biol* **132**, 15-23
203. Chen, J., Lobachev, K. S., Grindel, B. J., Farach-Carson, M. C., Hyzy, S. L., El-Baradie, K. B., Olivares-Navarrete, R., Doroudi, M., Boyan, B. D., and Schwartz, Z. (2013) Chaperone properties of pdia3 participate in rapid membrane actions of 1alpha,25-dihydroxyvitamin d3. *Mol Endocrinol* **27**, 1065-1077
204. Sammar, M., Sieber, C., and Knaus, P. (2009) Biochemical and functional characterization of the Ror2/BRIb receptor complex. *Biochem Biophys Res Commun* **381**, 1-6

205. Sammar, M., Stricker, S., Schwabe, G. C., Sieber, C., Hartung, A., Hanke, M., Oishi, I., Pohl, J., Minami, Y., Sebald, W., Mundlos, S., and Knaus, P. (2004) Modulation of GDF5/BRI-b signalling through interaction with the tyrosine kinase receptor Ror2. *Genes to cells : devoted to molecular & cellular mechanisms* **9**, 1227-1238
206. Oishi, I., Suzuki, H., Onishi, N., Takada, R., Kani, S., Ohkawara, B., Koshida, I., Suzuki, K., Yamada, G., Schwabe, G. C., Mundlos, S., Shibuya, H., Takada, S., and Minami, Y. (2003) The receptor tyrosine kinase Ror2 is involved in non-canonical Wnt5a/JNK signalling pathway. *Genes to cells : devoted to molecular & cellular mechanisms* **8**, 645-654
207. Afzal, A. R., Rajab, A., Fenske, C. D., Oldridge, M., Elanko, N., Ternes-Pereira, E., Tuysuz, B., Murday, V. A., Patton, M. A., Wilkie, A. O., and Jeffery, S. (2000) Recessive Robinow syndrome, allelic to dominant brachydactyly type B, is caused by mutation of ROR2. *Nat Genet* **25**, 419-422
208. van Bokhoven, H., Celli, J., Kayserili, H., van Beusekom, E., Balci, S., Brussel, W., Skovby, F., Kerr, B., Percin, E. F., Akarsu, N., and Brunner, H. G. (2000) Mutation of the gene encoding the ROR2 tyrosine kinase causes autosomal recessive Robinow syndrome. *Nat Genet* **25**, 423-426
209. Nishita, M., Yoo, S. K., Nomachi, A., Kani, S., Sougawa, N., Ohta, Y., Takada, S., Kikuchi, A., and Minami, Y. (2006) Filopodia formation mediated by receptor tyrosine kinase Ror2 is required for Wnt5a-induced cell migration. *J Cell Biol* **175**, 555-562

210. Cao, X., Teitelbaum, S. L., Zhu, H. J., Zhang, L., Feng, X., and Ross, F. P. (1996) Competition for a unique response element mediates retinoic acid inhibition of vitamin D3-stimulated transcription. *J Biol Chem* **271**, 20650-20654
211. Hakomori, S., Handa, K., Iwabuchi, K., Yamamura, S., and Prinetti, A. (1998) New insights in glycosphingolipid function: "glycosignaling domain," a cell surface assembly of glycosphingolipids with signal transducer molecules, involved in cell adhesion coupled with signaling. *Glycobiology* **8**, xi-xix
212. Brown, D. A., and London, E. (1998) Functions of lipid rafts in biological membranes. *Annual review of cell and developmental biology* **14**, 111-136
213. Pitha, J., Irie, T., Sklar, P. B., and Nye, J. S. (1988) Drug solubilizers to aid pharmacologists: amorphous cyclodextrin derivatives. *Life sciences* **43**, 493-502
214. Christian, A. E., Haynes, M. P., Phillips, M. C., and Rothblat, G. H. (1997) Use of cyclodextrins for manipulating cellular cholesterol content. *Journal of lipid research* **38**, 2264-2272
215. Singh, I., and Kishimoto, Y. (1983) Effect of cyclodextrins on the solubilization of lignoceric acid, ceramide, and cerebroside, and on the enzymatic reactions involving these compounds. *Journal of lipid research* **24**, 662-665

216. Shiraishi, T., Hiraiwa, M., and Uda, Y. (1993) Effects of cyclodextrins on the hydrolysis of ganglioside GM1 by acid beta-galactosidases. *Glycoconjugate journal* **10**, 170-174
217. Ottico, E., Prinetti, A., Prioni, S., Giannotta, C., Basso, L., Chigorno, V., and Sonnino, S. (2003) Dynamics of membrane lipid domains in neuronal cells differentiated in culture. *Journal of lipid research* **44**, 2142-2151
218. Okazaki, T., Bell, R. M., and Hannun, Y. A. (1989) Sphingomyelin turnover induced by vitamin D3 in HL-60 cells. Role in cell differentiation. *J Biol Chem* **264**, 19076-19080
219. Liu, R., Xu, Y., Farach-Carson, M. C., Vogel, J. J., and Karin, N. J. (2000) 1,25 dihydroxyvitamin D(3) activates sphingomyelin turnover in ROS17/2.8 osteosarcoma cells without sphingolipid-induced changes in cytosolic Ca(2+). *Biochem Biophys Res Commun* **273**, 95-100
220. Huwiler, A., Johansen, B., Skarstad, A., and Pfeilschifter, J. (2001) Ceramide binds to the CaLB domain of cytosolic phospholipase A2 and facilitates its membrane docking and arachidonic acid release. *FASEB journal : official publication of the Federation of American Societies for Experimental Biology* **15**, 7-9
221. Stahelin, R. V., Subramanian, P., Vora, M., Cho, W., and Chalfant, C. E. (2007) Ceramide-1-phosphate binds group IVA cytosolic phospholipase a2 via a novel site in the C2 domain. *J Biol Chem* **282**, 20467-20474

222. Shvartsman, D. E., Gutman, O., Tietz, A., and Henis, Y. I. (2006) Cyclodextrins but not compactin inhibit the lateral diffusion of membrane proteins independent of cholesterol. *Traffic* **7**, 917-926